Role of Aurora B-mediated phosphorylation during mitosis and interphase

Carmen Taveras

Submitted in partial fulfillment of the
requirements for the degree of
Doctor of Philosophy
under the Executive Committee
of the Graduate School of Arts and Science

COLUMBIA UNIVERSITY

2017

ABSTRACT

Role of Aurora B-mediated phosphorylation during mitosis and interphase

Carmen Taveras

Accurate chromosome segregation requires a spindle apparatus composed of microtubules that arise from the spindle to attach to the kinetochore, a protein complex assembled at the centromere of each chromosome. Failure to segregate chromosomes accurately may lead to lethal early developmental defects and tumorigenesis. To achieve proper kinetochore binding to microtubules, mammalian cells have evolved elaborate mechanisms to correct attachment errors and stabilize correct ones. Current models suggest that tension between kinetochore pairs (inter-kinetochore stretch) and tension at the kinetochore (intra-kinetochore stretch) produces a spatial separation of Aurora B kinase from kinetochore-associated and microtubule-binding substrates, subsequently reducing their phosphorylations and increasing their microtubule affinity. However, the tension-based models do not explain how the initial microtubule binding at unattached kinetochores occurs, where there is no tension and kinetochore-associated substrates are highly phosphorylated and, hence unable to bind to microtubules. Therefore, there must be a mechanism that explains how the phosphorylation of kinetochore substrates by Aurora B is reduced in the absence of tension.

In the first part of this thesis, I examine the structural features of the coiled-coil domain of the kinetochore-associated kinesin motor protein, CENP-E. Using Single-Molecule High-Resolution Colocalization (SHREC) microscopy analysis of kinetochore-associated CENP-E, I show that CENP-E undergoes structural rearrangements prior to and after tension generation at the kinetochore. Chemical inhibition of the motor motility or genetic perturbations of the coiled-coil domain of CENP-E increases Aurora B-mediated Ndc80 phosphorylation in a tension-independent

manner. Importantly, metaphase chromosome misalignment caused by inhibition of CENP-E can be rescued by chemical inhibition of Aurora B kinase. Therefore, CENP-E regulates the initial kinetochore binding to microtubules and the stabilization of kinetochore-microtubule attachments.

Formin-dependent actin assembly is known to play a role in multiple processes, including cytokinesis, filopodia formation, cell polarity, and cell adhesion. Thus, formin malfunction is directly linked to various pathologies, including defects in cell migration and tumor suppression. Although the role of formins in actin polymerization has been well described, the mechanistic processes that regulate the actin assembly function of formins remain poorly understood, especially the interplay among the various sub-families of formins and how they are spatiotemporally regulated.

In the second part of this thesis, I show that Aurora B-mediated phosphorylation of the formin, mDia3 regulates actin assembly. Previous studies identified two Aurora B phosphorylation sites in the FH2 domain of mDia3. To this end, phosphomimetic and non-phosphorylatable mutants of a constitutively active form of mDia3 were designed to test whether phosphorylation by Aurora B regulates actin assembly. Using an *in vitro* actin polymerization kinetic assay and expression of fluorescently-tagged constitutively active mDia3 in cells, I show that phosphorylation of mDia3 by Aurora B induces the actin assembly function of mDia3. Furthermore, using a phospho-specific antibody, I show that mDia3 is phosphorylated by Aurora B. Live-cell analysis shows that perturbations of these phosphorylation sites affect cell migration and cell spreading. Therefore, I illustrate a novel regulatory mechanism for the actin assembly function of mDia3 that is dependent on Aurora B kinase activity.

TABLE OF CONTENTS

LIST OF FIGURES

Chapter 1

Chapter 2

Chapter 3

Chapter 4

ACKNOWLEDGEMENTS

First and foremost, I would like to acknowledge and express my very special gratitude toward my thesis advisor, Dr. Yinghui Mao. Over the past 5 years, Dr. Mao has been an extraordinary mentor and teacher to me. He has guided me and enabled me to develop and conduct all the research necessary to write and defend this thesis. Above all, I am extremely grateful for the scientific platform Dr. Mao offered me to gain the confidence, technical and critical thinking skills necessary to develop my scientific ideas. On a personal level, Dr. Mao has been a role model to me; his commitment and curiosity for science influenced me throughout the years playing an essential role in my pursuit of the doctoral degree.

I want to thank the members of my thesis committee, Drs. Richard Valle, Julie Canman and Gregg Gundersen for their suggestions and support throughout the course of this thesis. The ideas and technical considerations they offered in my committee meetings helped me improve my thesis research tremendously. I also want to thank Dr. Geri Kreitzer for agreeing to serve as the additional examiner on my thesis committee.

I would also like to express my gratefulness to former members of the Mao Laboratory. Mainly, I would like to thank, Drs. Yige Guo and Chenshu Liu and Christine Kim. Dr. Guo help me launch the main focus of this thesis by offering technical guidance, engaging in very productive discussions. Dr. Liu was an invaluable labmate and colleague to me. Without his help, the super-resolution analysis of CENP-E would not have been possible. He developed the algorithm and helped me quantify the super-resolution data. Additionally, Dr. Liu continuously engaged with me in very productive scientific discussions and his contributions to the lab significantly made my graduate experience very special. Finally, I would like to thank Christine Kim with whom I collaborated for the mDia3 project. I would also like to thank her for helping me get started during my first years as a graduate student.

I am very grateful to the quantitative training I received from the Quantitative Imaging course at Cold Spring Harbor Laboratory. Specifically, I would like to thank Drs. Jennifer Waters Hunter Elliott, Torsten Wittmann and Talley Lambert for putting together an outstanding training course. I would also like to thank Theresa Swayne and Adam White at Herbert Irving

Comprehensive Cancer Center Shared Resources for technical support on the FRET analysis. I would also like to thank Dr. Michael Lampson for providing reagents and Dr. Geri Kreitzer for the mCherry-EmeraldGFP empty vector.

I would also like to thank members of the Pathology and Cell Biology Department for sharing reagents and making Columbia University Medical Center a great environment to conduct research. In particular, I would like to thank Dr. Francesca Bartolini for her collaboration on the mDia3 project. Also, members of the Gundersen Laboratory, Drs. Susumu Antoku, Wakam Chang, and Ruijun Zhu for offering technical advice and helping me design experiments.

I want to thank the Integrated/Cell Biology Graduate Program at Columbia University, the program directors, especially Dr. Ron Liem for admitting me to the Ph.D. program and setting a great environment for graduate students. A very special thank you goes to Zaia Sivo for being such a wonderful program coordinator. She offered immense help and guidance that helped me manage any problem or technical issues associated with graduate student life inside or outside the lab.

The undergraduate research experience I gained were invaluable to me during my years as a graduate student. Therefore, I would like to thank my undergraduate research mentors, Drs. Geri Kreitzer and Frida Kleiman. Their support and guidance were essential in helping me become a graduate student. I would like to thank NIH's Minority to Access to Research Career (MARC) program at Hunter College, especially, Dr. Derrick Brazil and program coordinators, Judith O'Brien and Susana Vargas for their support and guidance.

I am very grateful for all of the support I received from my family. I would like to give a warm thank you to my parents, Carmen and David and my siblings, Katherine, David, Johnathan, and Jason. Also, I would like to thank my extended family in the Dominican Republic and in Germany for all of their love and support throughout the development of this thesis.

Finally, I would like to dedicate this thesis to my best friend, Frank Mathmann. I would like to thank him for his patience and above all for his unconditional love and support. Without his support and encouragement, this thesis would not have been possible.

CHAPTER 1: Introduction

One of the most important issues in cell biology is to understand how chromosomes are segregated equally during cell division. Errors in this process may lead to aneuploidy, which results in severe developmental defects and may contribute to tumor progression (Hartwell and Kastan, 1994). Accurate chromosome segregation requires proper interactions between the kinetochore and the microtubules of the mitotic spindle apparatus (Cleveland et al., 2003; Guo et al., 2013). Because abnormal chromosome segregation has such severe consequences, cells have evolved elaborate mechanisms to oversee this process, such as the mitotic checkpoint to ensure that kinetochores form proper attachments with microtubules. In the first part of this chapter, I will introduce the molecular mechanisms involved in the stabilization of proper kinetochore-microtubule attachments with emphasis on the roles of Aurora B kinase and the kinetochore-associated kinesin motor protein, CENP-E (centromere-associated protein E).

Cell migration plays an important role in multiple developmental and homeostatic processes (Lauffenburger and Horwitz, 1996). As a consequence, failure of cells to migrate, or disruption of migratory movements, may lead to severe consequences, such as deficiencies of the immune response, defective wound repair, or metastatic cancer. Central to the understanding of the mechanisms associated with cell migration is the actin cytoskeleton (Insall and Machesky, 2009). The actin cytoskeleton is involved in a series of interrelated activities, including the generation of force and the morphological changes required for cell motility. In part two of this chapter, I will introduce the mechanisms associated with actin assembly in cells with a focus on the regulation of the actin nucleation and elongation factor, mDia3 (mouse Diaphanous homolog 3) of the diaphanous sub-family of formin proteins.

PART 1: Stabilization of kinetochore-microtubule attachments

Kinetochore-mediated microtubule capture

The mitotic spindle is a structure composed of microtubules that segregate the replicated chromosomes into two daughter cells. The spindle consists of polarized microtubule filaments that arranged in a head-to-tail configuration of α- and β-tubulin heterodimers (Nogales et al., 1998; Nogales et al., 1999). Microtubules switch from phases of growth and shrinkage, or the addition or loss of tubulin heterodimers, termed "dynamic instability" (Mitchison and Kirschner, 1984). The asymmetric configuration of the α- and β-tubulin heterodimers gives the microtubule structural polarity, in which the minus-end and the plus-end have different dynamic properties (Desai and Mitchison, 1997). The inherent polarity and the "dynamic instability" properties of microtubules are critical to generating the force necessary for chromosome segregation.

The kinetochore is a proteinaceous complex that assembles at the centromere region of each chromosome. Kinetochores mediate microtubule capture and chromosome transport (Cleveland et al., 2003; Guo et al., 2013). Many of the proteins that assemble into kinetochores are conserved among eukaryotic species, including the specialized histone H3 variant, CENP-A, which marks the site for kinetochore assembly (Van Hooser et al., 2001; Blower et al., 2002; Collins et al., 2005). The protein composition of outer kinetochores that mediate microtubule capture, includes the KMN network, which constitutes the core microtubule-binding activity of kinetochores. The KMN network is composed of the Knl1 protein, the hetero-tetrameric subcomplexes, Mis12 and Ndc80 (Wigge and Kilmartin, 2001; Deluca et al., 2002; McCleland et al., 2003; Cheeseman et al., 2004; Obuse et al., 2004; Kline et al., 2006; Kiyomitsu et al., 2007; Wang et al., 2008). The microtubule-binding and force-generating motors, Dynein and CENP-E

also localize to outer kinetochores and play critical roles in chromosome transport and segregation (Yen et al., 1992; Emanuele and Stukenberg, 2007; Cheeseman and Desai, 2008). Proteins required for the mitotic checkpoint that monitors the fidelity of kinetochore-microtubule attachments, also associate to outer kinetochores. These mitotic checkpoint proteins include Bub1, BubR1, Bub3, Mad1, Mad2, MPS1, Rod, Zw10, and Zwilch (Maiato et al., 2004; Musacchio and Salmon, 2007).

In metazoan cells, microtubules are nucleated by microtubule-organizing centers called centrosomes (Azimzadeh and Bornens, 2007). Because centrosomes are found outside the nucleus in interphase, kinetochores can only interact with microtubules after nuclear envelope breakdown (Sazer, 2005). Following nuclear envelope breakdown, kinetochore-mediated capture of microtubules occurs through a "search and capture" process (Kirschner and Mitchison, 1986) (**Figure 1.1A**). According to this model, centrosome-nucleated microtubules undergo phases of repeated growth and shrinkage until microtubules are captured and stabilized by kinetochores. During the first encounter of kinetochores with microtubules, kinetochores attach to the lateral surface of a microtubule. This a process is driven by the kinetochore-associated dynein, a minus-end-directed motor, which transport kinetochores towards the microtubule-dense environment of the spindle poles (Yang et al., 2007; Magidson et al., 2011). Poleward movement is then redirected towards the plus-end of the microtubule, a process mediated by the motor motility of CENP-E, to facilitate the attachment conversion to the plus-end tip of a microtubule (end-on attachment) and the congression of chromosomes to the cell equator, known as the metaphase plate (Kapoor et al., 2006; Cai et al., 2009).

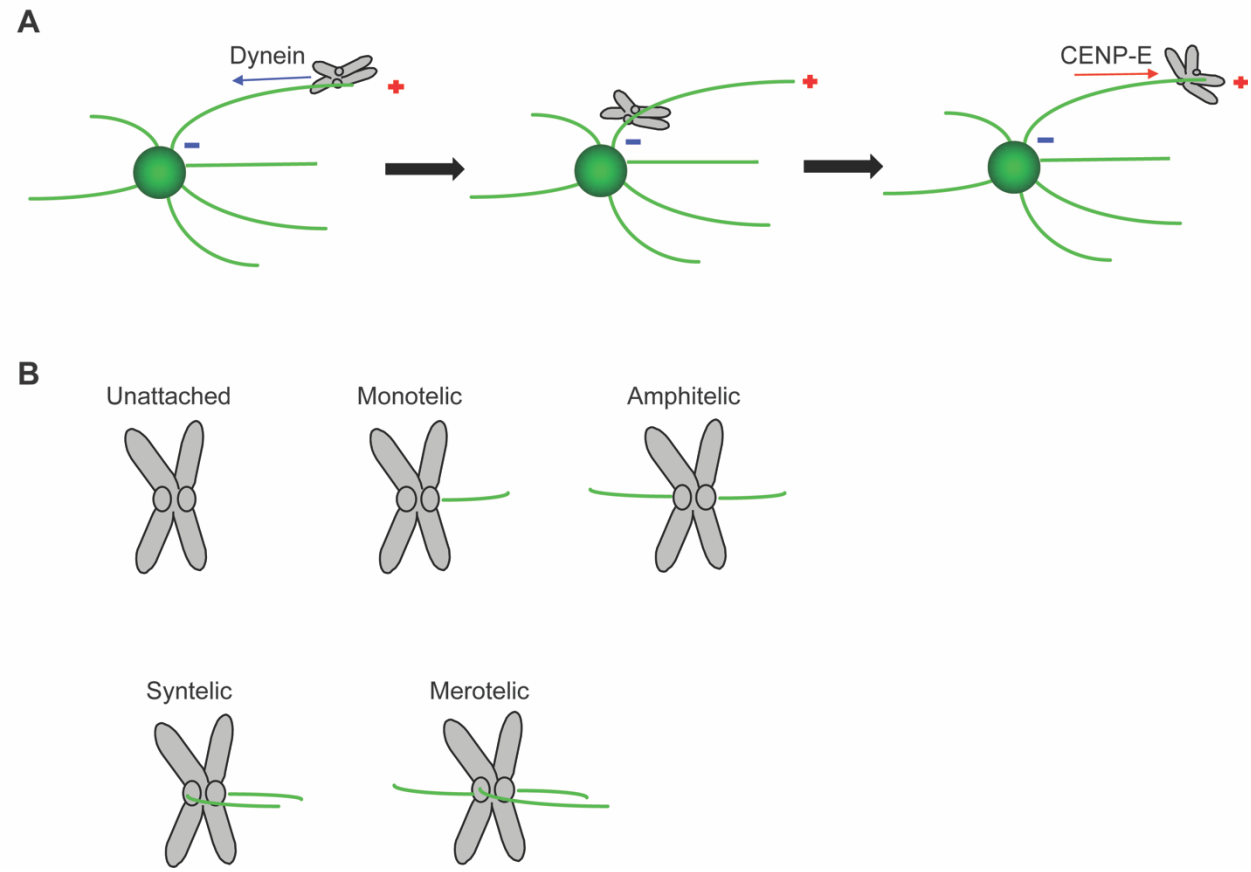

Figure 1.1 Initial microtubule capture by kinetochores. (**A**) Illustration depicting the initial microtubule capture by kinetochores using the proposed "search and capture" mechanism (Kirschner and Mitchison, 1986). Kinetochores first bind to the lateral surface of microtubules, a process mediated by the kinetochore-associated, minus-end directed dynein motor (Yang et al., 2007; Magidson et al., 2011). Plus-end motility is re-directed towards the plus-end of the microtubules by the plus-end directed CENP-E motor to facilitate the conversion to end-on attachment (Kapoor et al., 2006; Cai et al., 2009). (**B**) Depiction of the different microtubule-kinetochore configurations that can arise during the "search and capture" phase. Unattached kinetochore lack microtubules attachment, while monotelic attachments have one sister kinetochore attached to microtubules. An amphitelic configuration occurs when kinetochores capture microtubules emanating from the opposite spindle poles. Syntelic attachments occur when both sister kinetochores attach to microtubules emanating from the same spindle poles. Merotelic attachments occur when one sister attaches to microtubule emanating from both spindle poles.

To ensure accurate chromosome segregation, proper kinetochore-microtubule attachments must be stabilized. The term "proper" refers to an attachment in which one sister kinetochore captures microtubules from one spindle pole and the other sister captures microtubules emanating from the opposite spindle pole, this configuration is known as amphitelic attachment (**Figure 1.1B**). The amphitelic configuration is important to generate tension across sister kinetochores pairs and the establishment of end-on and stable bi-oriented attachments at the metaphase plate (Loncarek et al., 2007). However, because microtubule capture is a stochastic process, errors in kinetochore-microtubule attachments occur frequently in early prometaphase producing chromosomes that accumulate near the spindle poles (Ault and Rieder, 1992; Cimini et al., 2003; Hauf et al., 2003).

There are three major types of aberrant kinetochore-microtubule attachments that can arise during the "search and capture" phase (**Figure 1.1B**). Monotelic attachments occur when only one sister of a kinetochore pair binds to microtubules, while the other sister remains unattached. Syntelic attachments occur when both sister chromosomes are attached to microtubules emanating from the same spindle pole. Merotelic attachments, on the other hand, occur when one kinetochore binds to microtubules from both spindle poles. Monotelic and syntelic attachment errors are known to activate the mitotic checkpoint in response to lack of microtubule attachment and/or tension generation across sister kinetochore pairs, whereas merotelic attachments silence the mitotic checkpoint, but activate the Aurora B error correction pathway (King and Nicklas 2000; Cimini et al., 2003; Dewar et al., 2004).

Unattached kinetochores are known to prevent the anaphase onset until all kinetochores assemble into the proper amphitelic attachment configuration. Unattached kinetochores generate a diffusible signal that is conserved across eukaryotes, composed of Mad2, the human homologue

of yeast Mad3, BubR1, Bub3, Mad1, and Bub1 (Hoyt et al., 1991; Li and Murray, 1991). Other checkpoint-related proteins are essential for the localization and recruitment of checkpoint proteins onto unattached kinetochores including, Mps1, CENP-E and Aurora B (Abrieu et al., 2000; Liu et al., 2003; Vigneron et al., 2004; Weiss and Winey, 1996; Santaguida et al., 2011).

Mitotic progression is controlled by the anaphase promoting complex/cyclosome (APC/C), a multi-subunit E3 ubiquitin ligase (Fang et al., 1998). APC/C activity requires a specificity factor, CDC20 (cell-division-cycle 20 homolog), in order to recognize and interact with mitotic substrates (Hwang et al., 1998). Proteins that are targeted for degradation by APC/C include cyclin B1 and securin (Yamamoto et al., 1996; Glotzer et al., 1991). Degradation of securin leads to the activation of separase, which cleaves the cohesin links that hold together the sister chromatids. Degradation of cyclin B1, however, causes the inactivation of CDK1 (cyclin-dependent kinase 1) and initiates mitotic exit. In metazoans, dynein plays a major role in the removal of checkpoint proteins from kinetochores and thus silencing the mitotic checkpoint upon microtubule attachment (Howell et al., 2001; Wojcik et al., 2001). CENP-E also contributes to the mitotic checkpoint silencing through its microtubule capturing activity and the subsequent silencing of the BubR1 kinase activity (Mao et al., 2005).

Aneuploidy describes a state of abnormal chromosome number. Most cases of aneuploidy occurring at early developmental stages, result in the death of the developing fetus (miscarriage), however viable cases of extra autosomal chromosomes carriers specifically, chromosomes 21, 18 and 13 are common (Driscoll and Gross 2009). Aneuploidy occurring after development is the most common characteristic of solid tumors (Rajagopalan and Lengauer, 2004). However, the mechanism by which aneuploidy contributes to cancer development and progression remains elusive. Nonetheless, some pieces of evidence support the idea that aneuploidy contributes to

tumorigenesis. For instance, injection of MEFs with a reduced expression level of CENP-E into nude mice increased incidents of spontaneous lymphomas and lung tumors due to aneuploidy (Weaver et al., 2007). Furthermore, loss of function or haploinsufficiency of checkpoint-related proteins, such as Mad1, Cdc20, and Bub1 also increased the incidence of tumors in animal models (Iwanaga et al., 2007; Schliekelman et al., 2009).

Aurora B corrects kinetochore-microtubule attachment errors

Aurora B kinase is a key component involved in the attachment error correction process and the stabilization of proper kinetochore-microtubule attachments. Aurora B is a family member of the serine/threonine protein kinases with the preferred phosphorylation consensus sequence of [RK]x[TS][ILV] (Kimura et al., 1997; Cheeseman et al., 2002). It is the enzymatic component of the chromosomal passenger complex (CPC), which also contains INCENP, Borealin, and Survivin (Ruchaud et al., 2007). Aurora B has multiple localization during mitosis. It is first detected at centromeres, then relocalizes to the midzone of the central spindle, and finally associates at the midbody between dividing cells (Andrews et al., 2003; Carmena and Earnshaw, 2003; Meraldi et al., 2004).

Evidence supporting the role of Aurora B in the error correction process came first from observations of the budding yeast *Saccharomyces cerevisiae* homolog of Aurora B, Ipl1. In budding yeast, Ipl1 facilitates error correction by promoting the turnover of incorrect kinetochore-microtubule attachments (Biggins et al., 1999). In mammalian cells, inhibition of Aurora B kinase activity using small-molecule inhibitors, siRNA-mediated knockdown or Aurora B inhibition using antibodies produces stabilization of incorrect attachments and accumulation of incorrect syntelic attachments near the spindle poles (Kallio et al., 2002; Hauf et al., 2003; Ditchfield et al.,

2003). Furthermore, Aurora B selectively enriches at merotelic attachments, whereas at bi-oriented attachments it is less abundant (Knowlton et al., 2006).

Aurora B plays an important role in the error correction process in two major ways. First, by regulating the recruitment of multiple proteins involved in the generation of the mitotic checkpoint signal, including Mad1, Mad2, BubR1, Mps1, and CENP-E to prevent anaphase onset until all kinetochores have been properly attached (Ditchfield et al., 2003; Lens et al., 2003; Vigneron et al., 2004). The second way involves the phosphorylation of key substrates to facilitate the destabilization of aberrant kinetochore-microtubule attachments. Some of these substrates include, the centromere-localized microtubule depolymerase kinesin-13 protein, MCAK and the kinetochore-localized microtubule-binding proteins including, the KMN network, the formin mDia3, CENP-E and the budding yeast protein Dam1 (Lan et al., 2004; Cheeseman et al., 2006; Gestaut et al., 2008; Kim et al., 2010; Cheng et al., 2011).

One major substrate implicated in the error correction process is MCAK. Aurora B-mediated phosphorylation of MCAK is known to suppress MCAK depolymerizing activity as well as its accumulation at centromeres (Lan et al., 2004; Andrews et al., 2004; Ohi et al., 2004**).** In mammalian cells, depleting MCAK produces errors in kinetochore-microtubule attachments, including merotelic and syntelic attachments (Kline-Smith et al., 2004). In addition, MCAK selectively accumulates at merotelic attachment leading to microtubule destabilization (Knowlton et al., 2006; Wordeman et al., 2007).

The KMN network is also a major phosphorylation target of Aurora B. Phosphorylation of the Ndc80 complex, KNL1, Mis12 complex subunit Dsn1 by Aurora B strongly reduces the microtubule-binding affinity preventing the stabilization of incorrect kinetochore-microtubule

attachments (Cheeseman et al., 2006; DeLuca et al., 2006; Welburn et al., 2010). The Ndc80 complex is also regulated by Aurora B-mediated phosphorylation and the formation of stable kinetochore-microtubule attachments (Sundin et al., 2011). The Ndc80 complex is a 57 nm long heterotetrameric complex consisting of two dimers, Hec1 and Nuf2, and Spc24 and Spc2 (Wei et al., 2007; Cheeseman and Desai, 2008; Ciferri et al., 2008). The unstructured N-terminal tail of Hec1 has multiple phosphorylatable sites that upon phosphorylation by Aurora B decreases the affinity of Hec1 to microtubules (Cheeseman et al., 2006; DeLuca et al., 2006; Wei et al., 2007; Santaguida and Musacchio, 2009). Furthermore, Aurora B phosphorylation can also inhibit the microtubule binding cooperation of the Ndc80 complex with either the budding yeast protein Dam1 or the Ska complex in vertebrate cells (Lampert and Westermann, 2011; Chan et al., 2012)

Phosphatase recruitment to kinetochores counteract Aurora B kinase activity

Aurora B kinase activity can be regulated by modulating the activity of kinase directly or by the recruitment of phosphatases to kinetochores. Several mechanistic insights of Aurora B kinase activation have been elucidated using biochemical and structural approaches. The main sources of kinase activation and regulation can be found primarily through interactions with the components of the CPC complex. Interaction with INCENP is known to partially activate Aurora B and promote the subsequent auto-phosphorylation of Aurora B required for its kinase activation (Yasui et al., 2004). In addition, interaction with Survivin is known to enhance Aurora B kinase activity (Honda et al., 2003). The mitotic kinases Chk1, Mps1, and phosphorylation of Borealin have been also implicated in stimulating the kinase activity of Aurora B (Zachos et al., 2007; Jelluma et al., 2008). However, it remains unclear how the kinase activation of Aurora B is regulated at short-time scales during the repeated rounds of kinetochore-microtubule attachment and detachment that occurs during the correction process.

Phosphatase recruitment to kinetochores has been proposed to counteract Aurora B-mediated phosphorylation of the outer kinetochore substrates. Several studies have implicated protein phosphatase 1 (PP1) to be a major counteracting phosphatase of Aurora B (Francisco et al., 1994; Hsu et al., 2000; Emanuele et al., 2008). In budding yeast, studies of the PP1 orthologue, *glc7* have been shown to mediate the microtubule-binding activity of kinetochores *in vivo* and *in vitro* (Sassoon et al., 1999). The phosphatase activity of Glc7 is repressed by Glc8 (Inhibitor-2 [I-2] in vertebrates) *in vitro*, and mutants of Ipl1 (Aurora B) kinase can be rescued by overexpression of Glc8 (Tung et al., 1995). In vertebrates, isoforms PP1α and PP1γ localized to the outer kinetochore switching on and off by rapidly diffusing into the cytosol (Trinkle-Mulcahy et al., 2003; Trinkle-Mulcahy et al., 2006).

Two outer kinetochore-localized proteins, KNL1 and CENP-E are essential for the recruitment of PP1 to the outer kinetochores (Liu et al., 2010; Kim et al., 2010). KNL1, a component of the KMN network has a conserved docking motif for PP1 binding (Liu et al., 2010). Mutating this docking motif leads to an upregulation in Aurora B-mediated phosphorylation of outer kinetochores substrates leading to destabilization of kinetochore-microtubule attachments (Liu et al., 2010). CENP-E has been shown to be phosphorylated by Aurora B (Kim et al., 2010). Additionally, CENP-E has a PP1 docking site near its motor and PP1 recruitment to this site opposes Aurora B-mediated phosphorylation of CENP-E upon metaphase chromosome alignment (Kim et al., 2010). Inhibiting PP1-mediated dephosphorylation of CENP-E using blocking antibodies destabilizes stable kinetochore-microtubule attachments (Kim et al., 2010). However, PP1 has been shown to localize to kinetochores only after chromosomes have aligned at the metaphase plate and preventing PP1 targeting to kinetochores does not impair chromosome alignment (Liu et al., 2010; Posh et al., 2010). Therefore, the mechanistic implications by which

PP1 mediates stabilization of proper kinetochore-microtubule attachments prior to metaphase chromosome alignment needs further investigation.

The protein phosphate 2A (PP2A) and its regulatory subunit B56, however, have been shown to be important for metaphase chromosome alignment. Depletion of PP2A-B56 from mammalian cells leads to destabilization of kinetochore-microtubule attachments and metaphase chromosomes alignment defects (Foley et al., 2011). Furthermore, PP2A has been found to be enriched at centromeres and at kinetochores that lack microtubule attachments (Kitajima et al., 2006; Riedel et al., 2006; Tang et al., 2006; Foley et al., 2011). The outer kinetochore recruitment of PP2A-B56 is mediated by a conserved and a highly phosphorylatable (KARD) domain found in BubR1 (Suijkerbuijk et al., 2012b). Deletion of this domain or prevention of its phosphorylation prevents formation of stable kinetochore-microtubule attachments (Suijkerbuijk et al., 2012b).

The kinetochore phosphorylation/dephosphorylation balance is regulated by tension

The outcome of Aurora B-mediated phosphorylation has been shown to vary among the different substrates found at the kinetochore. However, a regulatory mechanism that integrates all of these phosphorylation events remains elusive. Nonetheless, several models, centered on Aurora B function have been proposed. These not mutually exclusive models include the tension-based models, the "spatial separation" model and the mechanical change of kinetochores, known as "intra-kinetochore stretch" (Lampson and Cheeseman, 2011; Maresca and Salmon, 2009; Uchida et al., 2009) (**Figure 1.2**).

The "spatial separation" model is based on previous observations in spermatocytes, in which induction of physical tension resulted in the stabilization of kinetochore-microtubule attachments (Nicklas and Koch, 1969; Nicklas and Ward, 1994). This model suggests that tension

exerted between sister kinetochores (inter-kinetochore stretch) results in a spatial separation of the inner centromere-localized Aurora B from the outer kinetochore-localized substrates (Lampson and Cheeseman, 2011) (**Figure 1.2**). This attachment configuration decreases Aurora B-mediated phosphorylation of the Ndc80 complex, increasing their binding affinities for microtubules and in turn promoting the stabilization of proper kinetochore-microtubule attachments (Keating et al., 2009; Liu et al., 2009). Conversely, when kinetochore-microtubule attachments are not correct and not under tension, these microtubule-binding proteins remain in close proximity to Aurora B and their phosphorylation is increased. This configuration results in a decreased microtubule binding activity and the release of kinetochores from microtubules. Essentially, the distance from the centromere-associated Aurora B to the outer kinetochores mediates the likelihood of phosphorylation (Liu et al., 2009; Lampson and Cheeseman, 2011; Tanaka, 2013).

This model relies on the distance between inner-centromere-localized Aurora B kinase from the outer-kinetochore-localized substrates. In mammalian cells, the distance between kinetochores under tension varies from 1 to 3 microns, whereas the relaxed or unattached state is approximately halved (Waters et al., 1998). Aurora B in complex with CPC has been found to be elongated at centromeres by approximately 50 nm (Bolton et al., 2002). Therefore, this model assumes that the diffusion of Aurora B must be very low (Kelly and Funabiki, 2009). Furthermore, an active population of Aurora B kinase has been shown to be enriched at the outer kinetochore in mammalian cells (DeLuca et al., 2011). However, the contributions of this outer kinetochore-targeted population remain unknown. In budding yeast, a study has found that centromere targeting of the homolog of Aurora B, Ipl1 is not necessary for Aurora B tension sensing (Campbell and Desai, 2013). Finally, this model can not explain how meiotic cells stabilize kinetochore-microtubule attachments as Aurora B remains closely associated with kinetochores during

metaphase I and metaphase II (Parra et al., 2003; Parra et al., 2006).

Kinetochore stretch has been proposed to play a critical role in the stabilization of proper kinetochore-microtubule attachments (**Figure 1.2**). Kinetochore stretch, known as intra-kinetochore stretch refers to the structural rearrangement of kinetochores that occurs upon microtubule attachment (Maresca and Salmon, 2009; Uchida et al., 2009). Changes in intra-kinetochore stretch have been studied by measuring the distance between an inner kinetochore component, such as CENP-A and an outer kinetochore component such as the Ndc80 complex or the Mis12 complex (Maresca and Salmon, 2009; Uchida et al., 2009). Components of the constitutive centromere-associated network (CCAN), CENP-T and CENP-C have been proposed to mediate changes in intra-kinetochore stretch due to the presence of long and extendable disordered domains found in both CENP-T and CENP-C (Suzuki et al., 2011; Suzuki et al., 2014). Changes in intra-kinetochore stretch have been shown to play an important role in silencing the mitotic checkpoint and correcting aberrant kinetochore-microtubule attachments (Maresca and Salmon, 2009; Uchida et al., 2009; Bakhoum et al., 2009; Silkworth and Cimini, 2012; Drpic et al., 2015).

Recent efforts, however, have found that the generation of stable kinetochore-microtubule attachments in the absence of intra-kinetochore stretch can silence the mitotic checkpoint and mediate mitotic progression (Etemad et al., 2015, Tauchman et al., 2015). Congruent with this evidence, another study has shown that intra-kinetochore stretch is not required, but rather the targeting of the outer kinetochore and the mitotic checkpoint component, Mad2 to unattached kinetochores alone regulates mitotic progression in mammalian cells (Magidson et al., 2016).

These tension-based models pose a paradox: the generation of tension requires the

formation of kinetochore-microtubule attachments and the generation of tension requires the stabilization of kinetochore-microtubule attachments. Therefore, there must be an intermediate step that stabilizes kinetochore-microtubule attachments in the absence of tension. This is the main subject of this thesis: to elucidate the mechanism that promotes microtubule-kinetochore attachments prior and after tension generation.

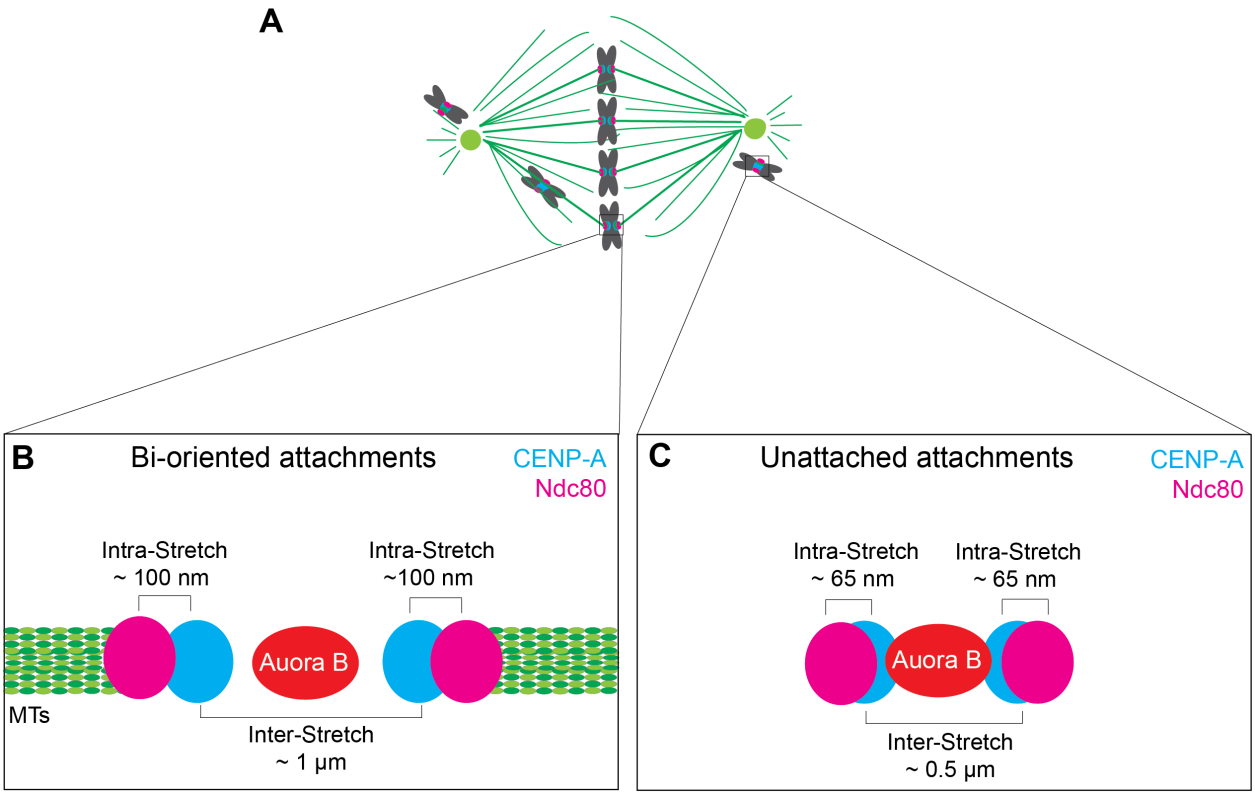

Figure 1.2 Illustration of the tension-based models. (**A**) The illustration depicts different types of kinetochore-microtubule attachments: unattached kinetochores that are not under tension, aligned bi-oriented attached kinetochores under tension. (**B**) When kinetochores are attached to microtubules from the opposite poles this leads to a physical separation of Aurora B from its phosphorylation substrates. This increase in separation leads to a decrease in phosphorylation of the core microtubule-binding component, Ndc80 complex and kinetochore-microtubule attachments are stabilized (middle panel). (**C**) Conversely, in unattached or mal-attached kinetochores, such as syntelically attached kinetochores, Aurora B remains in close proximity to the Ndc80 complex leading to an increase in phosphorylation and destabilization of kinetochore-microtubule attachments.

CENP-E facilitates the stabilization of kinetochore-microtubule attachments

As a kinetochore-associated plus-end directed motor, CENP-E has been proposed to power chromosome movement on the microtubules of the mitotic spindle (Kapoor et al., 2006) and/or to maintain a mechanical link between kinetochores and dynamic microtubule plus-ends (Lombillo et al., 1995; Gudimchuk et al., 2013). The role of CENP-E in microtubule capture and the unique structural features of CENP-E, make CENP-E an attractive candidate that might be involved in the stabilization of kinetochore-microtubule attachments prior to tension generation.

CENP-E was discovered as a kinetochore-associated protein with a molecular mass of 310 kDa (Yen et al., 1992). As a kinesin-7 member, CENP-E has a conserved kinesin motor domain at the N-terminus and a globular kinetochore targeting domain found at the C-terminus. The N- and C- terminus is separated via an extended discontinuous coiled-coil "stalk" domain. CENP-E accumulates in the late phase of the G2/M phase of the cell cycle and is degraded at the end of mitosis (Yen et al., 1992; Brown et al., 1994; Brown et al., 1996). Specifically, CENP-E localizes to the outermost region of the kinetochore at the corona fibers, with its motor domain positioned away from kinetochores (Yao et al., 1997). During prometaphase, there is an acute accumulation of CENP-E at unaligned kinetochores and as cells progress through mitosis CENP-E levels decrease persisting until early anaphase. At late anaphase, CENP-E translocates to the spindle midzone (Yen et al., 1992; Liao et al., 1994; Brown et al., 1994; Brown et al., 1996; Yao et al., 1997). Further *in vitro* studies characterized CENP-E as a plus-end directed microtubule motor that it is highly processive, but with a slow velocity of 8 nm/sec (Wood et al., 1997; Kim et al., 2008; Espeut et al., 2008; Yardimci et al., 2008).

Studies in multiple experimental systems support the roles of CENP-E in metaphase

chromosome alignment and tethering kinetochores to microtubules. In both developing flies and in mice, homozygous disruption of the *CENP-E* gene leads to early embryonic lethality as a result of mitotic abnormalities (Putkey et al., 2002; Yucel et al., 2000). Inhibition or removal of CENP-E from mammalian cells or disruption of the CENP-E gene in mice leads to an obvious metaphase plate with a few unaligned chromosomes left near the spindle poles (Yao et al., 1997; Martin-Luesma et al., 2002; McEwen et al., 2001; Putkey et al., 2002). In *Drosophila* cells and in *Xenopus* eggs extracts, loss of their respective CENP-E orthologue also results in a failure to achieve and/or maintain metaphase chromosome alignment (Wood et al., 1997; Goshima et al., 2003). The unaligned chromosomes in a later study were shown to congress to the metaphase plate via a CENP-E motility-dependent mechanism (Kapoor et al., 2006).

Besides the role in mediating chromosome transport, inhibition or depletion of CENP-E results in a reduction of the number of microtubules bound to kinetochores at both unaligned and aligned chromosomes (McEwen et al., 2001; Putkey et al., 2002; Weaver et al., 2003). Supporting its role in tethering kinetochores to microtubules, *in vitro* studies, have shown that CENP-E can converts from a lateral transporter into a microtubule tip-tracker, tracking both the depolymerizing and depolymerizing end of a microtubule (Gudimchuk et al., 2013). Supporting this function, a prior study showed that perturbing CENP-E function using function-blocking antibodies prevents the depolymerization-dependent motion of isolated chromosomes (Lombillo et al., 1994). In mammalian cells, CENP-E has been proposed to facilitate lateral to end-on conversion of kinetochore-microtubule attachments (Shrestha and Draviam 2013). Additionally, other *in vitro* studies, have implicated CENP-E to be involved in promoting microtubule plus-end elongation (Sardar et al., 2010; Musinipally et al., 2013).

In addition to tethering kinetochores to microtubules, CENP-E is a major component of the

mitotic checkpoint. In *Xenopus* egg extracts, immunodepletion or function-blocking antibodies of CENP-E disrupts the recruitment of two essential mitotic checkpoint components, Mad1 and Mad2 (Abrieu et al., 2000). CENP-E links microtubule capture to the mitotic checkpoint by directly binding and activating the kinase activity of BubR1 at unattached kinetochores (Mao et al., 2003). Biochemical studies of a ternary complex composed of BubR1, CENP-E, and microtubules is known to silence the mitotic checkpoint in *Xenopus* egg extracts (Mao et al., 2005). In support of this evidence, the addition of a motorless CENP-E mutant abolishes the ability of microtubules to suppress the CENP-E stimulation of BubR1 activity *in vitro* (Mao et al., 2005). Further studies of BubR1 kinase activation showed that BubR1 is auto-phosphorylated and this auto-phosphorylation event is CENP-E and microtubule attachment dependent (Guo et al., 2012). The BubR1 kinase activation by CENP-E is essential for accurate chromosome segregation, metaphase alignment, and a full-strength mitotic checkpoint in cancer cells (Guo et al., 2012). These data indicate that microtubule capture by CENP-E can be transduced through BubR1 kinase function.

CENP-E function at kinetochores can be regulated by several forms of post-translational modifications. Prenylation of CENP-E has been proposed to regulate the localization of CENP-E to kinetochores (Ashar et al., 2000; Schafer-Hales et al., 2007). The addition of a farnesyl transferase inhibitor to inhibit prenylation produces a similar phenotype of cells depleted of CENP-E (Ashar et al., 2000; Schafer-Hales et al., 2007). Furthermore, the localization of CENP-E to kinetochores is also regulated by SUMOylation, the covalent addition of SUMO peptides to a protein. Overexpression of the SUMO-specific isopeptidase, SENP2 leads to prometaphase cell cycle arrest with chromosomes near the spindle poles with reduced levels kinetochore-associated CENP-E (Zhang et al., 2008). Aurora B kinase function is also important for CENP-E localization through the upstream kinetochore targeting of Bub1 and BubR1 (Ditchfield et al., 2003).

CENP-E has ten potential phosphorylatable sites that have been identified using mass spectrometry (Nousiainen et al., 2006). Most of these have an unknown function, however, all have been shown to be important for mitotic progression (Kim et al., 2010). Some of these were found in the C-terminal motorless microtubule-binding domain of CENP-E and have been reported to regulate the microtubule binding activity of this domain (Liao et al., 1994). Studies in *Xenopus*, using purified truncated fragments of the motor domain and the C-terminal domain of CENP-E, showed that addition of the C-terminal fragment inhibits the motor activity of CENP-E (Espeut et al., 2008). Furthermore, phosphorylation of this C-terminal region by either cyclin B/Cdk1 or by Mps1 mitotic kinases was sufficient to relieve this inhibition (Espeut et al. 2008). However, the contributions of the long and highly flexible coiled-coil domain in this inhibitory process remains unknown.

As mentioned above, CENP-E is a known target of Aurora B. Aurora B-mediated phosphorylation near the motor domain of CENP-E, was shown to regulate its binding affinity for microtubules (Kim et al., 2010). Phosphorylation by both Aurora B and Aurora A (the kinase enriched at the spindle poles), reduces the affinity of CENP-E for microtubules (Kim et al., 2010). Phosphorylation of CENP-E at residue threonine 442, was shown to be higher at kinetochores near the poles compared to aligned kinetochores at the metaphase plate (Kim et al., 2010). Furthermore, Aurora-mediated phosphorylation of CENP-E opposes the direct recruitment of PP1, which is also found near the motor domain of CENP-E (Kim et al., 2010). Expressing a non-phosphorylatable mutant of CENP-E produces misaligned kinetochores left near the spindle poles. These data suggest that CENP-E has a direct role in stabilizing microtubule-kinetochore attachments through Aurora B kinase function.

In cancer, CENP-E is frequently overexpressed compared to non-cancerous tissues. For instance, lung adenocarcinomas have a five-fold and squamous cell carcinomas have a twenty-fold increase in protein expression (Wood et al., 2008). There are also cases in upregulation of the CENP-E mRNA from two to five fold in several cases of adenocarcinomas (Wood et al., 2008). Genetic studies of CENP-E using mouse models have shown that CENP-E can be either tumor-promoting or tumor-suppressive depending on the genetic background (Weaver et al., 2007). The mice that lacked one allele of CENP-E showed reduced expression of CENP-E, which led to a higher incidence of aneuploidy, or the presence of abnormal chromosome numbers (Weaver et al., 2007). These mice exhibited an increase in spontaneous lung adenomas and splenic lymphomas, which suggest a role for CENP-E in tumor suppression (Weaver et al., 2007). On the other hand, the incidence of liver tumors was reduced when tumors were induced chemically or genetically to increase the rate of aneuploidy. In this scenario, CENP-E showed an anti-tumor activity due to a higher frequency of aneuploidy (Weaver et al., 2007). Furthermore, CENP-E has been shown to interact directly and indirectly with BubR1 and BRCA2 known to have mutations that predispose to the development of cancer (Cahill 1998, Futamura et al., 2000).

Drug discovery efforts have led to the discovery of GSK923295, a highly specific allosteric inhibitor of CENP-E that inhibits the motor motility of CENP-E (Wood et al., 2010). GSK923295 inhibits the microtubule-stimulated ATPase cycle of CENP-E motor domain, by stabilizing the motor domain in a complex with ADP and preventing the nucleotide turnover, thus ‘‘locking’’ CENP-E in a microtubule-bound state (Wood et al., 2010). In multiple cancer cell lines, GSK923295 treatment inhibited proliferation, causing cell cycle arrest with misaligned chromosomes left near the spindle poles (Wood et al., 2010).

Rationale and objectives for chapter 2

Structural studies using electron microscopy of purified CENP-E found that CENP-E is a homodimeric motor with a discontinuous and highly flexible α-helical coiled-coil that is approximately 230 nm long (Kim et al., 2008) (**Figure 1.3**). While the motor domain is highly conserved among members of the kinesin family, this feature is strikingly different from conventional kinesin motors, which mainly have a much shorter coiled-coil either rigidly extended or folded through hinge segment found in the middle of the coiled-coil (Hirokawa et al.,1989; Verhey et al., 2011) (**Figure 1.3, B and C**). This highly flexible coiled-coil enables CENP-E to rearrange into a wide variety of different conformations (Kim et al., 2008). Further analysis of the protein sequence found in *Xenopus* and in humans revealed a predicted disruption of the coiled-coil structure by more than 20 times, potentially by segments containing proline or glycine amino acids (Kim et al., 2008).

The main goal for chapter 2 is to elucidate what is the role of the coiled-coil domain of CENP-E. Using genetic and chemical manipulations of the kinetochore function of CENP-E combined with super-resolution imaging, live-cell imaging, and immunofluorescence analysis, I elucidate the main function of CENP-E is to stabilize kinetochore-microtubule attachments before and after tension generation at the kinetochore. This function is facilitated by the unique structural features of CENP-E, which mediate the microtubule capture activity of CENP-E and the structural rearrangement of CENP-E at the kinetochore. Specifically, the structural changes of CENP-E play a critical role in the downregulation of Aurora B kinase activity and thus promoting the stabilization of kinetochore-microtubule attachments in a tension independent manner.

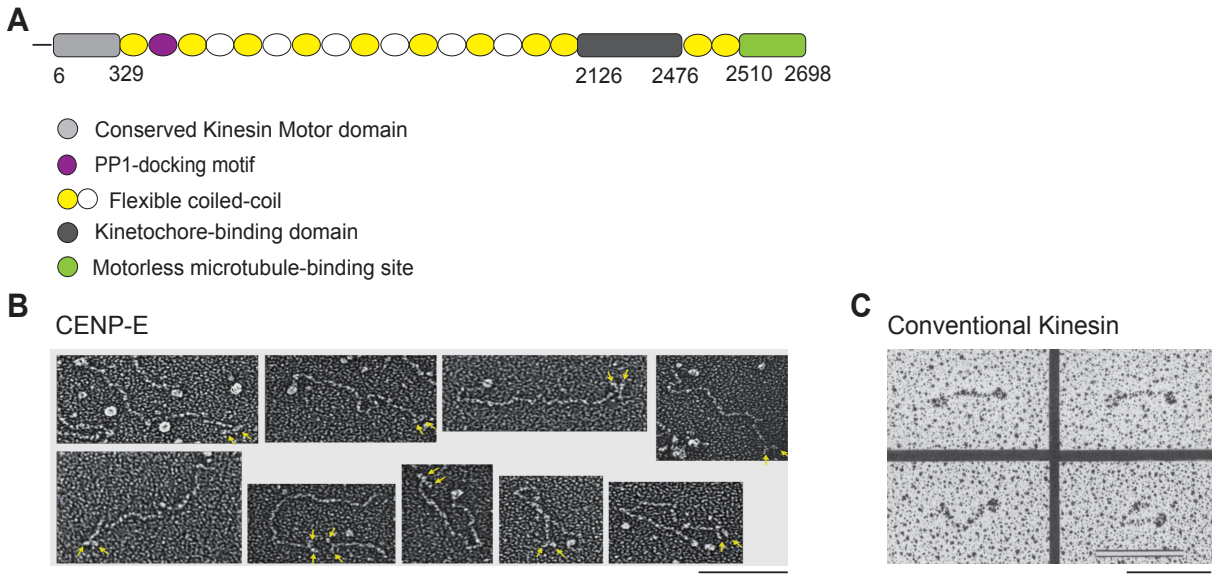

Figure 1.3. CENP-E has a long and flexible coiled-coil domain. (**A**) Illustration of the CENP-E protein sequence found in humans. The sequence includes a conserved motor domain at the N-terminus, and kinetochore targeting domain at the C-terminus. The N- and C-terminus are separated by a discontinuous coiled-coil. Near the motor domain, lies a PP1 targeting motif. (**B**) Electron micrographs of individual *Xenopus* CENP-E molecules from *Kim et al., 2008*. Arrows indicate the globular motor heads of CENP-E. Scale bar, 100 nm. (**C**) Electron micrographs of conventional kinesin motors from *Hirokawa et al.,1989*. Scale bar, 100 nm.

PART 2: Regulation of formin-mediated actin assembly

The actin cytoskeleton plays a major role in cell migration

Cell migration plays an essential role in many biological processes and is implicated in the development of many pathologies. During embryonic development, cell migration plays multiple roles, including the formation of the germ layers that give rise to tissue and organs (Keller, 2002). Tissue regeneration and repair is a prominent homeostatic process of the skin, in which cell migration plays an important role (Martin, 1997). The inflammatory response to fight foreign pathogens throughout the body involves the migration of immune cells from the lymph nodes to the circulatory system (Luster et al., 2005). Therefore, defects in cell migration or aberrant cell movements can lead to various diseases including immunosuppression, defects in tissue regeneration and metastatic cancer (Friedl and Gilmour, 2009; Martin and Leibovichb, 2005).

The migration of cells is a well-organized and multi-step process that involves the remodeling of the cytoskeleton in response to extracellular cues (Lauffenburger and Horwitz, 1996). The actin cytoskeleton plays a major role in cell morphology, adhesion sites and the generation of force by associating with motors of the myosin superfamily (Webb et al., 2004; Pollard, 2007). Although there are differences in the migratory process among different cell types, the role of actin assembly in the generation of a protrusion and cell adhesion machinery are common among migratory cells (Kole et al., 2005; Gardel et al., 2010). Actin assembly at the front of the cell drives the extension of membrane protrusions known as lamellipodia and filopodia (Mejillano et al., 2004). Retraction at the rear of the cell is mediated by combining the activities of the motor myosin and actin (actomyosin) (Pollard, 2007).

A protrusion is the *de novo* formation of membrane extensions that occurs at the leading

edge of a polarized cell. The protrusions are produced by local actin polymerization. These include the lamellipodia, a flat and "fan-like" protrusion, in which actin polymerization is often branched. The other form of a protrusion is known as the filopodia, a "spike-like" protrusion, which often are comprised of polymerized actin filaments that are arranged into linear parallel bundles (Mejillano et al., 2004). These two forms of protrusions are thought to have different roles during cell migration. Lamellipodia provides wide surfaces that generate traction for forwarding movement, whereas filopodia act as mechanosensory and exploratory machinery.

Actin is a highly abundant and ubiquitous expressed protein. It is among the most highly conserved proteins, with more than ninety-five percent of its primary sequence conserved (Elzinga et al., 1973). The monomeric, globular form of actin, known as G-actin, forms the basic unit for actin filaments. Actin polymerization is a highly dynamic process, in which the filaments grow and shrink in length (Watanabe, 2010). There are generally three phases by which actin polymerization occurs, a nucleation phase, elongation and a steady state phase. The formation of an "actin nucleus" occurs in the nucleation phase, in which three actin monomers form a complex (Dominguez, 2010). This "actin nucleus" facilitates the association of other actin monomers at the plus or barded end of the filament, known as the elongation phase. The steady state is reached once the speed of growth at the barded end is equal to the rate of shrinkage at the minus or the pointed end, a process known as actin treadmilling (Dominguez, 2010).

In cells, actin nucleation from actin monomers requires nucleation factors the help to overcome the kinetic barrier of the nucleation phase (Pollard, 2007). There are three major groups of nucleation factors; the Arp2/3 complex, WH2-containing nucleators, and formins. Arp2/3 complex is a heptamer complex that attaches itself to the side of a pre-existing actin filament and nucleates *de novo* actin polymerization at a fixed angle. This polarized branched-actin array is

maintained by rapid treadmilling by the coordinated action of actin-binding proteins, cofilin, profilin, and capping proteins (Schafer et al., 1996; Svitkina and Borisy, 1999; Yarmola and Bubb, 2006). The Arp2/3 complex is known to generate the mesh of branched actin filaments found in the lamellipodia.

Formin-mediated actin assembly

Formin-mediated actin assembly processes are involved in multiple cellular processes that includes cytokinesis, endocytosis, filopodia formation, cell polarity, cell-cell adhesion, and cell-matrix adhesion (Kovar 2006; Goode and Eck, 2007). In 1990, the term 'formin' was introduced to describe protein products of the *limb deformity* gene in mice (Woychik et al., 1990; Maas et al., 1990). The homologous formin protein was later found in *Drosophila* as the *diaphanous* locus, which was shown to be essential for cytokinesis (Castrillon and Wasserman, 1994). Therefore, the *Formin* (FMN) and *Diaphanous* (Dia) subfamilies became the founding members of the formin families.

The formin family of proteins are characterized by the presence of two conserved domains, the formin homology 1 and 2 (FH1 and FH2). The FH1 domain contains proline repeats that interact with SH3-domains containing proteins and profilin (Watanabe et al., 1997; Evangelista et al., 1997). The FH2 domain is necessary and sufficient to nucleate actin filaments by stabilizing an actin dimer (Pruyne et al., 2002; Sagot et al., 2002; Kovar et al., 2003; Pring et al., 2003). Furthermore, FH2 domains when bound to the actin-binding protein, profilin, can rapidly elongate actin filaments at a rate of approximately 100 actin subunits per second (Romero et al., 2004).

The crystal structure of the FH2 domain from the budding yeast formin, Bni1p revealed a "doughnut shape" with a flexible antiparallel dimeric configuration of the FH2 domains (Xu et al.,

2004). Furthermore, a linker found between the FH1 and FH2 domains was found to mediate the dimerization required for the nucleation activity of the FH2 domain (Shimada et al., 2004). In addition to its nucleation activity, the FH2 domain binds to the barbed end and acts as a "leaky capper" by slowing down the elongation and dissociation rates without affecting the critical concentration of actin (Pruyne et al., 2002; Pring et al., 2003; Zigmond et al., 2003).

Formins are regulated by auto-inhibition, in which the C-terminal DAD domain (diaphanous autoregulatory domain) interacts with the N-terminal DID (diaphanous inhibitory domain) resulting in the inhibition of the actin-nucleating activities of the FH2 domain (Alberts, 2001; Li and Higgs, 2003). Biochemical and structural studies, demonstrated that binding of Rho family of small GTPases to the N-terminal GBD/FH3 domain, which is present in most formin isoforms releases the autoinhibitory interaction leading to activation of the FH1 and FH2 domains (Lammers et al., 2005; Li and Higgs, 2003, Rose et al., 2005).

Evidence in multiple organisms shows the role of formins in filopodia formation downstream of Rho-GTPases signaling. In mammalian cells, the diaphanous-related formin mDia2 is known to localized to the tip of the filopodia (Pellegrin et al., 2005; Peng et al., 2003). Microinjection of function-blocking antibodies against mDia2 or expression of a dominant-negative form of mDia2 disrupts actin re-organization and filopodia formation in response to the small GTPase, Cdc42 activation in fibroblasts (Peng et al., 2003). Conversely, expression of a constitutively active form of mDia2 induced the formation of filopodia (Wallar et al., 2006). In *Dictyostelium*, dDia2 also localizes at the tip of filopodia and is required for their extension (Schirenbeck et al., 2005). Specifically, the Rho-GTPase, Rif, which also localizes to filopodia, was shown to play a prominent role in the formation of mDia2-dependent filopodia elongation (Pellegrin and Mellor, 2005).

Formin-mediated actin nucleation is essential for the formation of the contractile ring during cytokinesis in multiple organisms (Swan et al., 1998; Chang et al., 1997; Severson et al., 2002; Castrillon and Wasserman, 1994). Active small GTPase, RhoA is known to bind to the N-terminal domain of formins to relieve its autoinhibition leading to nucleation of actin filaments at the contractile ring (Alberts, 2001). Null mDia1 formin alleles in *Drosophila* results in early pupal lethality due to defects in cytokinesis (Castrillon and Wasserman, 1994). In mammalian cells, overexpression of nucleation-deficient formin mutants and microinjection of function-blocking antibodies against mDIa1 results in cytokinesis failure (Suetsugu, et al., 1999; Tominaga et al., 2000).

Besides the well-studied autoinhibitory process of formins, other forms of regulation are potentially possible, giving that most organisms express multiple formin isoforms. In humans, there are at least fifteen formin genes, six formin genes found in *Drosophila*, three formins found in fission yeast and two in budding yeast (Chang et al., 1997, Petersen et al., 1998; Feierbach and Chang, 2001; Higgs and Peterson, 2005). This leads to the hypothesis that different isoforms have distinct functions that are differentially regulated. Differences in the intrinsic actin nucleation activities of formin have been reported. For instance, the diaphanous-related formin, Daam1 (dishevelled-associated activator of morphogenesis-1), which is crucial to establish planar cell polarity in *Xenopus,* has a weaker actin assembly activity compared to other mammalian formins due to differences in secondary structural elements (Lu et al., 2007).

Besides structural differences, formins can also be differentially regulated by other binding effectors. Examples supporting this possibility have been reported in various organisms, in which the isoforms are differentially targeted to specific actin-based structures. The three isoforms expressed in fission yeast, are known to localized differentially to mediate different cellular

processes, including cytokinesis and cell polarity (Chang et al., 1997; Feierbach and Chang, 2001; Petersen et al., 1998; Nakano et al., 2002). The formins Bni1 and Bnr1 in budding yeast, mouse mDia2 and *Dictyostelium* dDia2 all were shown to assemble into unique structures in their respective organism (Evangelista et al., 1997 Imamura et al., 1997; Ozaki-Kuroda et al., 2001; Pellegrin and Mellor 2005; Schirenbeck et al., 2005). In mammalian cells, the diaphanous family of formins, mDia1, mDia2, and mDia3 have been shown to have non-redundant functions in cortical microtubule capture and actin-based processes (Goh, 2012; Yang et al., 2007; Daou et al., 2013).

Although evidence of compensatory functions has been reported, for instance, knockout of both mDia1 and mDia3 is necessary to induce developmental defects in mouse brains (Thumkeo et al., 2011; Shinohara et al., 2012). Mass spectrometry analysis, however, has found that the FH2 domain of mDia1, mDia2, and mDia3, have different binding partners (Daou et al., 2013). For instance, the FH2 of mDia1 specifically interacts with Rab6-interacting protein 2 (Daou et al., 2013). On the other hand, the FH2 of mDia2 was shown to interact with various nuclear proteins, including histones (Daou et al., 2013). Furthermore, mDia2, but not mDia1 or mDia3 accumulates in the nucleus (Miki et al., 2008). Further studies, reported that mDia2 nuclear accumulation is essential to maintain the histone variant H3, CENP-A at centromeres, whereas mDia3 does not affect this function (Liu and Mao, 2016).

Aurora B-mediated phosphorylation of mDia3 regulates mDia3 function

The formin mDia3 specifically have been shown to regulate the generation of stable kinetochore-microtubule attachments (Yasuda et al., 2004). Besides the role of the Diaphanous-related family in actin nucleation and elongation, mDia1, mDia2, and mDia3 have been implicated

in microtubule-dependent processes (Chesarone et al., 2010; Gaillard et al., 2011). Mutants of mDia2 that disrupts its dimerization of the FH1FH2 domains or their actin nucleation activities, were shown to induce microtubule stabilization in fibroblast (Bartolini et al., 2008). These results suggest that formins can also regulate microtubule dynamics independent of their actin functions, connecting both the actin and microtubule cytoskeleton. Further studies of mDia3, identified four phosphorylatable sites the have the preferred Aurora B consensus sequence (Cheng et al., 2011). mDia3 function in the stabilization of kinetochore-microtubule attachments was found to be independent of its actin function (Cheng et al., 2011). Furthermore, the kinetochore function of mDia3 is regulated by Aurora B-mediated phosphorylation at 4 residues (T66, S196, S820, and T882). Aurora B-mediated phosphorylation of mDia3 or expression of a phosphomimetic mutant form of mDia3 failed to bind or stabilize microtubules *in vitro* and rescue metaphase chromosome alignment in cells depleted of endogenous mDia3 (Cheng et al., 2011).

Apart from its stabilization function of kinetochore-microtubule attachment, mDia3 is involved in many actin-based processes including cytokinesis, filopodia formation, and oogenesis. In *Drosophila* and in humans, mutations in the *Dia* locus leads to disrupted oogenesis and premature ovarian failure due to failures in mitosis and in cytokinesis (Castrillon and Wasserman, 1994; Bione et al., 1998). In mammalian cells, depletion of mDia3 using siRNAs results in defective cell migration and disruption of cortical microtubule capture (Daou et al., 2013). Expression of mDia3 in neuroblastoma cells induces filopodia formation (Goh et al., 2012). Furthermore, mDia3 actin assembly activity induction by the small GTPase RhoD have been shown to control endosomal trafficking and filopodia formation in mammalian cells (Gasman et al., 2003; Koizumi et al., 2012).

As described in part 1 of this chapter, Aurora B has essential roles during cell division.

The expression of Aurora B is cell-cycle-regulated, with a sharp accumulation during G2 and M phases followed by a decrease after completion of cytokinesis (Honda et al., 2003). Ubiquitin-mediated proteolysis by the anaphase-promoting complex (APC/C) targets many mitotic substrates for degradation including Aurora B (Stewart and Fang, 2005). This proteolytic process has been proposed to dampened Aurora B kinase activity. However, the mechanism by which APC/C fine tunes Aurora B kinase activity after cell division remains unknown.

A study of the formin homology 2 domain-containing protein 1 (FHOD1) of the diaphanous-related formins (DRFs), found that FHOD1 is involved in targeting a pool of Aurora B to the cell periphery at the end of cytokinesis and as cells enter interphase (Floyd et al., 2013). The retention of Aurora B at the cell cortex was shown to be dependent on FHOD1. Furthermore, Aurora B was also found to phosphorylate FHOD1 at multiple sites, which affects the re-organization of filamentous actin during cell spreading (Floyd et al., 2013). These results suggest that Aurora B plays a role in regulating formin-mediated actin-dependent processes.

In cancer cells, Aurora B is frequently upregulated and overexpression of Aurora B is correlated with higher incidences of metastatic cancer (Keen et al., 2004; Giet et al., 2005). However, the role of Aurora B in metastasis remains largely unknown. Studies have reported that Aurora B regulates cell migration and invasion in tumors (Zhou et al., 2014; Zhu et al., 2014; Shan et al., 2014). Knockdown of Aurora B using shRNAs or inhibition of Aurora B using small-molecule inhibitors, perturbed cell migration and invasion in various cancer cell lines (Zhou et al., 2014; Zhu et al., 2014; Shan et al., 2014). Furthermore, Aurora A, a member of the Aurora family kinases, was also shown to disrupt cell migration in cancer cells (Wu et al., 2005). However, the molecular pathways involved in this process remain unknown.

Rationale and objectives for chapter 3

mDia3 has been previously shown to be phosphorylated by Aurora B (Cheng et al., 2011). Two of the phosphorylation sites are found in the FH2 domain of mDia3 (**Figure 1.4**). However, how this affects the actin assembly function of mDia3 remains unknown. Importantly, while one of these phosphorylation sites is conserved in mDia1 and mDia2 (T882), the other site, S820 is replaced with phosphomimetic amino acids (aspartic acid or glutamic acid). These observations lead to the hypothesis that these phospho-amino acid residues play an important role in the actin assembly activities of the diaphanou*s* subfamilies of formins, mDia1, mDia2, and mDia3.

The main objective of chapter 3 is to determine whether Aurora B-mediated phosphorylation of mDia3 differentially regulates the actin assembly function of mDia3. Using analysis of phosphomimetic and non-phosphorylatable mutants of a constitutively active form of mDia3 expression in cells and using an *in vitro* actin polymerization assay, I show that phosphorylation of mDia3 is essential for the actin assembly. Furthermore, using a phospho-specific antibody, I show that mDia3 is phosphorylated at the cell periphery. The disruption of Aurora B-mediated phosphorylation of mDia3 perturbs cell migration and cell spreading. Thus, in chapter 3, I elucidate a novel function for Aurora B kinase besides the well-characterized Aurora B function in microtubule-based processes. Importantly, this study can potentially help elucidate the contributions of the Aurora B-specific phospho-residues for the actin assembly function of the other diaphanous formin members, mDia1 and mDia2.

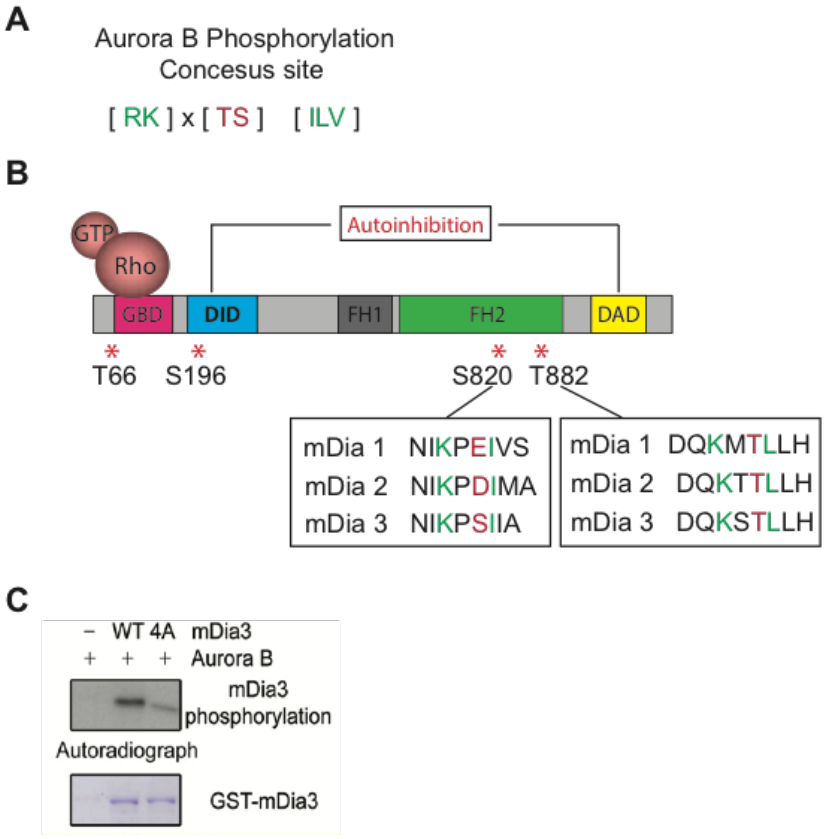

Figure 1.4 mDia3 is phosphorylated by Aurora B. (**A**) Representation of the preferred consensus sequence for Aurora B-mediated phosphorylation. (**B**) Schematic representation of the domains found in the protein sequence of the diaphanous formin mDia3. The DID and DAD domains are known to mediate the autoinhibition of mDia3, which can be relieved by the Rho family of small GTPases binding at the GBD domain. There are four phosphorylatable sites of Aurora B, including two in the FH2 domain. T882 is conserved in mDia1 and mDia2, while the other are phosphomimetic residues. (**C**) Autoradiograph of a SDS-PAGE gel of purified recombinant full-length wild-type and the nonphosphorylatable 4A-mDia3 adapted from *Cheng et al., 2011* confirming that mDia3 is a phosphorylated by Aurora B.

CHAPTER 2: CENP-E regulates Aurora B kinase activity at the kinetochore

Introduction

One of the most important issues in cell biology and cancer research is to understand how chromosomes are segregated equally during cell duplication. Errors in this process may cause aneuploidy, which results in severe developmental defects and is thought to contribute to the malignant progression of tumors (Hartwell and Kastan, 1994; Weaver and Cleveland, 2006). Accurate chromosome segregation requires proper interactions between chromosomes and microtubules of the mitotic spindle apparatus (Cleveland et al., 2003; Guo et al., 2013). The kinetochore, the proteinaceous complex assembled at the centromere region of each mitotic chromosome, serves as the microtubule attachment site and powers chromosome movement along the mitotic spindle. Because abnormal chromosome segregation has such severe consequences, mammalian cells have evolved elaborate mechanisms to oversee this process, such as the mitotic checkpoint, to ensure that kinetochores properly attach to microtubules.

To ensure accurate chromosome segregation, cells must stabilize proper bi-oriented attachments (one sister kinetochore captures microtubules from one spindle pole and the other one captures microtubule from the opposite pole), and resolve aberrant attachments, such as syntelic attachments (both sister kinetochores bind to microtubules from the same pole). Current studies have shown that Aurora B kinase is a key component involved in the attachment error correction process (Lampson and Cheeseman, 2011; Walczak and Heald, 2008). The "spatial separation" model (Lampson and Cheeseman, 2011), suggests that tension exerted between sister kinetochores (inter-kinetochore stretch) with correct stable attachments results in a spatial separation of the inner centromere-associated Aurora B from its substrates that are localized at the outer kinetochore. This

attachment configuration minimizes Aurora B-mediated phosphorylation of the core microtubule-binding proteins, e.g. Ndc80 complex, which would persist at kinetochores with incorrect attachments. This prevailing model relies on the distance between the inner-centromere-localized Aurora B kinase and outer-kinetochore-localized phosphatases as being critical for the balance of phosphorylation/dephosphorylation. However, evidence suggests that inner centromere-localized Aurora B is not required to resolve improper attachments. In the budding yeast, *Saccharomyces cerevisiae,* for instance, the centromere targeting of Aurora B is not necessary for Aurora B function as proposed in the "spatial separation" model (Campbell and Desai, 2013). In addition, in mammalian cells, there is a kinetochore-localized pool of Aurora B (Deluca et al., 2011), which has not been investigated in the context of the proposed "spatial separation" model.

In addition to inter-kinetochore stretch, studies have also emphasized that changes in kinetochore stretch (intra-kinetochore stretch) as a result of microtubule attachment, is critical to regulating the balance of phosphorylation/dephosphorylation at the kinetochore (Mascera and Salmon, 2009; Uchida et al., 2009; Suzuki et al., 2014; Drpic et al., 2015). However, recent efforts have found that the generation of stable kinetochore-microtubule attachments in the absence of kinetochore stretch can silence the mitotic checkpoint (Etemad et al., 2015; Tauchman et al., 2015). Furthermore, another study has shown that intra-kinetochore stretch is dispensable, but rather the targeting of the outer kinetochore component, Mad2 to unattached kinetochores alone regulates mitotic progression in mammalian cells (Magidson et al., 2016). These data indicate that the role of individual kinetochore-associated components, rather than changes in inter- and/or intra-kinetochore stretch should be analyzed.

As a kinetochore-associated and a plus-end directed motor, CENP-E has been proposed to power chromosome movement along the microtubule of the mitotic spindle (Kapoor et al., 2006),

and/or to maintain a mechanical link between kinetochores and the plus-end tip of a dynamic microtubule (Lombillo et al., 1995; Gudimchuk et al., 2013). Inhibition or removal of CENP-E from cells or mutational analysis in mice leads to an obvious metaphase plate with only a few unaligned chromosomes (Yao et al., 1997; Martin-Luesma et al., 2002; McEwen et al., 2001; Putkey et al., 2002). These data suggest that CENP-E plays a critical role in ensuring cells segregate their chromosomes accurately.

Structural studies of CENP-E have revealed that unlike conventional kinesin motors, which have a short coiled-coil domain either rigidly extended or folded through hinge segments in the middle, CENP-E has a discontinuous coiled-coil domain that is approximately 230 nm long. This unique coiled-coil enables CENP-E to rearrange into different conformations *in vitro* (Kim et al., 2008). In this chapter, we elucidate the role of this unique coiled-coil in mediating the kinetochore function of CENP-E. We found that kinetochore-associated CENP-E undergoes a conformational change that is responsive to kinetochore bi-orientation. Furthermore, here we show that the flexibility of the coiled-coil domain of CENP-E is required to regulate Aurora B-mediated phosphorylation of the Ndc80 complex to ensure that proper kinetochore-microtubule attachments are stabilized.

Materials and Methods

Tissue Culture, Transfection, and Drug Treatment

T98G and HeLa cells were cultured in DMEM supplemented with 10% Fetal Bovine Serum at 37°C in 5% CO2. Co-transfections of CENP-E siRNA (5' - AGAUAAGGGAACAGGAAAUUU - 3') and GFP-tagged, double-tagged mCherry and EmeraldGFP CENP-E or the Aurora B phosphorylation FRET biosensors transgenes into T98G cells were performed using DharmaFECT

Duo Transfection Reagent (GE Dharmacon) according to the manufacturer's instruction. 48 hrs after transfection, cells were synchronized with 100 μM monastrol (Sigma-Aldrich) for 4 hrs, then either fixed or released into 10 μM MG132 for 20-30 min. Nocodazole (Sigma-Aldrich) treatment was performed at 3.3 μM for 4 hrs. For live-cell imaging experiments, HeLa cells stably expressing YFP-H2B were treated 10 μM MG132 (Sigma-Aldrich) for 30 min prior to imaging then treated with 10 μM MG132 with or without 50 nM GSK923295 (Selleckchem) and/or 2 μM ZM447434 (Tocris Bioscience) upon imaging or fixed after 30 min. Taxol (Tocris Bioscience) treatment was performed at 1 μM for 5 min.

Antibody Labelling

Phospho-Hec1 (pS55-Hec1) and ACA antibodies were purchased from GeneTex and Antibodies Incorporated, respectively. CENP-E and Mad1 antibodies from Santa Cruz. All other antibodies were purchased from Abcam. Cells were grown on poly-l-lysine–coated No. 1.5 coverslips and fixed with -20°C Methanol for 10 min. Prior to phospho-staining of pS55-Hec1, cells were pre-extracted with 0.1% Triton X-100 (Fisher Scientific) in microtubule stabilizing buffer, MTSB (100 mM PIPES, 1 mM EGTA, 1 mM $MgSO_4$, and 30% of glycerol) for 30-90 sec and immediately fixed with -20°C Methanol for 10 min. Fixed cells were blocked in PBS containing 0.1% Triton X-100 and 5% Bovine Serum Albumin (Sigma-Aldrich) for 1 hr at room temperature or overnight at 4°C. Coverslips were subjected to primary antibodies diluted in blocking buffer for 1 hr at room temperature or overnight at 4°C and then secondary antibodies conjugated to Alexa 488 (Invitrogen), Rhodamine or Cy5 (Jackson Immuno-Research Laboratories, Inc.) were incubated for 45 min at room temperature followed by DAPI counterstaining. Coverslips were mounted with an antifade reagent (SouthernBiotech).

Image Acquisitions

Image acquisitions were performed at room temperature using an inverted microscope (IX81; Olympus) with a 60X, NA 1.42 Plan Apochromat oil immersion objective lens (Olympus), a monochrome charge-coupled device camera (Sensicam QE; Cooke Corporation), and the SlideBook imaging software (Intelligent Imaging Innovations, 3i) was used to acquire the 500 nm Z-sections or 200 nm Z-sections for the K-SHREC analysis of CENP-E. To quantify fluorescence intensities, all images were collected on the same day using identical exposure times. For live-cell imaging experiments, HeLa cells were plated onto 4 compartment glass-bottom dishes No. 1.5 (Greiner Bio-One) and imaged at 37°C in 5% CO2. Images were acquired using a 40X, NA 0.6 dry objective lens using the SlideBook imaging software. Cells expressing the Aurora B phosphorylation biosensor were imaged lived using a Nikon Ti Eclipse inverted microscope with a 100x NA 1.49 oil immersion objective lens and the NIS-Elements (Nikon) software.

Data and Statistical Analysis

Quantitative analysis of the raw 16-bitt tiff stacks or maximum Z-projected fluorescence images was performed using ImageJ (NIH). Kinetochore fluorescence intensities were quantified as a modified version of Hoffman et al., 2001 by drawing a small 6 X 6-pixel and a large 12 X 12-pixel circular regions centered over each kinetochore to obtain the total integrated fluorescence of each region. The final total integrated fluorescence was obtained by subtracting the total integrated fluorescence of the large circular region from the smaller total integrated fluorescence. This local background subtraction method controls for background fluorescence heterogeneity. The fluorescence intensities were normalized to the total integrated fluorescence of ACA and then normalized to the total integrated fluorescence obtain from nocodazole-treated cells. The centroid

positions of kinetochores and centrosomes were obtained by drawing a circular mask over the ACA and γ-tubulin fluorescence signals, respectively. For the K-SHREC analysis, custom MATLAB script was coded to automatically read in and process the cropped uncompressed 16-bitt image stacks (Liu and Mao, 2016; Wan et al., 2009). The X, Y, and Z coordinates of mCherry-CENP-E-EmGFP constructs and CENP-A centroids were determined by a nonlinear curve fitting function of segmented kinetochore volume with 3D Gaussian fitting in MATLAB (lsqcurvefit, R2016a; MathWorks). The X, Y, and Z coordinates were then corrected for chromatic aberration using 100 nm multi-coated fluorescent microspheres (Fisher Scientific). The inter-kinetochore distance (except those in K-SHREC analysis) was measured as described in Waters et al., 1998 by using line-scans of CENP-A immunofluorescence signal of sister kinetochore pairs in the same focal plane to obtain the distance between the brightest pixels of the kinetochore pairs. Representative images were subjected to no-neighbor deconvolution using Slidebook imaging software and maximum Z-projection of selected stacks and subsequently scaled in ImageJ (NIH). Statistical analyses were performed using GraphPad Prism (GraphPad, version 7a) using unpaired, two-tailed t-tests to compare the means between two groups or a One-way ANOVA was used to compare the means of 3 or more groups. Histogram analysis and Hartigans' dip test (Hartigan and Hartigan, 1985) statistical analysis of multimodality was performed in R (version 3.3.2). Plots were prepared in GraphPad Prism, Matlab or in R.

Results

The long and flexible coiled-coil domain of CENP-E is essential for the kinetochore function of CENP-E

To test the role of the long and flexible coiled-coil, we designed several CENP-E constructs tagged with GFP at the carboxyl-termini (**Figure 2.1**) including a Full-length construct as a control and a Tail construct that lacks the motor domain and parts of the coiled-coil. A Mini construct was

generated by combining the motor, Tail and a shorter segment of the coiled-coil domain of CENP-E. Furthermore, a part of the flexible coiled-coil of CENP-E was replaced with a more rigid coiled-coil domain from a Kinesin-1 family member, Kif5B, to construct a Chimera.

Cells were co-transfected with the CENP-E constructs along with the siRNA that binds the 3' untranslated region of CENP-E mRNA to target CENP-E for degradation. Cells were synchronized using monastrol and released into MG132 and metaphase chromosome alignment was assessed by indirect immunofluorescence. All CENP-E constructs associated with kinetochores at a similar level to unattached, aligned and unaligned kinetochores (**Figure 2.1, D and E**) phenocopying the kinetochore localization patterns of endogenous CENP-E (**Figure 2.1, B and C**).

Consistent with what has been shown before (Yao et al., 2000; McEwen et al., 2001), the majority of cells (77.7%) depleted of CENP-E showed an obvious metaphase plate with a few polar chromosomes (**Figure 2.2A**), whereas expressing the Full-length rescued the chromosome alignment defect (**Figure 2.2A**). By contrast, expressing the Mini or the Chimera caused metaphase chromosome misalignment, which was similar to cells expressing the tail mutant (**Figure 2.2A**). More detailed analysis on the number of polar chromosomes per cell showed that most of the CENP-E-depleted cells (~80%) had only 1-4 polar chromosomes whereas, expressing the Tail, Mini, or the Chimera mutants led to a ~20-40% increase in cells with more than 4 polar chromosomes (**Figure 2.2C**). This increase in the number of misaligned chromosomes was similar to cells treated with GSK923295, an ATPase antagonist of CENP-E that inhibits the motor motility of CENP-E (Wood et al., 2010) (**Figure 2.2, A and C**). These results suggest that expressing a motorless, a shorter and/or less flexible CENP-E or chemical inhibition of CENP-E motility not

only cannot rescue the chromosome misalignment defects caused by CENP-E depletion, but also exacerbates the misalignment phenotype characteristic of CENP-E depleted cells.

It has been shown that the coiled-coil of CENP-E regulates the motor function of CENP-E *in vitro* (Vitre et al., 2014). To directly test whether the Mini or the Chimera have a defective motility in cells, we measured chromosome ejection from mono-poles upon inhibition of Kinesin-5 (Kapoor et al., 2000). We found that depletion of CENP-E or inhibition of CENP-E motility with GSK923295 results in reduced distances between kinetochores and centrosomes (**Figure 2.2, B and D**), consistent with previous findings (Barisic et al., 2014). Furthermore, only the Full-length, but not the Mini or the Chimera was able to completely rescue the chromosome ejection defect caused by CENP-E depletion (**Figure 2.2, B and D**). This result supports that both the length and the flexibility of the coiled-coil are required for the motility of CENP-E.

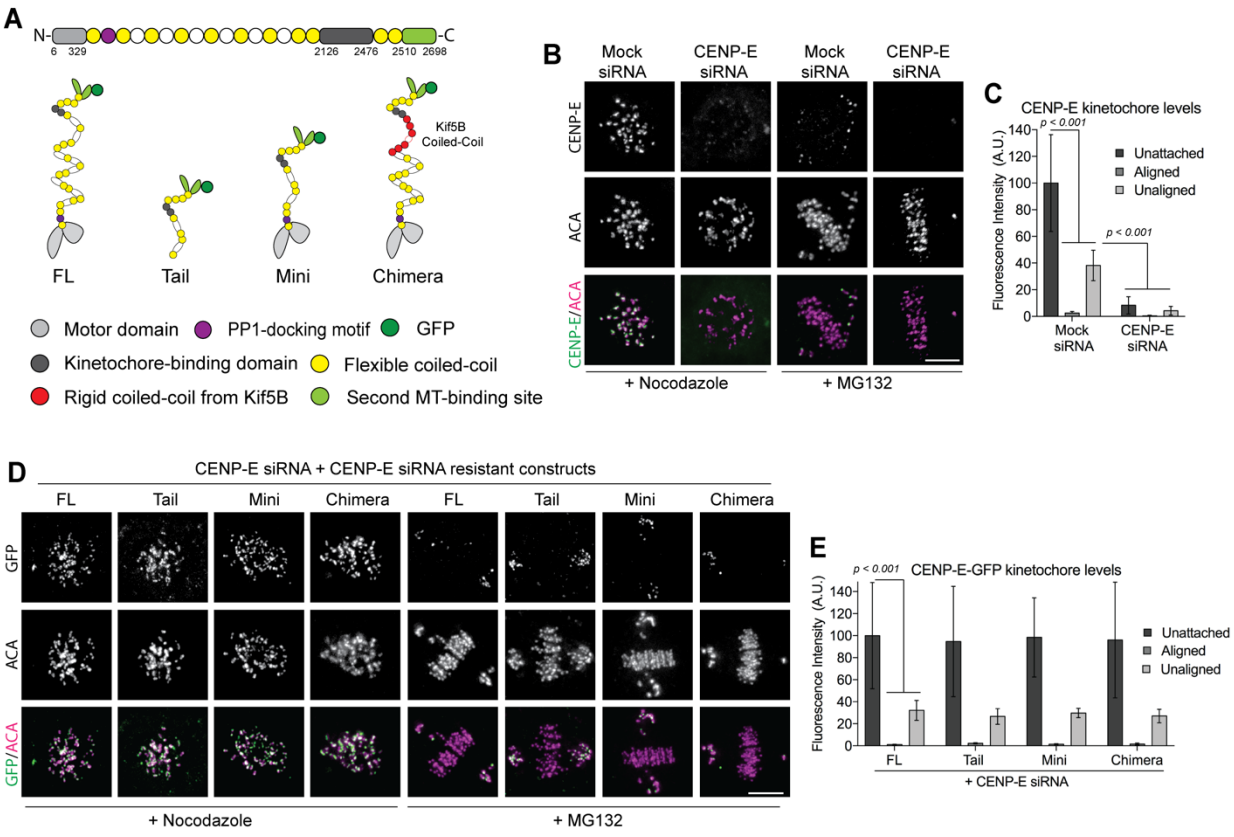

Figure 2.1. Perturbation of the coiled-coil domain does not affect the kinetochore localization of CENP-E. (**A**) The illustration depicts the different domains of CENP-E. All constructs were tagged with GFP at the carboxyl-termini. (**B**) Immunostaining analysis showing the knockdown of CENP-E by siRNA targeting the 3'UTR of CENP-E in nocodazole-treated and MG132-treated cells. T98G cells were stained with antibodies to CENP-E and ACA, DNA was stained using DAPI. Scale bar, 5 µm. (**C**) Quantification of CENP-E levels in nocodazole-treated (unattached kinetochores) and MG132-treated pseudo-metaphase cells with fully aligned kinetochores and unaligned kinetochores. Fluorescence intensity was normalized to ACA. Mean ± SD are shown of three independent experiments, unattached: Mock siRNA: n = 215, CENP-E siRNA: n = 226; aligned kinetochores: Mock siRNA: n = 249, CENP-E siRNA: n = 233; unaligned kinetochores Mock siRNA: n = 119, CENP-E siRNA: n = 199. (**D**) Immunostaining analysis showing exogenously expressed CENP-E constructs in nocodazole-treated and MG132-treated cells. T98G cells were stained with antibodies to GFP and ACA. Scale bar, 5 µm. (**E**) Quantification of CENP-E-GFP levels in nocodazole-treated (unattached kinetochores) and MG132-treated pseudo-metaphase cells with fully aligned kinetochores and unaligned kinetochores. Fluorescence intensity was normalized to ACA. Mean ± SD are shown of three independent experiments, unattached kinetochores: FL: n = 219, Tail: n = 203, Mini: n = 226, Chimera: n = 230; aligned kinetochores: FL: n = 193, Tail: n = 207, Mini: n = 197, Chimera: n = 171; unaligned kinetochores: FL: n = 100, Tail: n = 134, Mini: n = 118, Chimera: n = 91.

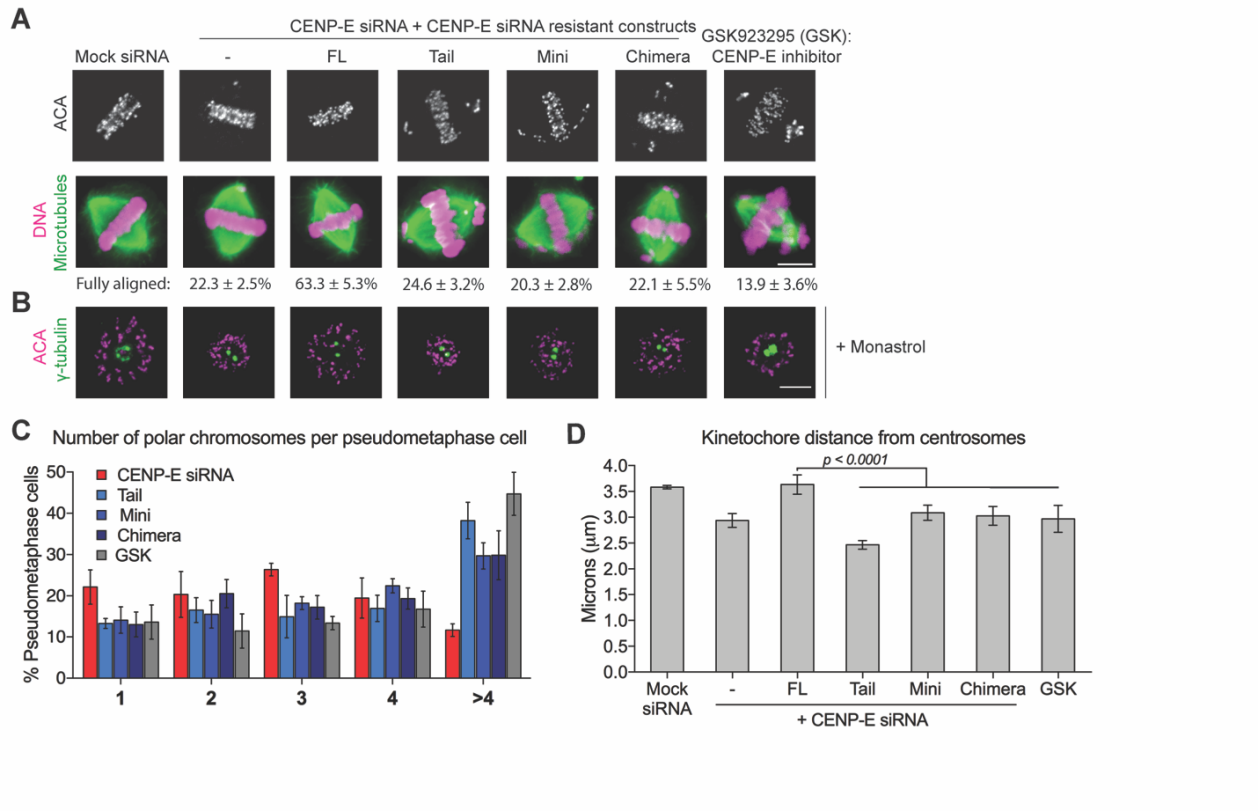

Figure 2.2. The long and highly flexible coiled-coil domain of CENP-E is essential for its kinetochore function. (**A**) CENP-E mutants with a shorter or more rigid coiled coil cannot rescue chromosome alignment defects caused by depletion of endogenous CENP-E. T98G cells were fixed and then stained with an anti-centromere antibody (ACA), microtubules (tubulin), and DNA (DAPI). Mean ± SD percentages of mitotic cells with fully aligned chromosomes of three independent experiments are indicated, Mock siRNA: n = 644, CENP-E siRNA: n = 680, FL: n = 699, Tail: n = 621, Mini: n = 458, Chimera n = 614, CENP-E inhibitor, GSK923295 (GSK) n = 686 cells quantified. Scale bar, 5 μm. (**B**) Immunofluorescence images of monastrol-treated cells expressing CENP-E constructs in CENP-E depleted cells or treated with GSK. Centrosomes and kinetochores were stained using a γ-tubulin and ACA antibodies, respectively. Scale bar, 5 μm. (**C**) Histogram showing the number of polar chromosomes per metaphase cell in cells co-transfected with CENP-E siRNA and CENP-E constructs as indicated. Mean ± SD are shown of three independent experiments, CENP-E siRNA: n = 272, Tail: n = 376, Mini: n = 186, Chimera n = 324, GSK n = 404 pseudo-metaphase cells quantified. (**D**) Quantification of the distance of kinetochores from centrosomes. Mean ± SD are shown of three independent experiments, n = 30 cells per group were quantified.

The coiled-coil domain of CENP-E mediates the structural behavior of kinetochore-localized CENP-E

To investigate whether the coiled-coil domain of CENP-E regulates the structural flexibility of CENP-E at the kinetochore with sub-pixel accuracy, we sub-cloned the Full-length-CENP-E, Mini, and the Chimera constructs into a double-tagged, mCherry and EmeraldGFP vector (**Figure 2.3A**). To measure the intra-molecular distance of the kinetochore-associated CENP-E below the diffraction limit of the light microscope, we used Single Molecule High-Resolution Co-localization (SHREC) microscopy (Churchman et al., 2005). This super-resolution technique allowed us to obtain the 3-dimensional centroid position of the different ends of kinetochore-associated CENP-E molecules based on the 3D-Gaussian distribution of the fluorescence mCherry and EmeraldGFP signals (**Figure 2.3, B and C**).

We first validated our SHREC imaging method by measuring the distance of the outer-kinetochore component, Hec1 from the inner kinetochore marker, YFP-CENP-A (**Figure 2.4A**). After kinetochore tilt correction using the 3D K-SHREC analysis, we found a similar length of Hec1 relative to YFP-CENP-A as previously measured in *Wan et al., 2009* (**Figure 2.4B**). Nonetheless, because the "delta method" does not allow us to measure the intra-molecular distance of CENP-E directly, we used the "raw distance method" as previously described in *Magidson et al., 2016* (**Figure 2.4C**). The "raw distance method" was also validated by measuring the distance between Hec1 and YFP-CENP-A after chromatic shift correction as previously measured in *Magidson et al., 2016* (**Figure 2.4C**). Using this method, we also found a similar distance of Hec1 relative to YFP-CENP-A. Therefore, we proceeded to with this method application for the CENP-E distance analysis.

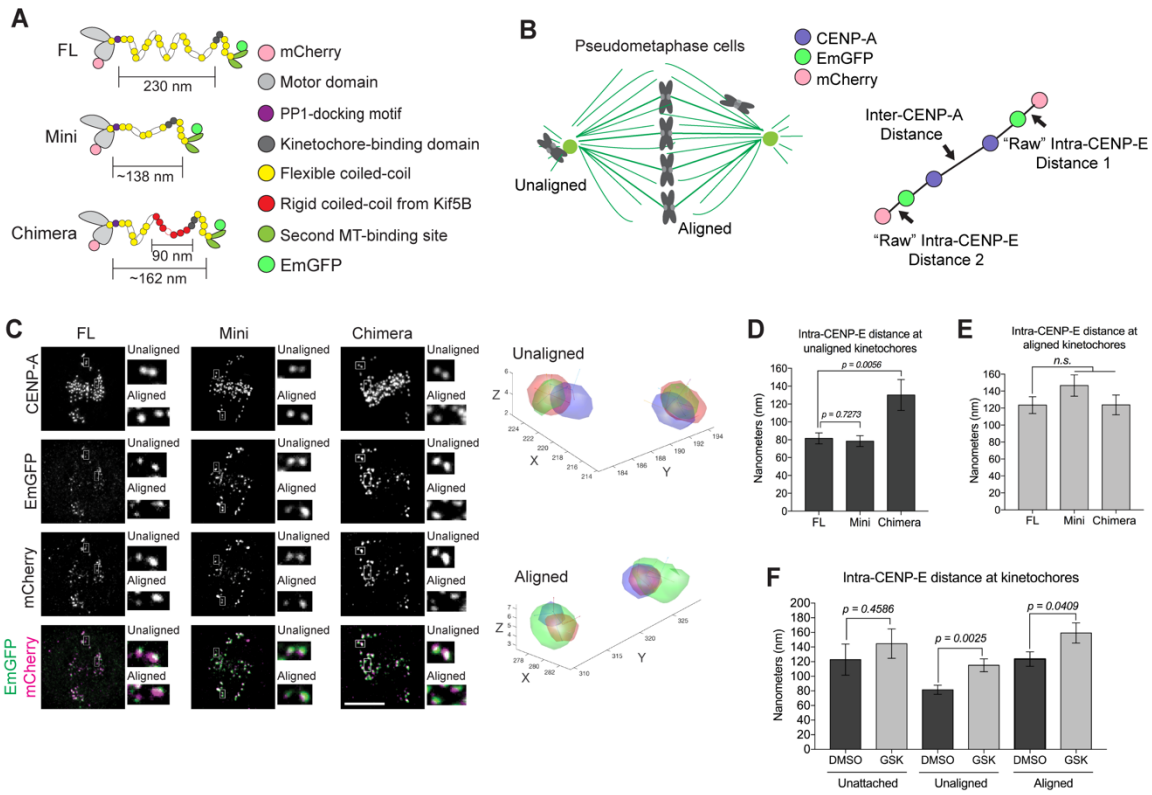

Figure 2.3. The length and flexibility of the coiled-coil domain of CENP-E mediate the folding conformation of CENP-E at the kinetochore. (**A**) Illustration of the transgenes of CENP-E used for CENP-E SHREC analysis. (**B**) Illustration of pseudo-metaphase cells depicting unaligned and aligned kinetochores used to analyze the inter-kinetochore distance of CENP-A and intra-kinetochore distance of CENP-E. (**C**) Immunofluorescence images of T98G cells expressing the CENP-E constructs (FL, Mini, and Chimera) in pseudo-metaphase cells. T98G cells were stained with antibodies to mCherry, EmGFP and kinetochores were stained using a CENP-A antibody. Scale bar, 5 μm. Graphs show representative isosurface plots of all three channels' intensity data (blue: CENP-A, red: mCherry(CENP-E), green: EmGFP(CENP-E) at unaligned and aligned kinetochores. Axes are shown in pixel (one pixel = 67.1875 nm). (**D**) Quantification of the intra-molecular distance of cells expressing FL, Mini, Chimera constructs at unaligned kinetochores. Mean ± SEM of three independent experiment are shown, FL n = 72, Mini n = 66, Chimera n = 66. (**E**) Quantification of the intra-molecular distance of cells expressing FL, Mini, Chimera constructs at aligned kinetochores. Mean ± SEM of three independent experiment are shown, FL n = 66, Mini n = 60, Chimera n = 66. (**F**) Bar graph showing the intra-molecular distance at unattached, unaligned and aligned kinetochores of cells treated with DMSO or GSK923295 (GSK). Mean ± SEM of three independent experiment are shown, unattached kinetochores: DMSO: n = 30, GSK: n = 32, unaligned kinetochores: DMSO: n = 72, GSK: n = 78, aligned kinetochores: DMSO: n = 66, GSK: n = 72.

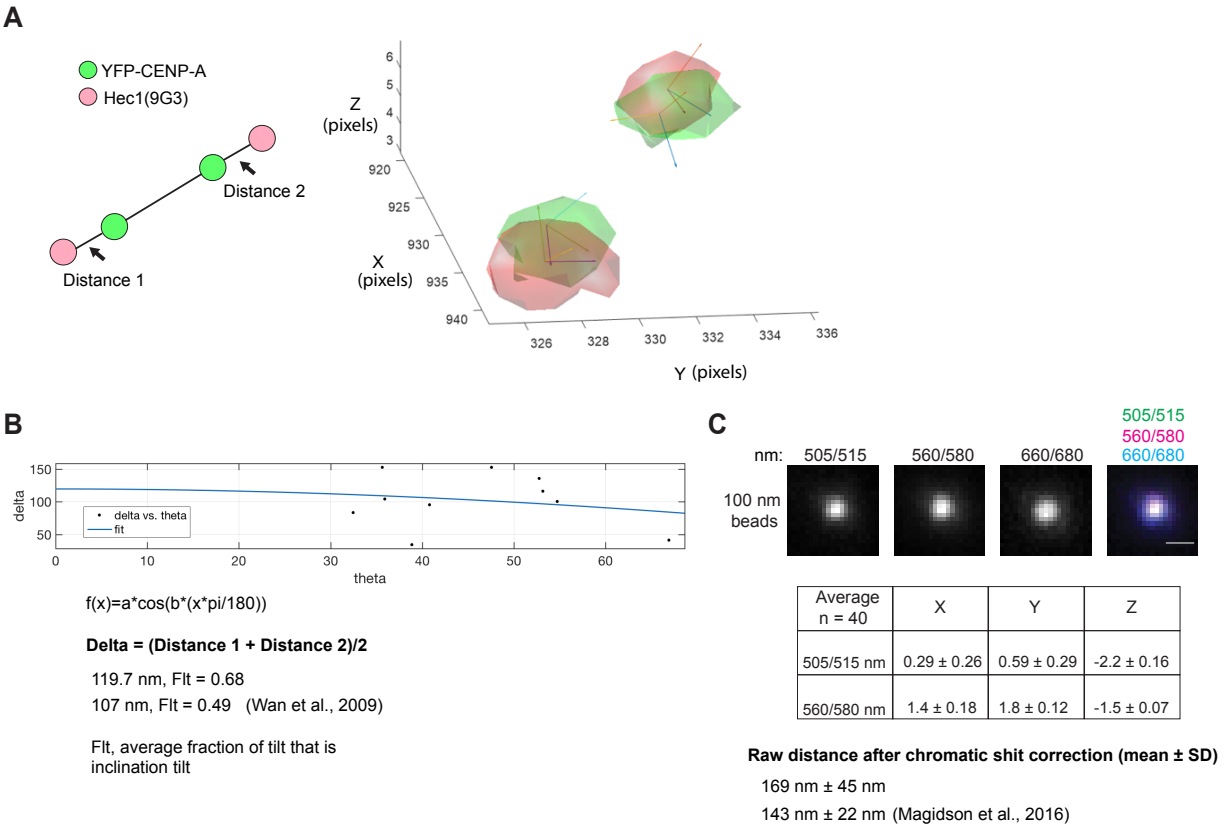

Figure 2.4. Validation of the 3-dimensional SHREC method. (**A**) Graphs showing representative isosurface plots of Hec1 (red) and YFP-CENP-A (green) in 3D space. Axes are shown in pixels (one pixel = 67.1875 nm). (**B**) Delta measurements of Hec1 relative to YFP-CENP-A after tilt correction as previously measured in *Wan et al., 2009*. (**C**) 100-nm multicoated beads fluorescence images used for chromatic shift correction as described in *Magidson et al., 2016*. Below it shows the "raw" distance of Hec1 relative to YFP-CENP-A. Scale Bar, 5 µm

To determine whether microtubule capture by kinetochores and subsequent kinetochore bi-orientation affects the structural behaviour of CENP-E, we analyzed pseudo-metaphase cells that had an obvious metaphase plate with aligned kinetochores and a few unaligned kinetochores near the centrosomes (**Figure 2.3, B and C**). We assessed the attachment status of the aligned and unaligned kinetochores using indirect immunofluorescence analysis of Mad1, a microtubule attachment marker (Waters et al., 1998) (**Figure 2.5**). Cells expressing the Full-length, the Mini or the Chimera showed little to no fluorescence signal of Mad1 at aligned kinetochores, indicative of the presence of kinetochore-microtubule attachments (**Figure 2.5, A and B**). Prior to end-on microtubule attachment, kinetochores initially attach to the lateral surface of a microtubule via the kinetochore-associated motor minus-end-directed dynein, which transport kinetochores towards the microtubule-dense environment of the spindle poles (Yang et al., 2007; Magidson et al., 2011). The unaligned kinetochores showed an increase in Mad1 fluorescence signal relative to the aligned kinetochores, but less than that of nocodazole-treated cells, which lack microtubule attachments (**Figure 2.5, A and B**). Bi-orientation was further confirmed by measuring the distance between the kinetochore marker, CENP-A (inter-CENP-A) in sister kinetochore pairs (**Figure 2.5C**). The inter-kinetochore stretch increased at aligned kinetochores, confirming bi-orientation, whereas at unaligned kinetochores this distance was approximately halved as previously reported (Liu et al., 2009). Taken together, we conclude that the aligned kinetochores represent pairs of bi-oriented end-on attached kinetochores, whereas the unaligned kinetochores constitute primarily of laterally attached kinetochores, with some unattached kinetochores.

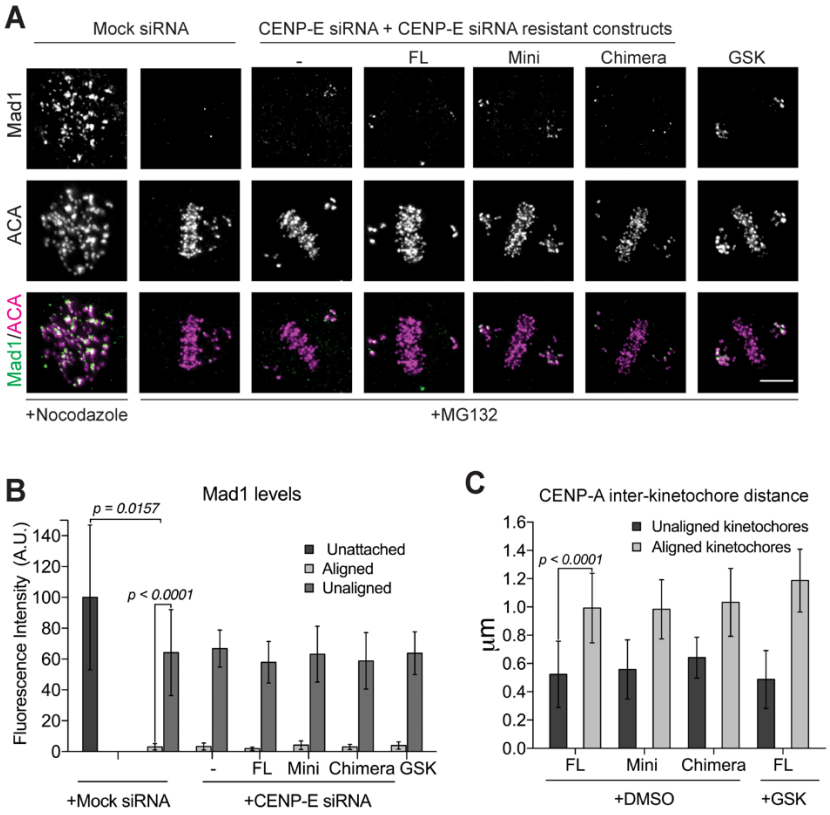

Figure 2.5. Mad1 immunofluorescence levels are significantly reduced at aligned kinetochores. (**A**) Immunofluorescence images shows Mad1 levels are reduced at the metaphase plate compared to nocodazole-treated cells. T98G cells were stained with antibodies to Mad1 and kinetochores were stained with ACA. Scale bar, 5 µm. (**B**) Quantification of Mad1 fluorescence intensity normalized to ACA kinetochore signal at unattached (nocodazole-treated), aligned and unaligned kinetochores (MG132-treated) shows Mad1 levels are reduced at unaligned kinetochores compared to unattached kinetochores. Mean ± SD of three independent experiments are shown, Mock siRNA: Nocodazole n = 214, MG132 aligned: n = 200, MG132 unaligned: n = 197; CENP-E siRNA aligned: n = 200, CENP-E siRNA unaligned: n = 219; FL aligned: n = 200, FL unaligned: n = 214; Mini aligned: n = 140, Mini unaligned: n = 238; Chimera aligned: n = 200, Chimera unaligned: n = 182; GSK aligned: n = 200, GSK unaligned: n = 239. (**C**) Quantification of CENP-A of the inter-kinetochore distance of CENP-A at bi-oriented kinetochores and unaligned kinetochores. Mean ± SD of three independent experiments are shown, unaligned DMSO: FL: n = 36, Mini: n = 33, Chimera: n = 32; aligned DMSO: FL: n = 33, Mini: n = 30, Chimera n = 33; unaligned GSK: FL: n = 39; aligned GSK: FL: n = 36.

To establish the "resting" distance of the intra-molecular distance of CENP-E, we first analyzed kinetochores that lack microtubule attachments. To produce unattached kinetochores, we treated cells with nocodazole to depolymerize the microtubules (**Figure 2.6, A and B**). Short treatment with nocodazole (15 min) depolymerized all of the microtubules, but prevented the kinetochore protein expansion that occurs after prolonged nocodazole treatment (Thrower et al., 1996) (**Figure 2.6B**). The distance between sister kinetochore pairs (inter-CENP-A) was measured at approximately 0.5 μm, as previously reported (Liu et al., 2009) and was not affected by expression of the Mini or the Chimera mutants compared to cells expressing the Full-length control (**Figure 2.6C**). The predicted length of a fully-extended CENP-E molecule was previously measured at approximately 230 nm by electron microscopy (Kim et al., 2008). At unattached kinetochores, however, the intra-molecular distance of the Full-length was halved of the predicted fully-extended length, averaging at 122.8 nm (**Figure 2.6D**). The intra-molecular distance of the Mini was found to have an average of 144.8 nm (**Figure 2.6D**). However, the coiled-coil domain truncation of the Mini mutant has a counter length of approximately 138 nm, which suggest that the Mini mutant has a fully-extended configuration at unattached kinetochores. Similarly, replacing the flexible coiled-coil domain with Kif5B's coiled-coil (Chimera) resulted in an almost fully-extended configuration (contour length is approximately 162 nm compared to the measured distance of approximately 120 nm) (**Figure 2.6D**). These data suggest that there is an intramolecular conformation of FL-CENP-E, at least on unattached kinetochores, such that the CENP-E intramolecular distances do not simply scale linearly with the constructs' contour lengths.

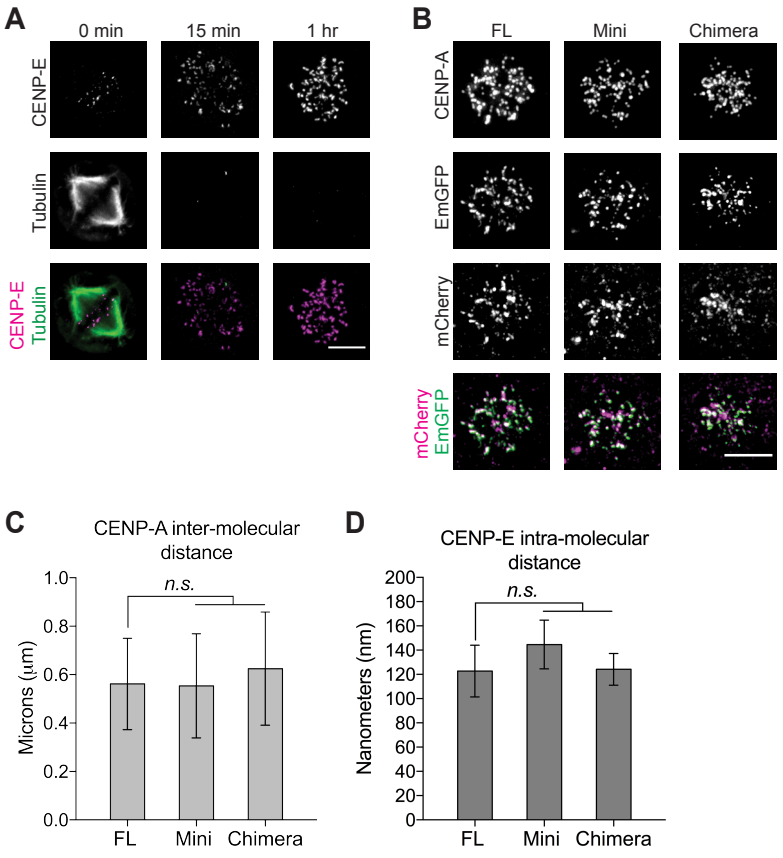

Figure 2.6. Perturbing the coiled-coil domain of CENP-E disrupts the folding conformation of CENP-E at unattached kinetochores (**A**) Immunofluorescence images of T98G cells treated nocodazole for 0 min, 15 min and 1 hr. Kinetochores were stained against CENP-E and microtubules were stained with a tubulin antibody. Scale bar, 5 µm**.** (**B**) Immunofluorescence images of T98G cells expressing FL, Mini and the Chimera CENP-E constructs treated with nocodazole for 15 min. Kinetochores were stained with a CENP-A antibody and the N-terminal mCherry and C-terminal EmGFP CENP-E tags were stained using mCherry and GFP antibodies, respectively. Scale bar, 5 µm. (**C**) Bar graph showing the distance from the CENP-A to CENP-A (inter-CENP-A) distance in cells expressing the FL, Mini and Chimera CENP-E constructs. Mean ± SEM of three independent experiments are shown, FL: n = 15, Mini: n = 15 Chimera n = 16 kinetochore pairs. (**D**) Bar graph showing the distance from the CENP-E N-terminal mCherry and CENP-E C-terminal EmGFP tags (intra-CENP-E) distance in cells expressing the FL, Mini and Chimera CENP-E constructs. Mean ± SEM of three independent experiments are shown, FL: n = 30, Mini: n = 30 Chimera n = 32 kinetochores.

Distance analysis of the Full-length at unaligned kinetochores showed a significant decrease in the intra-molecular distance of CNEP-E compared to unattached kinetochores (from 122.8 nm at unattached kinetochores to 81.5 nm at unaligned kinetochores) (**Figure 2.3D and Figure 2.6D**). Conversely, expressing the Chimera mutant remained in an extended configuration in all conditions analyzed, remaining at approximately 120 nm at unattached, unaligned and aligned kinetochores (**Figure 2.3, D and E and Figure 2.6D**). However, the Mini mutant showed a decrease in the intra-molecular distance that was similar to the Full-length control at unaligned kinetochores (**Figure 2.3D**). These results suggest that the Full-length undergoes a conformational change at unaligned kinetochores that is abolished when parts of the coiled-coil domain of CENP-E is replaced with a shorter and more rigid coiled-coil domain.

To test whether the motor motility of CENP-E plays a role in regulating the structural flexibility of CENP-E after bi-orientation, we treated cells with GSK923295 (**Figure 2.3F**). Motility inhibition of the Full-length-CENP-E construct resulted in a significant increase in the intra-molecular distance at both aligned and unaligned kinetochores, but not at kinetochores that lacked microtubule attachments. (**Figure 2.3F**). Therefore, the motor motility of CENP-E plays an essential role in regulating the structural flexibility of kinetochore-localized CENP-E prior and after bi-orientation.

Analysis of the intra-molecular distance of the Mini mutant showed a similar pattern at unaligned and aligned kinetochores compared to the Full-length control (**Figure 2.3, D and E**). This was unexpected given that the Mini-CENP-E mutant has a reduced coiled-coil contour length and a motor motility defect that is similar to the Chimera mutant (**Figure 2.2, C and E**). Therefore, we conducted a structural analysis of kinetochore-associated CENP-E by examining the angular distribution of CENP-E relative to the kinetochore axis (inter-CENP-A) in 3-dimensional space

(**Figure 2.7A**). Angular analysis of the Full-length-CENP-E at bi-oriented kinetochores revealed a two population cluster that followed a bi-modal Gaussian distribution with local maxima at approximately 14° and 68° (**Figure 2.7B**). However, we did not find this bi-modal Gaussian distribution in cells expressing the Mini mutant or in all other conditions analyzed (**Figure 2.8**). Density plotting of the angular distributions of cells treated with Taxol, which disrupt microtubule dynamics, affected the bi-modal Gaussian distribution of the Full-length causing a shift towards a local maximum of 72° (**Figure 2.7C**). Taken together, these data suggest CENP-E sustains a two-conformational state at bi-oriented kinetochores, which is regulated by the growing and shrinking ends of microtubules.

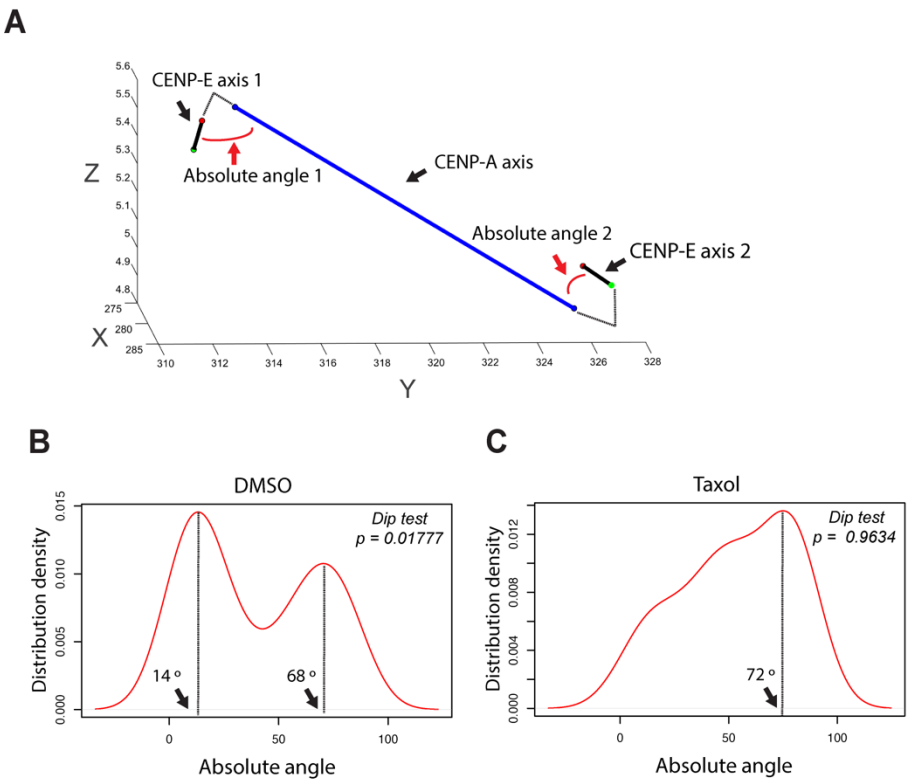

Figure 2.7. CENP-E displays a two-state conformation at bi-oriented kinetochore-microtubule attachments. (**A**) Representative plots of CENP-E axis and CENP-A axis in 3-dimensinoal space used to calculate the angular distribution of CENP-E along the kinetochore (CENP-A) axis. Axes are shown in pixel (pixel = 67.1875 nm). For the CENP-E axes, two termini are depicted in red (N-terminus) and green (C-terminus) respectively. (**B and C**) Density plots of the angular distribution of Full-CENP-E in T98G cells treated with DMSO (**B**) and Taxol (**C**) from three independent experiments, DMSO: n = 66, Taxol: n = 30. Hartigans' dip test statistical analysis, p-value less .05 indicates significant bimodality.

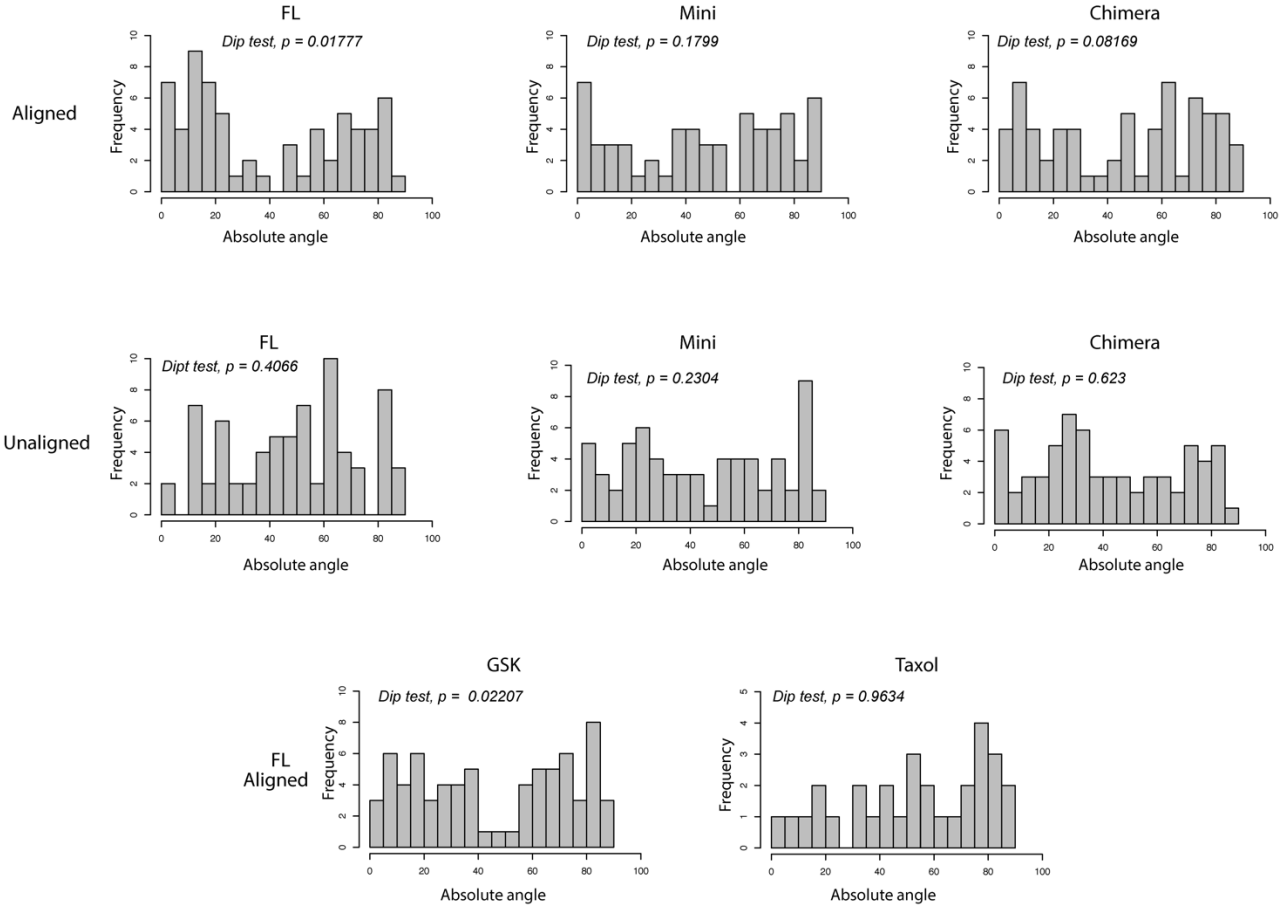

Figure 2.8. **Angular distribution analysis of Full-length-CENP-E show a two-state conformation at aligned kinetochores**. Histograms shows Full-length CENP-E at aligned kinetochores assumes a bi-modal Gaussian distribution not observed at unaligned or in cells expressing the Mini or the Chimera mutants. Histogram plots are from three independent experiments, Aligned: FL: n = 66, Mini: n = 60, Chimera: n = 66, Unaligned: FL: n = 72, Mini: n = 66, Chimera: n = 66, GSK: n = 72, Taxol: n=30. multimodality (Hartigans' dip test) statistical analysis. p-value less .05 indicates significant bimodality.

Chromosome misalignment caused by chemical inhibition of CENP-E can be rescued by chemical inhibition of Aurora B kinase

Inhibiting the motor motility of CENP-E during metaphase with GSK923295 results in a loss of metaphase chromosome alignment with chromosomes accumulated near the spindle poles (Gudimchuk et al., 2013). This finding suggests CENP-E continues to be an active motor at bi-oriented kinetochores to enhance their links with dynamic microtubule ends. Using live-cell imaging and indirect immunofluorescence analysis of fixed cells, we found that the loss of chromosome alignment in metaphase cells caused by GSK923295 treatment was prevented by the simultaneous treatment of ZM447439, an Aurora B kinase inhibitor (**Figure 2.9, A–C**). The addition of GSK923295, but not ZM447439, to metaphase cells with fully aligned chromosomes produced misaligned chromosomes that accumulated near the centrosomes. By contrast, metaphase alignment was not disrupted upon co-treatment with GSK923295 and ZM447439. These results indicate that instead of being a physical link between kinetochores and dynamic microtubules, CENP-E plays an important role in regulating the Aurora B pathway at end-on microtubule attachments.

To directly test whether inhibition of CENP-E affects Aurora B pathway, we examined the levels of phosphorylated Hec1 (pS55-Hec1), a component of the Ndc80 complex and a major Aurora B substrate at outer kinetochores (DeLuca et al., 2006). This revealed higher levels of kinetochore-associated pS55-Hec1 signals on chromosomes aligned at the metaphase plate upon addition of the CENP-E inhibitor, GSK923295 (**Figure 2.9, D and F**). By contrast, the kinetochore localization of Hec1 itself was not affected under this condition (**Figure 2.9G**). To test whether the increase of pS55-Hec1 signal was due to the loss of tension observed after treatment with GSK923295 (**Figure 2.9E**), we treated cells with taxol, a treatment that affects both the inter- and

intra- kinetochore stretch (Mascera and Salmon, 2009; Magidson et al., 2016). Short treatment with (5 min at 1 μM) taxol resulted in a decrease in tension as expected, but did not cause elevated levels of pS55-Hec1 relative to GSK923295 treatment. (**Figure 2.9, D, E, and F**). Collectively, these results suggest that in addition to transporting misaligned chromosome to the metaphase plate (Kapoor et al., 2006), a major functional role of CENP-E at aligned kinetochores is to reduce Aurora B phosphorylation, thus enhancing the microtubule binding activity of the Ndc80 complex to prevent metaphase chromosome misalignment.

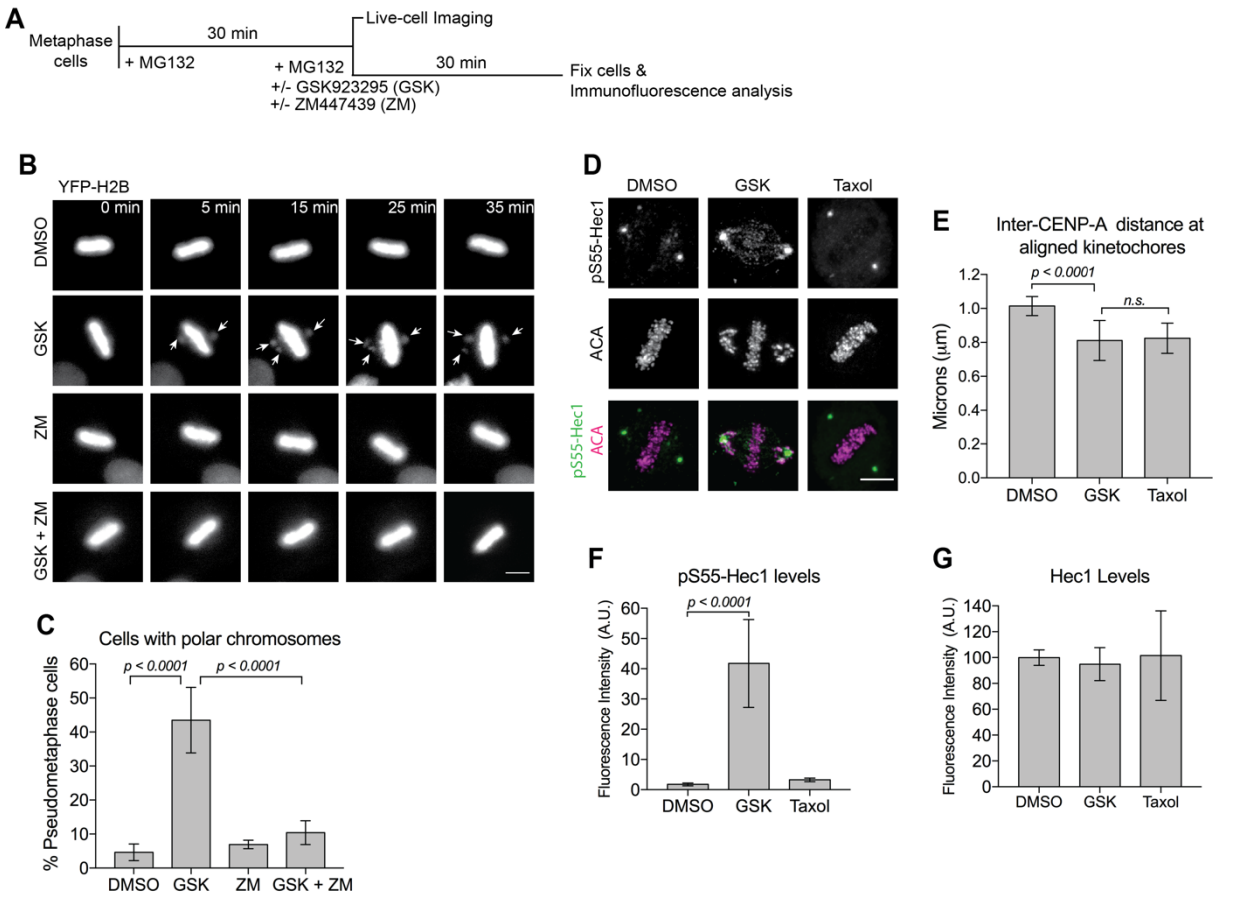

Figure 2.9 The motor motility of CENP-E is essential to maintain low levels of Aurora B-mediated phosphorylation on attached kinetochores at the metaphase plate. (**A**) Schematic representation of chemical inhibition treatments protocol. (**B**) Aurora B inhibition can rescue chromosome misalignment caused by inhibition of CENP-E motility. Representative still frames of live-cell imaging of YFP-H2B HeLa cells treated with or without a CENP-E inhibitor, GSK923295 (GSK), and an Aurora B inhibitor, ZM447439 (ZM). Arrows indicate misaligned chromosomes. Scale bar, 20 μm. (**C**) Quantification of T98G metaphase cells with fully aligned chromosomes or pseudo-metaphase cells with polar chromosomes after drug treatment. Mean ± SD are shown of three independent experiments, DMSO: n = 465, GSK: n = 487, ZM: n = 328, GSK + ZM: n = 332 cells quantified. (**D**) Inhibition of CENP-E motility caused an increase of Aurora B-mediated Hec1 phosphorylation. Immunofluorescence images showing Hec1 phosphorylation (pS55-Hec1) at aligned kinetochores. Kinetochores were stained using anti-centromere antigen (ACA). Scale bar, 5 μm. (E) Quantification of the relative fluorescence intensity of pS55-Hec1 levels at kinetochores normalized to ACA. Mean ± SD are shown of three independent experiments, DSMO: n = 223, GSK: n = 244, Taxol: n = 202 aligned kinetochores quantified. (F) Quantification of the relative fluorescence intensity of Hec1 at aligned kinetochores normalized to ACA fluorescence intensity. Mean ± SD are shown of three independent experiments, n > 200 aligned kinetochores per group were quantified. (G) Distance between sister kinetochore pairs (inter-kinetochore stretch) after drug treatment. Mean ± SD are shown of three independent experiments, DSMO: n = 215, GSK: n = 240, Taxol: n = 214 kinetochores pairs quantified.

The coiled-coil-mediated conformational change of CENP-E regulates Aurora B-mediated phosphorylation at bi-oriented kinetochores

CENP-E regulates the mitotic checkpoint through its interaction with BubR1 (Chan et al., 1999; Abrieu et al., 2000; Mao et al., 2003; Weaver et al., 2003; Mao et al., 2005; Guo et al., 2012). Phosphorylation of BubR1 at Threonine 608 depends on CENP-E and is sensitive to kinetochore-microtubule attachment. Expression of a non-phosphorylatable mutant of BubR1 or depletion of CENP-E reduces the levels of Aurora B-mediated phosphorylation of Hec1 (pS55-Hec1) at unattached kinetochores (Guo et al., 2012). We found that cells expressing the mini or the chimera, as well as the tail of CENP-E, rescued the levels of pS55-Hec1 as effective as the full-length at unattached kinetochores (**Figure 2.10, A and B**), suggesting the kinetochore-binding tail domain of CENP-E is sufficient to stimulate Aurora B-mediated phosphorylation of the outer kinetochore component, Hec1.

As inhibition of CENP-E by GSK923295 elevates Aurora B-mediated Ndc80 phosphorylation on attached kinetochores at the metaphase plate, we evaluated the levels of pS55-Hec1 in pseudo-metaphase with an obvious metaphase plate and few misaligned chromosomes near the poles in cells expressing the full-length or the mutants with an altered coiled-coil. This revealed that in contrast to the full-length, both the mini and chimera behaved like the tail increasing the levels of pS55-Hec1 on attached kinetochores at the metaphase plate and at unaligned kinetochores (**Figure 2.10, C and D**). Furthermore, in contrast to unattached kinetochores, inter-kinetochore stretch (tension) on attached kinetochores was only reduced slightly in cells expressing the mutants in comparison to those with full-length CENP-E (**Figure 2.10E**). However, this slight decrease was not significantly different from cells treated with GSK923295. These results suggest that the structural behavior of CENP-E at the aligned

kinetochores is essential to regulate Aurora B-mediated phosphorylation of Hec1, rather than a tension-dependent mechanism.

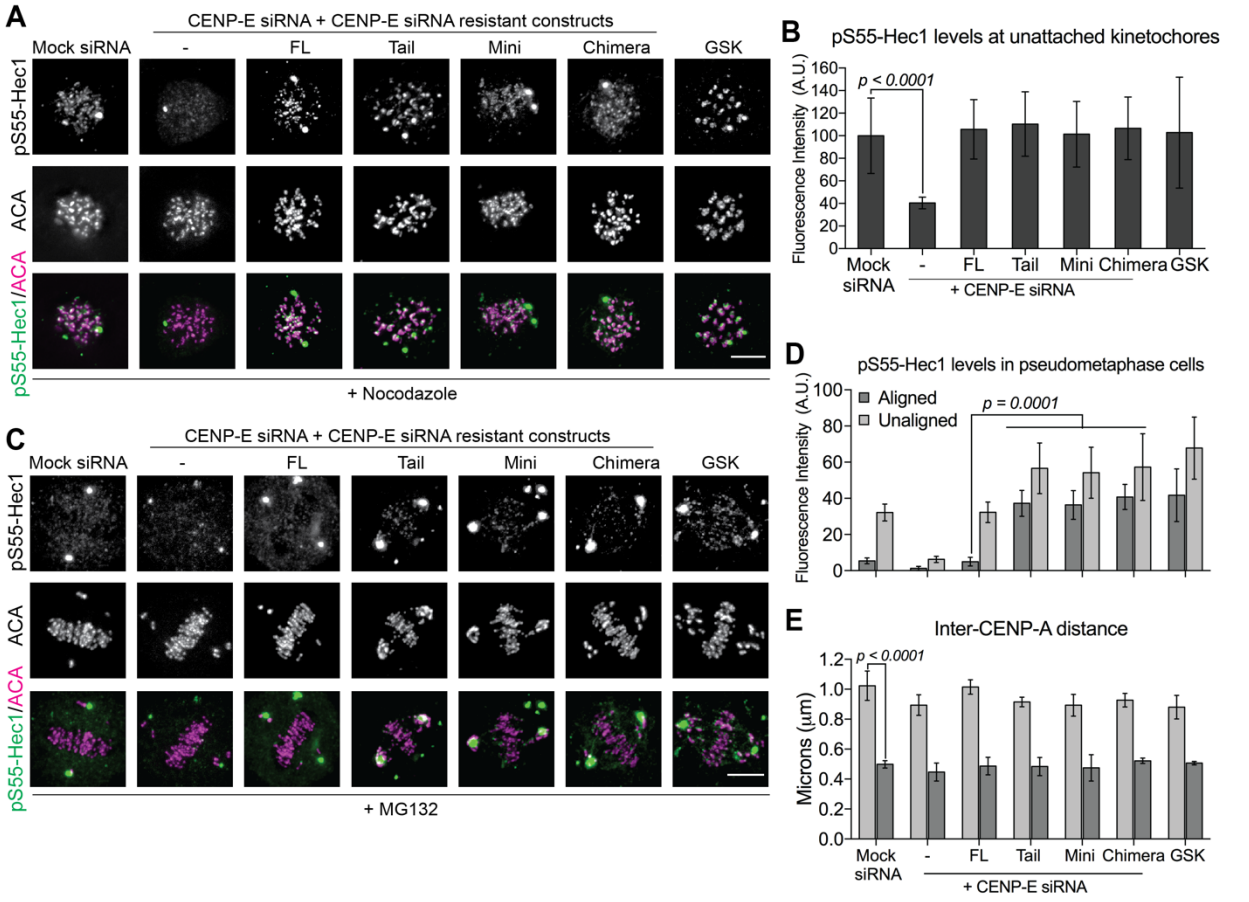

Figure 2.10 CENP-E-tail is sufficient to increase Aurora B-mediated Hec1 phosphorylation at unattached kinetochores, but deficient to sustain low levels of Aurora B phosphorylation on attached kinetochores. (**A**) Immunofluorescence analysis of nocodazole-treated T98G cells. Phosphorylation of Hec1 was assessed with a pS55-Hec1 antibody and kinetochores were stained with ACA. Scale bar, 5 μm. (**B**) Quantification of the relative fluorescence intensity of pS55-Hec1 at unattached kinetochores. Mean ± SD of three independent experiments are shown, Mock siRNA: n = 215, CENP-E siRNA: n = 222, FL: n = 219, Tail: n = 203, Mini: n = 226, Chimera: n = 230, GSK n = 212 kinetochores quantified. (**C**) Immunofluorescence analysis of MG132-treated pseudo-metaphase T98G cells. Phosphorylation of Hec1 was assessed with a pS55-Hec1 antibody and kinetochores were stained with ACA. Scale bar, 5 μm. (**D**) Quantification of the relative fluorescence intensity of pS55-Hec1 in aligned and unaligned kinetochores. Mean ± SD of three independent experiments are shown, aligned: Mock siRNA: n = 249, CENP-E siRNA: n = 233, FL: n = 193, Tail: n = 207, Mini: n = 197, Chimera: n = 171, GSK n = 215, unaligned: Mock siRNA: n = 119, CENP-E siRNA: n = 199, FL: n = 100, Tail: n = 134, Mini: n = 118, Chimera: n = 191, GSK n = 223 kinetochores quantified. (**E**) The distance between kinetochore pairs (inter-CENP-A stretch) of aligned and unaligned kinetochores. Mean ± SD are shown of three independent experiments, n = 200 kinetochores pairs per group quantified.

CENP-E regulates Aurora B-mediated phosphorylation in response to microtubule attachment

To test whether CENP-E regulates Aurora B-mediated phosphorylation pathway in response to microtubule attachment directly, we examined the levels of kinetochore-associated pS55-Hec1 in mono-polar spindles upon treatment with monastrol, an Eg5 inhibitor that prevents the separation of the spindle poles (Kapoor et al., 2000). The mono-polar spindle generates monotelic attachments, in which one sister kinetochore captures microtubules from spindle poles, whereas the other sister kinetochore remains unattached (**Figure 2.11, A and B**). Analysis of Aurora B phosphorylation using an established FRET probe (Liu et al., 2009) confirmed the asymmetric levels of phosphorylation on monotelic sister kinetochores in the mono-polar spindles (**Figure 2.11, C and D**), which was sensitive to the treatment of ZM447439, the inhibitor of Aurora B kinase.

The asymmetric attachment status of these monotelic kinetochores was further confirmed using indirect immunofluorescence of Mad1 (**Figure 2.11, E and F**). The distal kinetochore showed an increased Mad1 signal relative to the proximal in pairs of sister kinetochores, indicating that distal kinetochore is unattached and proximal kinetochore is attached to microtubules. This asymmetric pattern of monotelic sister kinetochores was similar when we immunostained for CENP-E (**Figure 2.11, E and G**). Replacing endogenous CENP-E with CENP-E mutants (Mini, Chimera, or the Tail) did not alter the asymmetric localization pattern of CENP-E on monotelic sister kinetochores (**Figure 2.11H**). These results collectively demonstrate the existence of a microtubule attachment pathway that regulates Aurora B-mediated phosphorylation of outer kinetochore components at the kinetochore before bi-orientation is established.

To further examine the role of CENP-E in regulating Aurora B phosphorylation, we

assessed the effect of CENP-E mutants on the levels of pS55-Hec1 at monotelic sister kinetochores in the mono-polar spindles. The kinetochore-associated pS55-Hec1 levels exhibited similar asymmetry as CENP-E levels on monotelic sister kinetochores (**Figure 2.12, A and B**). By contrast, the total Hec1 levels regardless of its phosphorylation status remained the same on both sister kinetochores (**Figure 2.12C**). The expression of the CENP-E mutants (Mini, Chimera, or the Tail) did not affect Hec1 fluorescence levels, but affected the phosphorylation of Hec1 remaining highly phosphorylated on attached sister kinetochores with decreased levels of CENP-E (**Figure 2.12**). Taken together this suggest that CENP-E regulates Aurora B-mediated phosphorylation of the outer kinetochores components during the early phases of mitosis, before sister kinetochores have been established, to facilitate stabilization of kinetochore-microtubule attachments before tension generation.

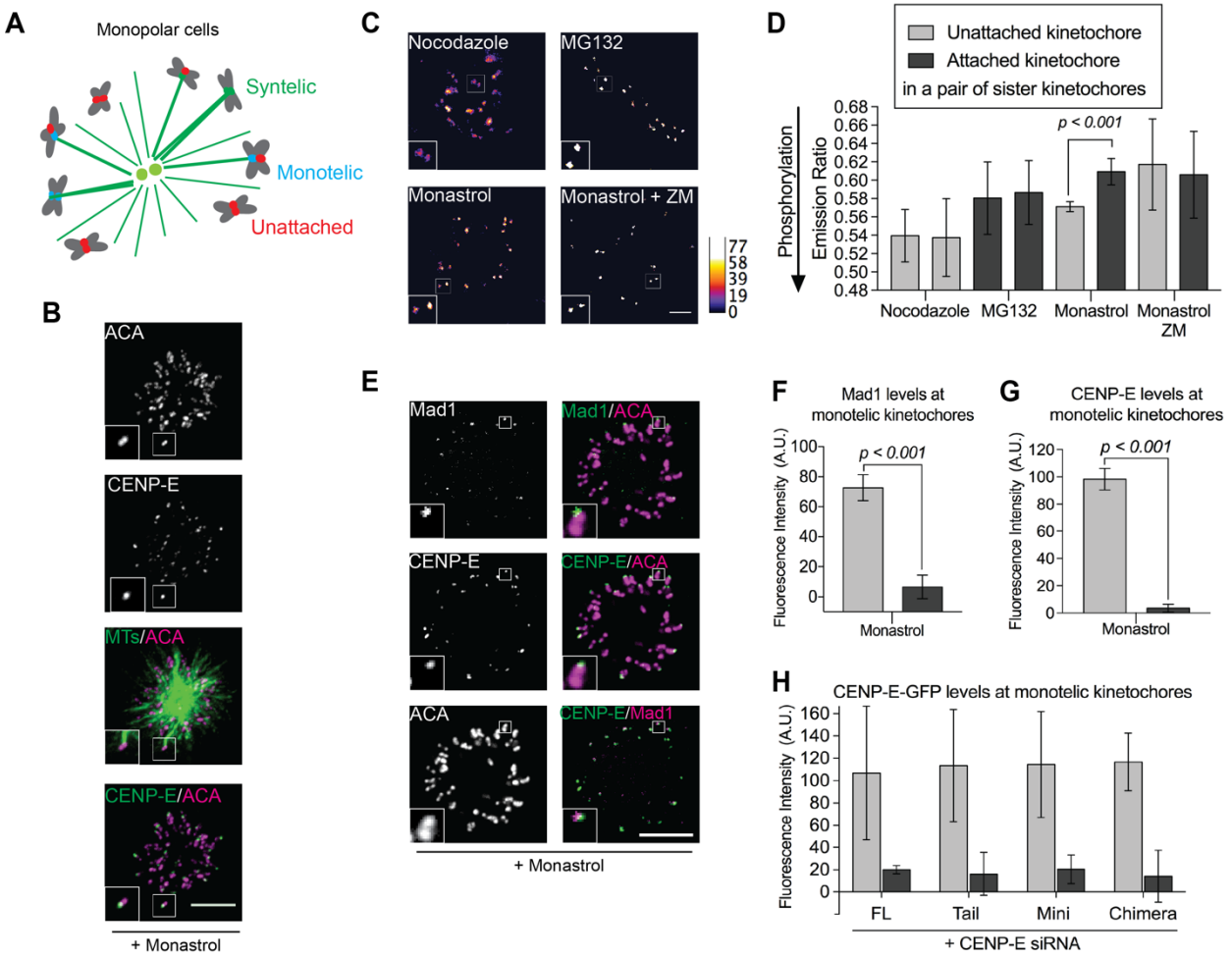

Figure 2.11 Monotelic sister kinetochores have asymmetric levels of Aurora B-mediated phosphorylation of Hec1. (**A**) Diagram depicting the three types of microtubule-kinetochore attachments in monastrol-treated cells. (**B**) CENP-E levels are asymmetric in sister kinetochores pairs of monotelic-attached kinetochores. Immunofluorescence images of monastrol-treated cells were stained with antibodies to CENP-E, ACA, and tubulin (microtubules). Scale bar, 5 µm. Insets represent a pair of monotelic-attached kinetochores. **(C)** FRET images of T98G cells expressing the kinetochore-targeted Aurora B phosphorylation biosensor. Cells were treated as indicated in image panels. Scale bar, 5 µm. Insets represent a pair of monotelic-attached kinetochores. (**D**) Quantification of YFP/TFP emission ratios of kinetochore pairs of fully attached kinetochores (MG132-treated), unattached kinetochores (nocodazole-treated) and monotelic attachments in of monastrol-treated cells with or without ZM447434 treatment. Mean ± SD of three independent experiments are shown. **(E)** Immunofluorescence images shows Mad1 and CENP-E levels are asymmetric and localized to the distal-proximal kinetochore in a pair of monotelic attached kinetochores. T98G cells were stained with antibodies to Mad1, CENP-E and kinetochores were stained with ACA. Scale bar, 5 µm. Insets represent a pair of monotelic-attached kinetochores. (**F, G, and H**) Quantification of the relative fluorescence intensity of Mad1 (**F**), CENP-E (**G**), and GFP (**H**) at monotelic kinetochores normalized to ACA fluorescence intensity. Mean ± SD are shown of three independent experiments, n > 200 aligned kinetochores per group quantified.

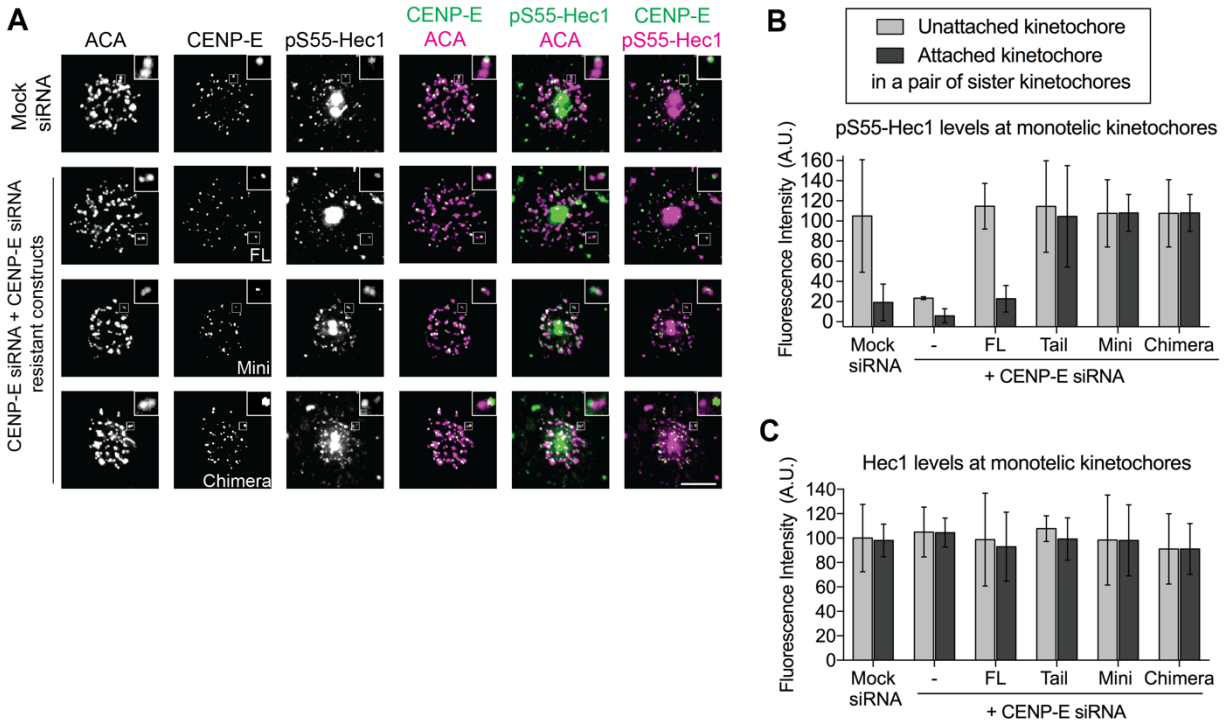

Figure 2.12. Microtubule attachment results in reduced levels of Aurora B phosphorylation on the attached kinetochore in a pair of monotelic sister kinetochore and this requires CENP-E function. (**A**) The levels of pS55-Hec1 are also asymmetric in sister kinetochores pairs of monotelic-attached kinetochores and this requires normal CENP-E function. Monastrol-treated cells were stained with antibodies to ACA, CENP-E, and pS55-Hec1. Scale bar, 5 μm. Insets represent a pair of monotelic-attached kinetochores. (**B**) Quantification of relative fluorescence intensity pS55-Hec1 normalized to ACA kinetochore signal in monotelic kinetochores. Mean ± SD are shown of three independent experiments, Mock siRNA: n = 49, CENP-E siRNA: n = 50, FL: n = 39, Tail: n = 32, Mini: n = 42, Chimera n = 35 kinetochores pairs quantified (**C**) Hec1 fluorescence intensity normalized to ACA kinetochore signal in monotelic kinetochores. Mean ± SD are shown of three independent experiments, Mock siRNA: n = 35, CENP-E siRNA: n = 31, FL: n = 32, Tail: n = 31, Mini: n = 32, Chimera n = 31 kinetochores pairs quantified.

Discussion

Current models for regulation of Aurora B-mediated phosphorylation emphasize the distance (tension or inter-kinetochore stretch) between sister kinetochores to move inner centromere-localized Aurora B away from its substrates (e.g. the Ndc80 complex) at outer kinetochores and to balance phosphorylation by phosphatases (Lampson and Cheeseman, 2011; Foley and Kapoor, 2013). The asymmetric Hec1 phosphorylation levels exhibited on monotelic sister kinetochores clearly suggests the existence of other mechanisms to regulate Aurora B phosphorylation independent of tension. It has been shown that active Aurora B is able to discriminate between correct and incorrect attachments regardless to its localization clustering on either centromeric chromatin or microtubules (Campbell and Desai, 2013). Besides an inter-kinetochore stretch (tension), an intra-kinetochore stretch has also been observed upon microtubule attachment (Maresca and Salmon, 2009; Uchida et al., 2009), which could represent structural changes within the kinetochore (Wan et al., 2009). However, recent efforts show that intra-kinetochore stretch is not necessary to mediate stabilization of kinetochore-microtubule attachments (Etemad et al., 2015; Tauchman et al., 2015; Magidson et al., 2016). Our findings also support that the kinetochore-associated motor CENP-E can regulate Aurora B-mediated phosphorylation in response to microtubule attachment and not tension. This mechanism depends on the motor activity and the elongated, flexible coiled-coil of CENP-E. The long and flexible coiled-coil of CENP-E not only is important for its motor activity (Vitre et al., 2014), but also can produce different conformations *in vitro* (Kim et al., 2008). Therefore, the force produced by CENP-E motility upon microtubule capture may lead to changes in susceptibility of Aurora B substrates at outer kinetochores to phosphorylation.

Several functional roles, which are not mutually exclusive, have been demonstrated for the kinetochore-associated kinesin motor CENP-E: (1) an essential motile tether between kinetochores and microtubules (Yao et al., 2000; McEwen et al., 2001; Putkey et al., 2002; Kim et al., 2008); (2) transporting misaligned (polar) chromosomes to the metaphase plate (Kapoor et al., 2006); (3) a processive bi-directional tracker of dynamic microtubule ends (Gudimchuk et al., 2013); and (4) regulating the mitotic checkpoint through its interaction with BubR1 (Abrieu et al., 2000; Chan et al., 1999; Guo et al., 2012; Mao et al., 2003; Weaver et al., 2003; Mao et al., 2005). Our results suggest that the major functional role of CENP-E on attached kinetochores at aligned metaphase plate is to reduce Aurora B phosphorylation and, thus, to enhance the microtubule binding activity of microtubule-binding proteins, including the Ndc80 complex, at outer kinetochores. Inhibition of CENP-E motor activity can produce elevated Aurora B phosphorylation and misaligned chromosomes, which can be rescued by inhibiting Aurora kinase activity.

In addition to the microtubule capture activity at lateral microtubules, CENP-E also actively maintains bi-oriented, end-on attachment at the metaphase plate (Gudimchuk et al., 2013). Consistent with this function, we found an upregulation in the Aurora B-mediated phosphorylation of the Ndc80 complex upon inhibition of the motor motility of CENP-E or perturbations of the coiled-coil domain. Strikingly, analysis of the angular distribution of the Full-length-CENP-E along the kinetochore yielded a bi-modal distribution. Previous studies on the configuration of kinetochore components identified a bent and rigid lateral linkage of the Ndc80 complex through an elongated interaction with the Mis12 complex and KNL1 (Wan et al., 2009). The study proposed the existence of a flexible linkage that could transmit the pulling forces generated by curling protofilaments of a microtubule to the inner kinetochore at bi-oriented kinetochores (Wan et al., 2009). However, no such linkage in vertebrate cells has been identified. We found that

CENP-E undergoes a two-state conformational change that is dependent on microtubule dynamics. Therefore, we propose CENP-E acts as a flexible linkage that help track the depolymerizing and polymerizing ends of microtubules through the rigid binding of the Ndc80 complex at bi-oriented kinetochores. Indeed, *in vitro* studies have characterized CENP-E as a microtubule tip-tracker, tracking both the growing and shrinking end of microtubules (Gudimchuk et al., 2013).

The asymmetric Hec1 phosphorylation levels exhibited upon microtubule attachment suggests that CENP-E regulates Aurora B phosphorylation of outer kinetochores localized substrates through structural changes propagated through CENP-E's unique coiled-coil domain. Reducing or replacing the coiled-coil domain of CENP-E with a shorter/less flexible coiled-coil domain affected the structural rearrangement of kinetochore-associated CENP-E. This leads us to postulate that the coiled-coil domain is involved in the recruitment of phosphatases to regulate the balance of phosphorylation/dephosphorylation. Indeed, a previous study has shown that Aurora B-mediated phosphorylation of CENP-E regulates microtubule capture by CENP-E through a phosphatase targeting pathway involving the Protein Phosphatase 1, PP1. Importantly, the kinetochore PP1 targeting motif is found at coiled-coil domain near the motor domain of CENP-E (Kim et al., 2010). Therefore, future work will elucidate the interplay between phosphorylation and dephosphorylation that is dependent on microtubule capture function of CENP-E.

.

CHAPTER 3: Aurora B regulates the actin assembly function of mDia3

Introduction

Formin-mediated actin assembly is known to play essential roles in multiple processes, including cytokinesis, endocytosis, filopodia formation, cell polarity, cell spreading, cell-cell adhesion, and cell-matrix adhesion (Kovar 2006; Goode and Eck, 2007). The presence of formin homology 2 (FH2) domain defines the family of formins, which nucleates and elongates unbranched actin filaments by binding to the barded ends (Pruyne et al., 2002; Sagot et al., 2002). The actin assembly activity of formins and the subcellular localization of formins are regulated by direct binding of the Rho family of small GTPases, which bind to the N-terminal GBD (GTPase binding domain) releasing the interaction of the N-terminal DID (diaphanous inhibitory domain) from the C-terminal the DAD domain (diaphanous autoregulatory domain), and thus promoting the nucleation of the FH2 domain (Alberts, 2001; Li and Higgs, 2003; Rose et al., 2005; Lammers et al., 2005).

Besides the well-characterized autoinhibitory process that inhibits the actin polymerization function of the FH2 domain, other regulatory mechanisms have been proposed. For instance, the diaphanous-related formin, Daam1 (dishevelled-associated activator of morphogenesis-1), has a weaker actin assembly activity compared to other mammalian formins due to differences in secondary structural elements (Lu et al., 2007). Furthermore, mass spectrometry analysis of the FH2 domain of has found differential interactions among the FH2 domains of mDia1, mDia2, and mDia3 (Daou et al., 2013). For instance, the FH2 of mDia1 specifically interacts with Rab6-interacting protein 2, whereas the FH2 domain was found to interact with various nuclear proteins (Daou et al., 2013). These suggest formins can be differentially regulated by binding to specific

effector molecules to the FH2 domain. However, the contributions of these differential FH2 domain interactions remains largely unknown.

The formin mDia3 has been shown to regulate the generation of stable microtubule attachments at the kinetochore (Yasuda et al., 2004). Further studies of mDia3, identified four sites that are phosphorylated by Aurora B (Cheng et al., 2011). Two of the phosphorylation sites are found in the FH2 domain of mDia3. While one of the phosphorylation sites is conserved in both mDia1 and mDia2, the other is replaced with phosphomimetic amino acids (aspartic acid or glutamic acid). This leads one to hypothesize that these phospho-amino acid residues are important for the actin assembly function of the diaphanous (Dia) subfamilies of formins, mDia1, mDia2, and mDia3. Here, we show that Aurora B-mediated phosphorylation of mDia3 regulates the actin polymerization activity of mDia3. Perturbations of mDia3 phosphorylation by Aurora B disrupts mDia3 localization to actin-based structures affecting cell migration and cell spreading.

Materials and Methods

Tissue culture, transfection and drug treatment

NIH3T3 cells were cultured in DMEM supplemented with 10% Calf Serum at 37°C in 5% CO_2. Transfections of mDia3 siRNA (5' – GAGAAGAGCAGGAGGAGCAAU - 3') and mDia3 constructs, GFP-FH1-FH2 WT and phosphomimetic and non-phosphorylatable mutants were performed using DharmaFECT Duo Transfection Reagent (GE Dharmacon) according to the manufacturer's instruction. ZM447439 (2 μM) (Tocris Bioscience) treatment was performed for 6 hrs 24 hrs post-transfection. LPA, L-α-Lysophosphatidic acid (Avanti Polar Lipids) stimulation of serum-starved cells was performed at 10 μM for 2 hrs.

Antibody labeling

For indirect immunofluorescence analysis, NIH3T3 cells were grown on acid washed No. 1.5 coverslips. Coverslips were fixed in either −20°C methanol for 10 min or 4% paraformaldehyde for 20 min at room temperature. Fixed cells were blocked in PBS containing 0.1% Triton X-100 and 5% Bovine Serum Albumin (Sigma-Aldrich) for 1 hr at room temperature or overnight at 4°C. To assess centrosome re-orientation and nuclear movement paraformaldehyde-fixed cells were stained suing pericentrin (BD Bioscience) to label the centrosomes, tubulin (sigma) to label the microtubules and nucleus was stained with DAPI. Actin filaments were imaged using Rhodamine-labelled Phalloidin (Sigma) and mDia3 GFP-tagged constructs where stained using a GFP antibody (Abcam). A myosin 10 antibody (Millipore) was used to label cellular protrusions. The phospho-mDia3 antibody (p820) was custom-ordered from Yenzym Antibodies. To confirm RNAi-mediated knockdown of mDia3 in NIH3T3 lysates a 8% SDS-PAGE gel was performed. mDia3 was detected using s mDia3 antibody (Santa Cruz) and a tubulin antibody (Sigma) was used the loading control.

Image acquisitions, data, and statistical analysis

All images were acquired using an inverted microscope (IX81; Olympus) a monochrome charge-coupled device camera (Sensicam QE; Cooke Corporation), and the SlideBook imaging software (Intelligent Imaging Innovations, 3i). To image cell migration in a wound healing assay, were cultured in DMEM with 10% calf serum, serum starved for 2 days, wounded and stimulated with 2% serum in the absence or presence of 2 μM ZM447439 upon imaging. Images were acquired every 5 min for 12 hrs using a 10X phase contrast objective lens (Olympus) at 37°C in 5% CO_2. To image migration of single cells, cells were serum starved for one day, trypsinized and

re-platted on Fibronectin (Sigma) coated imaging 35mm dishes with No. 1.5 coverslips. 30 min after re-platting, cells were imaged using a 20X phase contrast objective lens (Olympus) at 37°C in 5% CO_2 for 10 hrs images were acquired every 10 min. Fixed cells were imaged using a 60X, NA 1.42 Plan Apochromat oil immersion objective lens (Olympus), Measurement of the velocity and the persistence of cells, the centroid position of migratory cells was obtained using the GFP channel to threshold the contour of the cells or circular region was drawn on the nucleus. All statistical analyses were performed using GraphPad Prism (GraphPad, version 7a) using unpaired, two-tailed t-tests to compare the means between two groups or a One-way ANOVA was used to compare the means of 3 or more groups. All plots were prepared in GraphPad Prism.

Protein purification and actin pyrene assay

GST-tagged proteins mDia3 FH1-FH2, WT, phosphomimetic and non-phosphorylatable mutants were expressed in *E. coli* cells and affinity purified on agarose-coupled glutathione (GE Healthcare) according to the manufacturer's recommended protocols. The GST tag FH1-FH2-mDia3 was cleaved using thrombin-mediated (Sigma) cleavage according to the manufacturer's instructions. Purified proteins were resuspended in 5 mM Tris-HCl pH 8.0 and 0.2 mM CaCl2 buffer in Sephadex G-25 PD-10 desalting columns (GE Healthcare). Protein expression was confirmed using 8% SDS-PAGE gel and stained with Coomassie (Teknova). Actin pyrene assays were performed on the same day of purification, using 2 μM muscle actin from rabbit (5% pyrene labeled) (Cytoskeleton, Inc). Actin polymerization was induced using 50 mM KCl, 2 mM MgCl2, and 0.2 mM ATP (Cytoskeleton, In). Purified GST-tagged mDia3 recombinant proteins were incubated with an active form of Aurora B kinase (SignalChem) in the presence of Kinase Buffer (5 mM MOPS, pH7.2, 2.5 mM ß-glycerol-phosphate, 1 mM EGTA, 0.4 mM EDTA, 5 mM MgCl2, 0.05 mM DTT, 20 μM ATP) for 30 min at room temperature. Actin polymerization kinetics was

monitor by the increase in fluorescence emission at 407 nm every 60 sec at room temperature with excitation wavelength at 350 nm.

Results

The kinase activity of Aurora B kinase is required for cell migration

Previous studies using a GFP-tagged full-length Aurora B construct found that although Aurora B is mostly found in the nucleus, a significant percentage remained in the cytoplasm (Rannou et al., 2008). Furthermore, RNAi-mediated knockdown of Aurora B or inhibition of Aurora B using small-molecule inhibitors, have found that Aurora B function is essential for cell migration and invasion in various cancer cell lines (Zhou et al., 2014; Zhu et al., 2014; Shan et al., 2014). To confirm whether Aurora B kinase activity affects the cell migration of non-tumorigenic mouse fibroblasts, we conducted a wound healing assay. Wounded monolayers of serum-starved cells stimulated with 2% serum in the presence of Aurora B inhibitor, ZM447439, caused a decrease in the rate of wound closure compared to cells treated with DMSO (**Figure 3.1A**). We first confirmed whether the migration defect was caused by a disruption in cell polarization by assessing the rearward positioning of the nucleus and the centrosome re-positioning towards the leading edge, hallmarks of a polarized cell (Gundersen and Worman, 2013; Gomes et al., 2005). However, we did not find any defect in the rearward positioning of the nucleus or the centrosome re-positioning in the presence of LPA and upon inhibition of Aurora B kinase function (**Figure 3.1B**). Quantification of single cell migration on a fibronectin-coated surface showed a significant decrease in velocity, but not in the ability of cells to persist with directional movement (endpoint displacement/total path) (**Figure 3.1, C – F**). These data suggest the kinase activity of Aurora B is not essential for cells to polarize, but is required for cells to maintain the migratory rate.

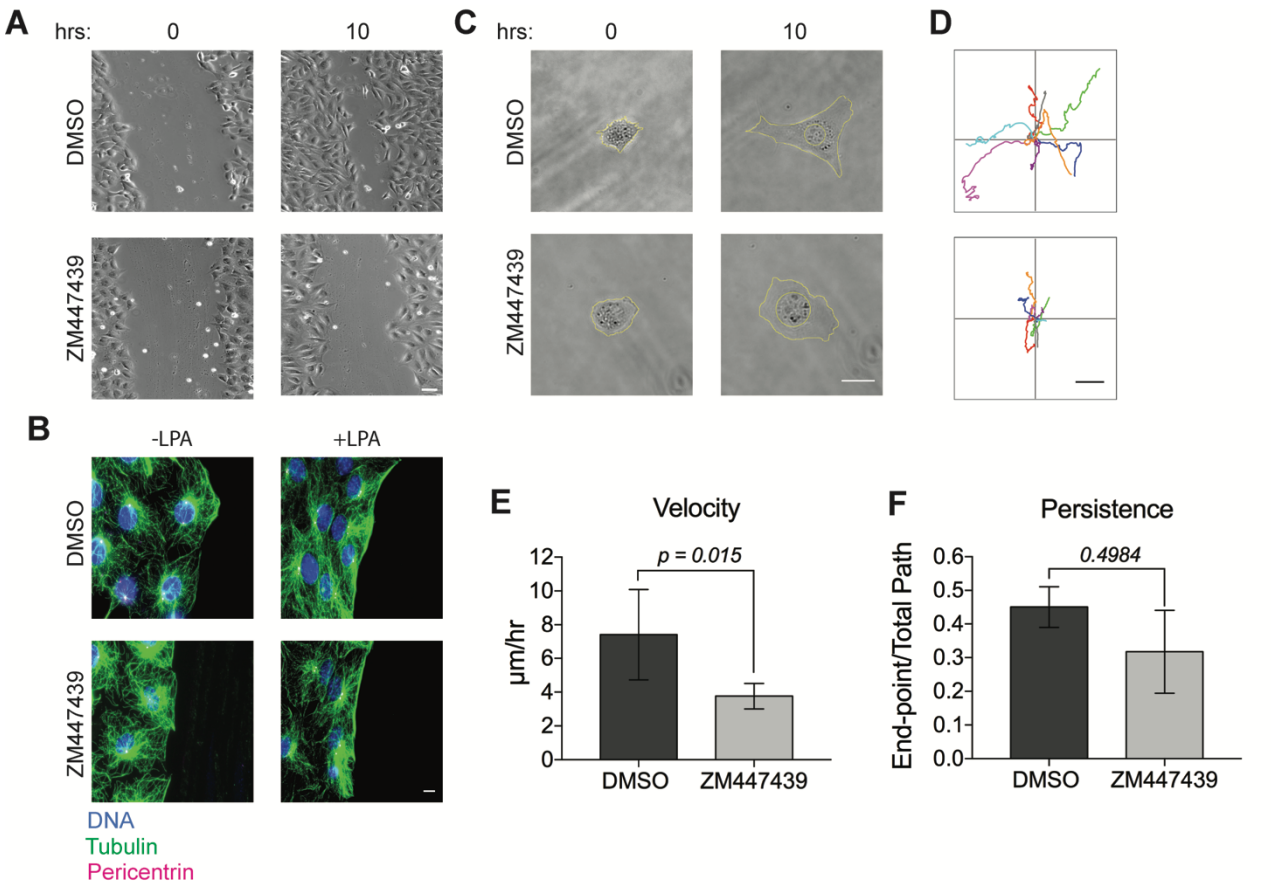

Figure 3.1. Inhibition of Aurora B kinase activity reduces the velocity of migratory mouse fibroblasts. (**A**) Phase-contrast images of wound healing assay. NIH3T3 cells were serum-starved for 1 day and stimulated with 2% serum with or without 2 μM ZM447439 upon time-lapse imaging. Scale Bar, 25 μm. (**B**) Immunofluorescence images of 2-day serum-starved NIH3T3 cells stimulated with or without LPA in the presence or absence of 2 μM ZM447439 shows Aurora B kinase activity is not required for rearward nuclear positioning and centrosome re-orientation. Microtubules and centrosomes were stained with a tubulin and a pericentrin antibody, respectively. DNA was stained with DAPI. Scale bar, 10 μm. (**C**) Phase-contrast images of single cell migration. NIH3T3 cells were serum-starved for 1 day, trypsinized, re-plated and stimulated with 2% serum with or without 2 μM ZM447439 upon time-lapse imaging. Scale Bar, 25 μm. (**D**) Representatives 10-hr trajectories of single cells treated with or without 2 μM ZM447439. Scale bar, 5 μm. (**E**) Bar graph plot of velocity, mean ± SEM of three independent experiments is shown. DMSO: n = 13, ZM447439: n = 20 cells were quantified. (**F**) Bar graph plot of persistence, mean ± SEM of three independent experiments is shown. DMSO: n = 13, ZM447439: n = 20 were quantified.

Aurora B-mediated phosphorylation of mDia3 regulates the actin nucleation and elongation function of mDia3

Many of the substrates of Aurora B have been shown to function almost exclusively during mitosis and cytokinesis (Minoshima et al., 2003; Lan et al., 2004; Cheeseman et al., 2006; Cheng et al., 2011; Kim et al., 2010; Gestaut et al., 2008). However, previous studies have identified the ubiquitously expressed diaphanous-related formin, FHOD1 as an Aurora B substrate (Floyd et al., 2013). Phosphorylation by Aurora B was found to increase the actin assembly function of FHOD1 (Floyd et al., 2013). Furthermore, previous studies of mDia3, identified four sites that are phosphorylated by Aurora B (Cheng et al., 2011). Two of the phosphorylation sites are found in the FH2 domain of mDia3 (**Figure 3.2A**).

To test whether phosphorylation of the FH2 domain of mDia3 affects the actin polymerization function of mDia3, we designed constitutively active forms of mDia3, including a phosphomimetic (2E), non-phosphorylatable (2A), and the wild-type as the control (**Figure 3.2B**). The constructs with tagged with either GFP or GST and included the FH1 domain, which is important for the interactions with actin and profilin (Watanabe et al., 1997; Evangelista et al., 1997).

To test the actin assembly function of these constructs, we first purified recombinant proteins and tested them for actin assembly using pyrene-labeled actin in a kinetic assay (**Figure 3.2, C-F**). While the phosphomimetic, 2E mutant substantially increased the actin assembly function of mDia3, the wild-type and non-phosphorylatable mutant minimally induced the actin nucleation function of mDia3 (**Figure 3.2D and F**). To further confirm this phosphorylation-mediated dependent actin assembly function of mDia3, we incubated the wild-type construct with a purified active form of Aurora B in the presence of ATP (**Figure 3.2E and F**). As expected, pre-

incubation of the wild-type FH1FH2 domain of mDia3 with Aurora B, increased the actin assembly function of the FH2 domain of mDia3. These results suggest Aurora B-mediated phosphorylation of mDia3 induces the actin assembly function of mDia3 *in vitro*.

To test whether the actin polymerization defect *in vitro* is correlated with a loss of activity in cells, we transfected constitutively active mutant forms and the wild-type GFP-tagged FH1FH2-mDia3 into serum-starved NIH3T3 cells, which have low levels of assembled actin. Actin filaments were assessed using Phalloidin staining (**Figure 3.2G**). Expressing the phosphomimetic, non-phosphorylatable and the wild-type recapitulated the *in vitro* findings. Furthermore, treating cells with the Aurora B inhibitor, ZM447439 decreased the levels of assembled actin in cells expressing the wild-type GFP-FH1FH2-mDia3, but not the phosphomimetic (**Figure 3.2G**). Taken together, these results suggest Aurora B-mediated phosphorylation of mDia3 induces the actin assembly function of mDia3 *in vitro* and in cells.

mDia3 has been shown to be involved in multiple actin-based processes including, cytokinesis, filopodia formation, and oogenesis (Castrillon and Wasserman, 1994; Bione et al., 1998). RNAi-mediated depletion of mDia3 affects cell migration and disruption of cortical microtubule capture in a breast cancer cell line (Daou et al., 2013). To confirm whether mDia3 is required for mouse fibroblasts, we reduced mDia3 levels using RNAi-mediated knockdown (**Figure 3.3A**). Reducing mDia3 levels did not cause any defect in the cell spreading and cell polarization, as shown by the rearward positioning of the nucleus (**Figure 3.3B)**. However, reduced levels of mDia3 caused a significant decreased in the velocity, but not the persistence of cell migratory fibroblasts reminiscent of Aurora B-inhibited cells (**Figure 3.3, B – E**). This suggests mDia3 plays an essential role in cell migration as previously reported.

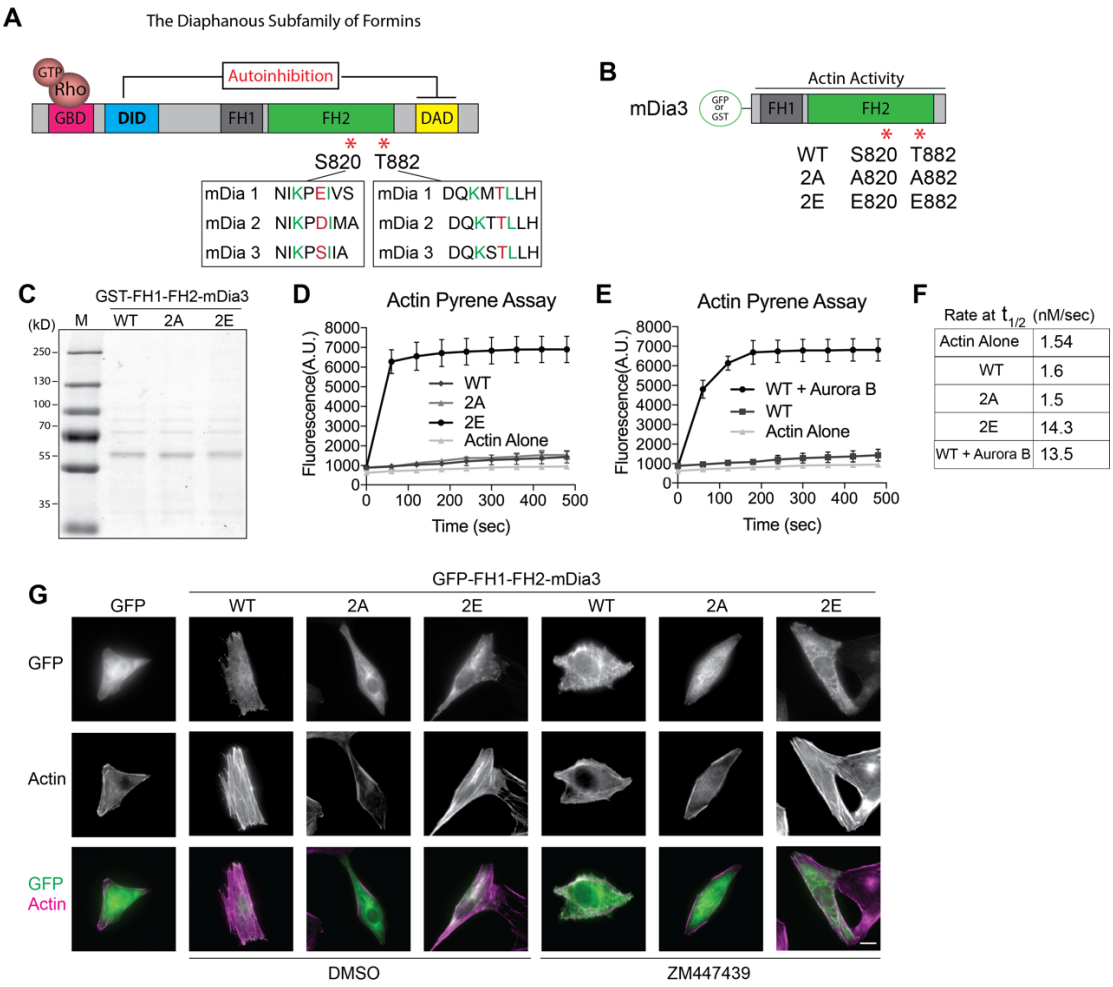

Figure 3.2. Phosphorylation of the FH2 domain of mDia3 by Aurora B mediates the actin polymerization activity of mDia3. (A) Illustration depicting mDia3 domains. The FH2 domain of mDia3 contains two Aurora B phosphorylation consensus site, [RK] x [TS] [ILV]. The T882 site is conserved among the subfamily of diaphanous formins, while S820 are phosphomimetic residues in mDia1 and mDia2. **(B)** Illustration depicting the phosphomimetic and non-phosphorylatable point mutations at S820 and T882 introduced into a constitutively active fragment of mDia3 that includes the FH1 and FH2 domains, but lack the regulatory GBD and DAD domains. (**C**) Coomassie stained 8% SDS-PAGE gel of mDia3 WT and mutants FH1-FH2 fragments expressed in *Escherichia coli* and affinity purified. M, protein marker. (**D**) Actin pyrene assay using 5% pyrene-labeled monomeric actin. The WT and mutant fragments were introduced after cleavage of the GST tag at 10 nM concentration. Mean ± SEM of three independent experiment using identical conditions is shown. (**E**) Actin pyrene assay using 5% pyrene-labeled monomeric actin. The WT fragment was pre-incubated in the absence or presence of active Aurora B protein. Mean ± SEM of three independent experiment using identical conditions is shown. (**F**) Rates of actin assembly at $t_{1/2}$ polymerization of the graphs shown in C and D. (**G**) Immunofluorescence images of serum-starved NIH3T3 cells transfected with the GFP-labeled WT and mutants FH1-FH2 fragments, treated with or without 2 µM ZM447439. GFP was detected with an antibody against GFP and polymerized actin was visualized using Rhodamine-labeled Phalloidin. Scale bar, 10 µm.

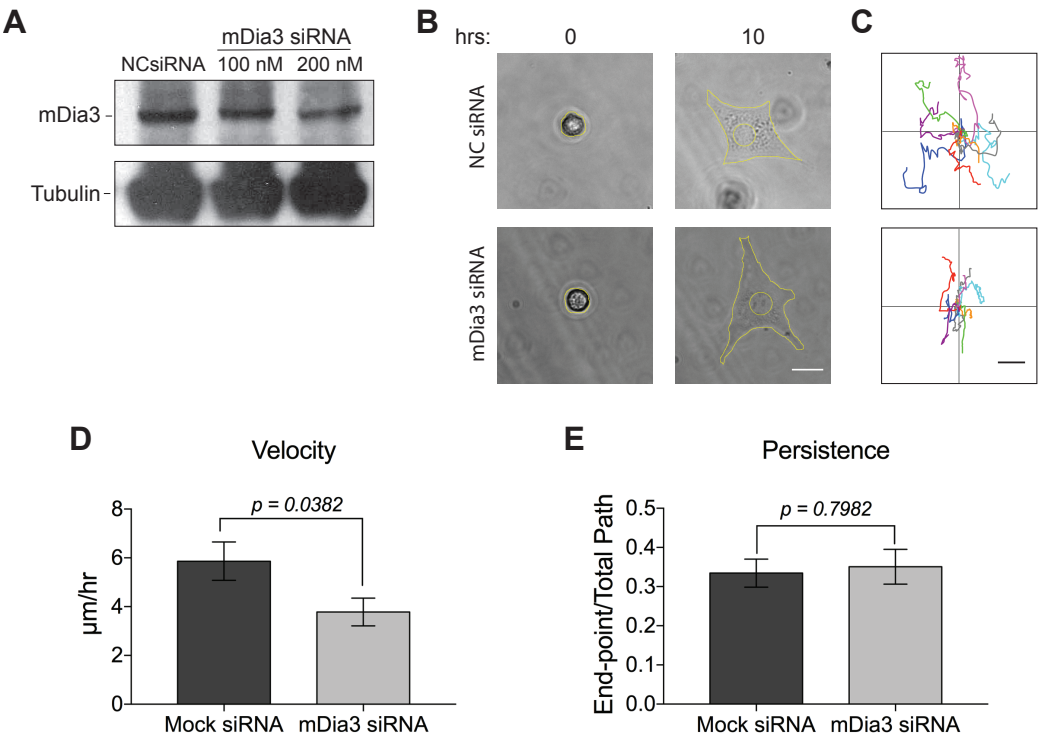

Figure 3.3. The formin mDia3 is required for cell migration and has two Aurora B phosphorylation consensus sites in the FH2 domain. (**A**) Western blot images of NIH3T3 cells transfected with an mDia3 siRNA or a Mock siRNA as the control. An mDia3 antibody was used to detect mDia3 and tubulin staining was used as the loading control. (**B**) Phase-contrast images of single cell migration. NIH3T3 cells were transfected with 200 nM mDia3 siRNA or Mock siRNA, after 1 day of transfection, cells were serum-starved for 1 day, trypsinized, re-plated and stimulated with 2% serum upon time-lapse imaging. Scale Bar, 25 µm. (**C**) Representative 10-hr trajectories of single cells transfected with mDia3 siRNA or Mock siRNA. Scale bar, 5 µm. (**D**) Bar graph plot of velocity, mean ± SEM. Mock siRNA: n = 11, mDia 3 siRNA: n = 19. (**E**) Bar graph plot of persistence, Mean ± SEM. Mock siRNA: n = 11, mDia3 siRNA: n = 19 cells were quantified.

The FH2 domain of mDia3 is phosphorylated by Aurora B at the cell periphery

Exogenous expression of mDia3 is known to induces filopodia formation neuroblastoma cells (Goh et al., 2012). Furthermore, mDia3 nucleation activation by the small GTPase RhoD has been shown to induce filopodia formation in mammalian cells (Gasman et al., 2003; Koizumi et al., 2012). To test whether Aurora B-mediated phosphorylation of regulates the localization of mDia3 in mouse fibroblasts by co-staining with Myosin-X, which is known to accumulate at the cell periphery (Berg et al., 2002). The GFP-FH1FH2-mDia3 wild-type and the phosphomimetic mutant co-localized with Myosin-X in serum-grown cells in the presence or absence of the Aurora B inhibitor, ZM447439 (**Figure 3.4A**). However, the non-phosphorylatable mutant signal remained mostly in the cytosol and did not co-localize with Myosin-X (**Figure 3.4A**). These results suggest the non-phosphorylatable mutant form of mDia3 abrogates the association of mDia3 at the barded-ends of growing actin filaments.

We generated a rabbit polyclonal antibody specific for phosphorylated mammalian mDia3 at serine 820 (pS820-mDia3). Using indirect immunofluorescence analysis of phosphorylated mDia3, we found that mDia3 is phosphorylated at the tip of filopodia upon expression of the wild-type GFP-FH1FH2-mDia3, which is sensitive to Aurora B kinase inhibition (**Figure 3.4B**). Cells expressing the phosphomimetic mutant was also recognized by this phospho-specific antibody, and as expected was not sensitive to Aurora B kinase inhibition (**Figure 3.4B**). Furthermore, consistent with results shown in figure 3.4A, expression of the non-phosphorylatable mutant did not produced any obvious phosphorylation signal at the cell periphery (**Figure 3.4B**). Taken together these results suggests Aurora B phosphorylates mDia3.

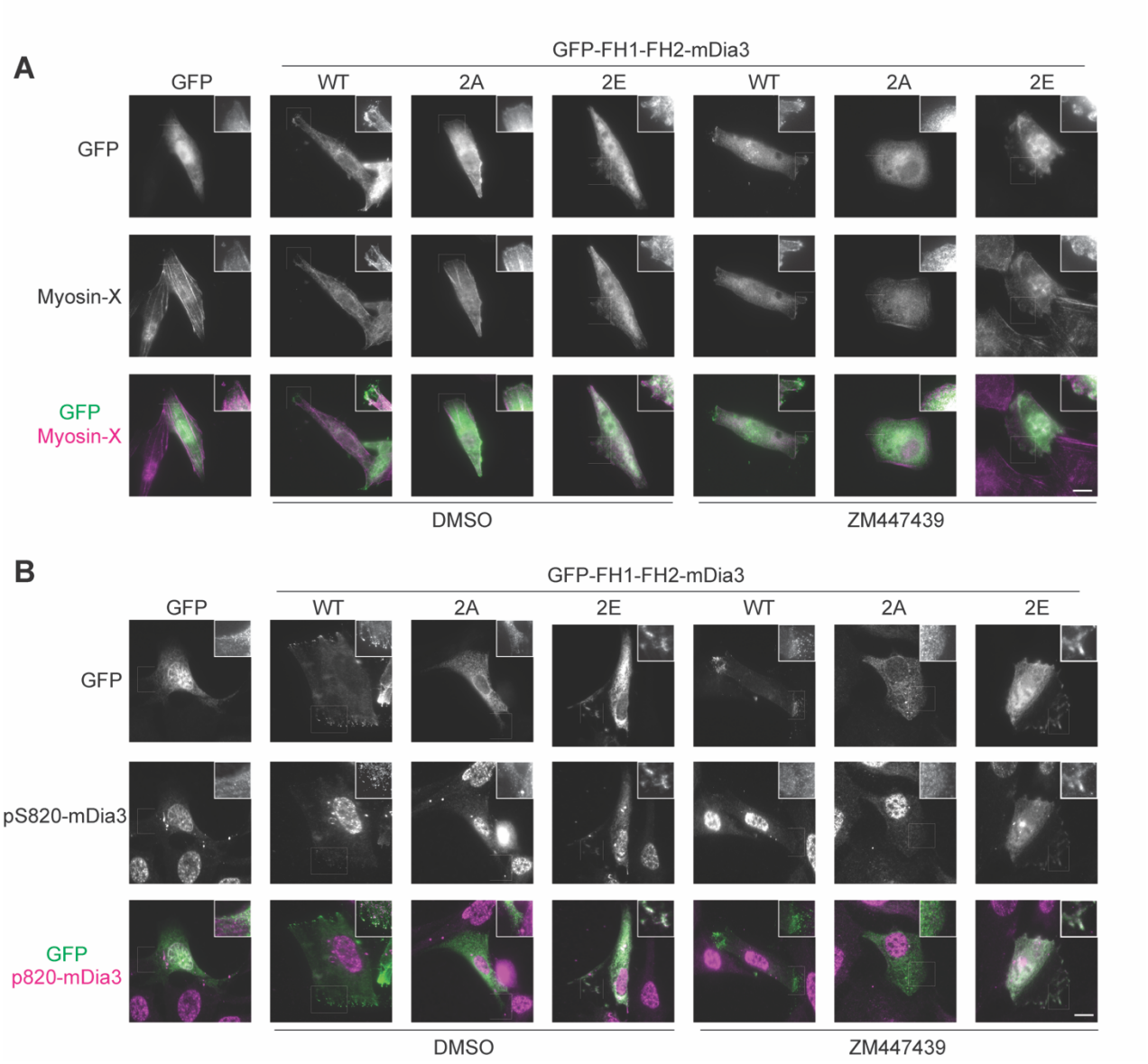

Figure 3.4. The FH2 domain of mDia3 is phosphorylated by Aurora B at the cell periphery. (**A**) Immunofluorescence images of NIH3T3 cells transfected with the GFP-labeled WT and mutants FH1-FH2 fragments, treated with or without 2 μM ZM447439. GFP was detected with an antibody against GFP and Myosin 10 antibody was used to detect filopodia structures. Scale bar, 10 μm. (**B**) Immunofluorescence images of NIH3T3 cells transfected with the GFP-labeled WT and mutants FH1-FH2 fragments, treated with or without 2 μM ZM447439. GFP was detected with an antibody against GFP and a phospho-antibody against residue 820 of the FH2 domain of mDia3 was used to visualize phosphorylation at the tip of filopodia structures. Scale bar, 10 μm.

Aurora B-mediated phosphorylation of mDia3 is required for cell migration and cell spreading

To test the effects of Aurora B-mediated phosphorylation, we imaged single cells and analyzed their ability to migrate upon Aurora B inhibition in cells expressing the wild-type, phosphomimetic and non-phosphorylatable mutant forms of GFP-FH1FH2-mDia3 (**Figure 3.5**). Consistent with the actin assembly function of the phosphorylated form mDia3, the phosphomimetic mutant migrated at a similar rate compared to the wild-type in the absence of the Aurora B inhibitor, ZM447439 (**Figure 3.5, A – D**). Importantly, expression of the phosphomimetic mutant showed comparable migration rates in the absence or presence of Aurora B inhibition (**Figure 3.5, A – D**). However, cells expressing the non-phosphorylatable mutant significantly reduced the velocity and the persistence of cells (**Figure 3.5, C and D**). These data corroborate the Aurora B-mediated phosphorylation-dependent mechanism of mDia3 in regulating the actin assembly function of mDia3.

We noticed distinct morphological changes in cells expressing of the non-phosphorylatable mutant. In our migration assay, cells appeared smaller and spent more time in a rounded-shaped. We quantified the number of cells that fully spread after 1 hr of time-lapse imaging (**Figure 3.6, A – C**). Expressing the non-phosphorylatable mutant increased the number of cells with a rounded-shaped compared to the wild-type control (**Figure 3.6C**). Treatment with the Aurora B inhibitor increased the number of cells with a rounded-shaped in cells expressing the wild-type control, but not in cells expressing the phosphomimetic mutant (**Figure 3.6C**). These data suggest the non-phosphorylatable mutant of mDia3 behaves as a dominant negative mutation severely disrupting the actin nucleation and elongation activity of mDia3.

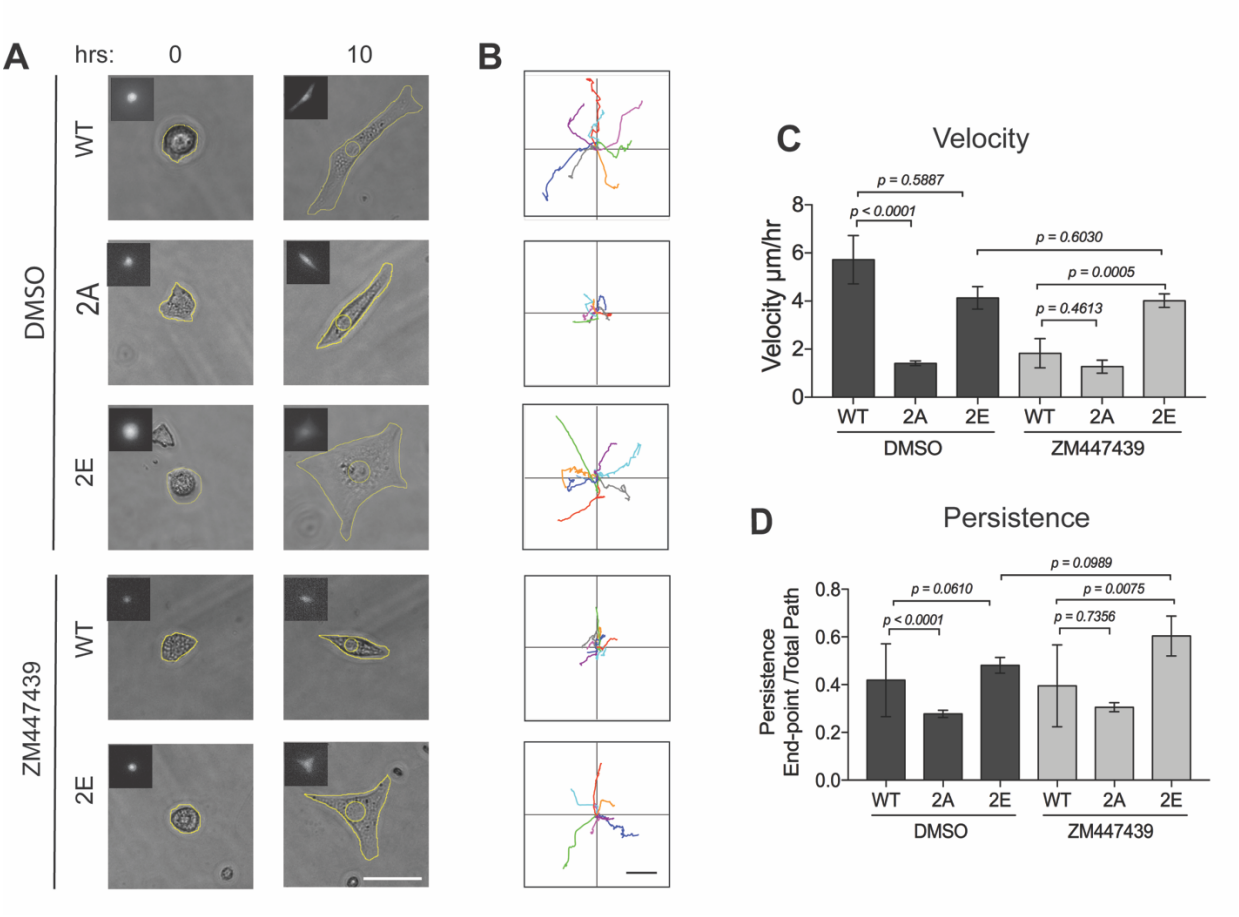

Figure 3.5. Aurora B-mediated phosphorylation of the FH2 domain of mDia3 is required for cell migration. (**A**) Phase-contrast images of single cell migration. NIH3T3 cells were transfected with GFP-labeled WT and mutants FH1-FH2 fragments, after 1 day of transfection, cells were serum-starved for 1 day, trypsinized, re-platted and stimulated with 2% serum in the absence or presence of 2 µM ZM447439 upon time-lapse imaging. Insets show GFP expression. Scale Bar, 25 µm. (**B**) Representative 10-hr trajectories of single cells transfected with GFP-labeled WT and mutants FH1-FH2 mDia3 fragments in the absence or presence of 2 µM ZM447439. Scale Bar, 5 µm. (**C**) Bar graph plot of velocity, mean ± SEM of three independent experiments is shown. WT DSMO: n = 9, WT ZM447439: n = 19, 2A DSMO: n = 18, 2A ZM447439: n = 10, 2E DSMO: n = 13, 2E ZM447439: n = 7 cells were quantified. (**D**) Bar graph plot of persistence, Mean ± SEM of three independent experiments is shown. WT DSMO: n = 9, WT ZM447439: n = 19, 2A DSMO: n = 18, 2A ZM447439: n = 10, 2E DSMO: n = 13, 2E ZM447439: n = 7 cells were quantified.

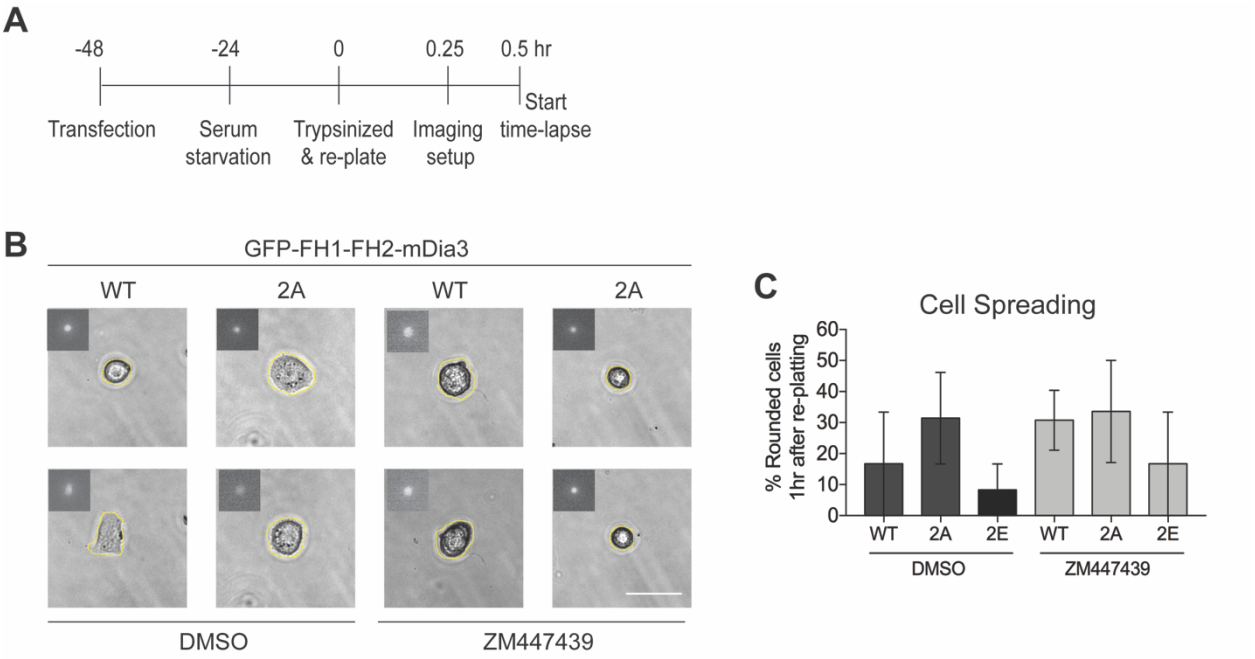

Figure 3.6. Aurora B-mediated phosphorylation of the FH2 domain of mDia3 is required for cell spreading. (**A**) Schematic depiction of the assay used to assess cell spreading. (**B**) Phase-contrast images of single NIH3T3 cells transfected with GFP-labeled WT and the non-phosphorylatable mutant of mDia3 FH1-FH2 fragments, after 1 day of transfection, cells were serum-starved for 1 day, trypsinized, re-plated and stimulated with 2% serum in the absence or presence of 2 μM ZM447439. The Inset shows GFP expression. Scale Bar, 25 μm. (**C**) Quantification of the percentage of cells spread after 1hr of re-plating or re-rounding throughout the course of a 10 hr time-lapse movie. Mean ± SEM of three independent experiments is shown. WT DSMO: n = 12, WT ZM447439: n = 21, 2A DSMO: n = 19, 2A ZM447439: n = 10, 2E DSMO: n = 14, 2E ZM447439: n = 11 cells were quantified.

Discussion

The roles of the formin in nucleating and elongating unbranched actin filaments are well-characterized (Goode and Eck, 2007). However, many different isoforms are ubiquitously expressed in cells and the mechanisms by which their function are spatiotemporally regulated remains largely unknown. Here, I show Aurora B-mediated phosphorylation of the FH2 domain of mDia3 regulates the nucleation and elongation function of mDia3. Previous studies have found that Aurora B shuffles from the nucleus to the cytoplasm via the exportin1-mediated nuclear export-dependent pathway (Rannou et al., 2008). However, the contribution of this cytoplasmic pool during interphase remains elusive. My results suggest Aurora B kinase is a master regulator of both actin and microtubule cytoskeletons, by regulating both the actin assembly and the microtubule stabilization functions of mDia3 at different phases of the cell cycle (Cheng, 2011).

Structural studies of the isolated FH2 domain have shown a specific region that is highly conserved "GNXMN" motif among various formins in multiple species (Shimada et al., 2004). Furthermore, several lysine residues near this motif have been shown to play a critical role in actin assembly function of the FH2 domain of mDia1 (Ishizaki et al., 2001). Importantly, the Aurora B phosphorylation consensus sites of mDia3, including the phosphomimetic residues of mammalian mDia1 and mDia2 are found near or flanking these critical regions. All three mDia formins have been shown to have non-redundant functions in cortical microtubule capture and Ebr2-depedent cell migration (Daou et al., 2013). Therefore, future structural and biochemical work of the mDia1-3 subfamily of formins should elucidate the effects of Aurora B-mediated phosphorylation on the actin nucleation and elongation activities and the actin assembly-independent mechanism of microtubule stabilization.

CHAPTER 4: Discussion and Future Directions

PART 1: CENP-E regulates Aurora B kinase activity at the kinetochore

Aurora B-mediated phosphorylation of outer-localized kinetochore substrates are regulated by microtubule attachment not tension

To ensure accurate chromosome segregation, pairs of sister kinetochores must bind to microtubules emanating from the opposite pole of the mitotic spindle apparatus, known as bi-orientation. This configuration characterizes a pair of stable kinetochore-microtubule attachments. Conversely, unstable kinetochore-microtubule attachments constitute pairs of sister kinetochores not bound to microtubules from the opposite poles of the mitotic spindle apparatus, i.e. syntelic attachments, in which both kinetochores from a sister pair binds to microtubule emanating from the same spindle pole. Aurora B kinase is a major regulator that monitors the fidelity of kinetochore-microtubule attachments by selectively destabilizing incorrect kinetochore-microtubule attachments and providing a new opportunity for incorrect kinetochore-microtubule attachments to rearrange into the proper bi-oriented configuration.

The "spatial separation" model (Lampson and Cheeseman, 2011), postulates that tension exerted across a pair of bi-oriented sister kinetochores, separates the inner-centromere-localized Aurora B from the outer-localized kinetochores substrates leading to a decrease in phosphorylation and, in turn stabilizing kinetochore-microtubule attachments (**Figure 4.1A**). Evidence that supports this model were first observed in spermatocytes, in which inducing a physical pulling force using a glass needle at monotelic attachments led to the selective stabilization of the kinetochore-microtubule attachment that would otherwise be unstable (Nicklas and Koch, 1969;

Nicklas, 1997). Subsequent experiments in fungi and in mammals led to the discovery of Aurora B in mediating this tension-sensing pathway, based on the proximity from the inner-centromere-localized Aurora B to the outer-localized kinetochore substrates, known as inter-kinetochore stretch. However, some assumptions that support this model need reassessment.

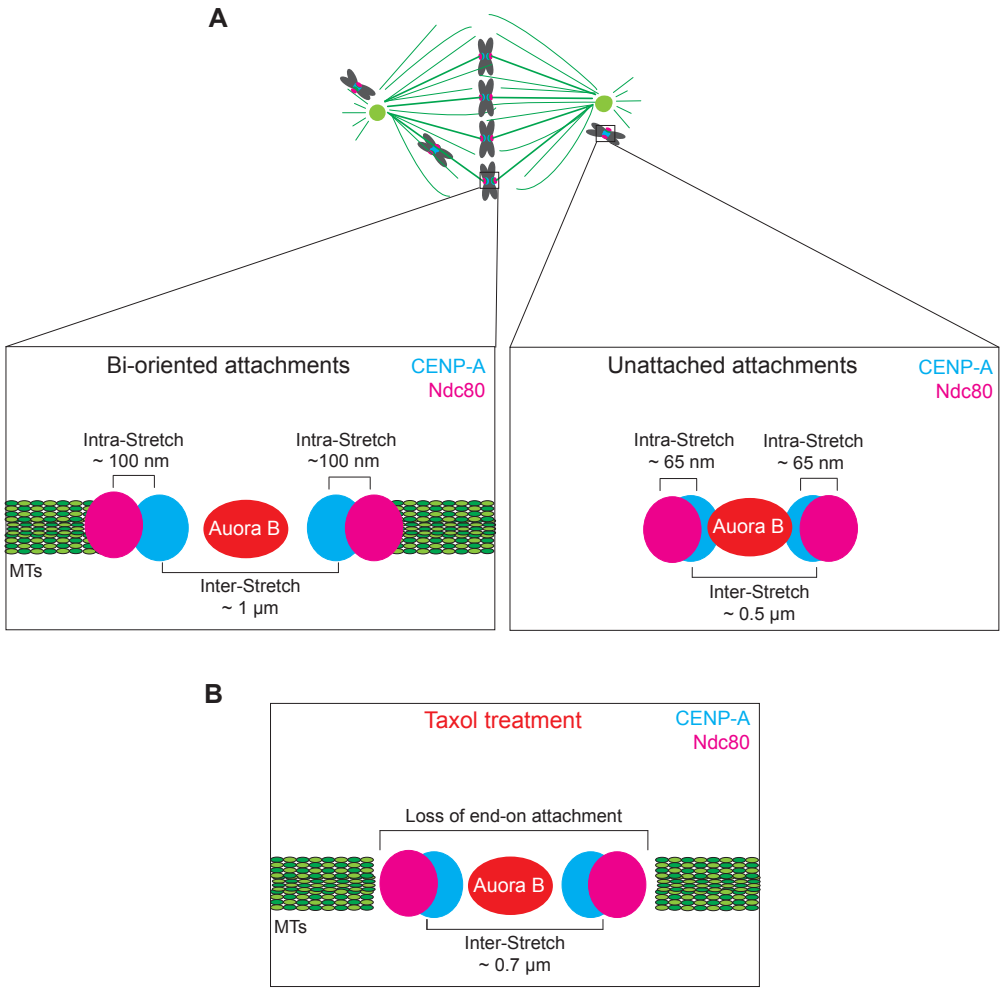

Figure 4.1 The proposed tension-based models. (**A**) Illustration of pseudo-metaphase cells depicting bi-oriented and unattached kinetochores. According to the "spatial separation" and the "kinetochore stretch" models, kinetochores that capture microtubules emanating from the opposite spindle pole generate tension that separates Aurora B from the Ndc80 complex. This configuration decreases the phosphorylation of the Ndc80 complex and thus, promoting the stabilization of kinetochore-microtubule attachments. At unattached kinetochores or mal-attached kinetochores, Aurora B remains in close proximity to the Ndc80 complex, increasing its phosphorylation that leads to the destabilization of mal-attached kinetochores. (**B**) Illustration depicting how taxol treatment affects inter-kinetochore stretch and intra-kinetochore after bi-orientation. Taxol treatment decreases the inter-kinetochore to ~0.7 µm by affecting the end-on attachment configuration.

First, the proximity-based model assumes that the kinase activity of Aurora B remains constant, but rather the main source of kinase activity regulation is predicted by the relative distance between the kinase and its substrates, i.e. a close proximity of a substrate to the kinase increases the likelihood of phosphorylation. A study using an Aurora B phosphorylation FRET (Förster Resonance Energy Transfer) biosensor provide evidence that supports this assumption (Liu et al., 2009). Measurements using the FRET phosphorylation sensor revealed a differential FRET emission signal based on the position of the FRET biosensor along the centromeres and kinetochores. While the centromere-targeted sensor was constitutively phosphorylated in a tension independent manner, the kinetochore-targeted sensor was phosphorylated when tension was low and dephosphorylated when tension was high (Liu et al., 2009; Welburn et al., 2010). Furthermore, re-positioning Aurora B from the centromeres to the outer kinetochore using genetic manipulations, resulted in the constitutive phosphorylation of the outer kinetochore substrates, supporting the proximity of Aurora B to its substrate model (Liu et al., 2009). However, the same study also showed a highly variable phosphorylation pattern at outer kinetochores that were under tension, which suggest that phosphorylation of outer-localized kinetochore substrates is highly dynamic and tension alone cannot explain this variation.

Second, besides the proximity of the kinase to its substrates, the "spatial separation" model also assumes Aurora B remains at the inner centromere with a low diffusion rate. However, several studies suggest otherwise. First, in complex with the CPC, Aurora B have been shown to have an elongated "diffusive-like" shape that extends approximately 40-50 nm from the centromere region towards the kinetochore (Bolton et al., 2002). Second, fluorescence recovery after photobleaching (FRAP) analyses, showed that the exchange of Aurora B between the centromeric and cytoplasmic pool before anaphase onset is highly dynamic, occurring within seconds (Murata-Hori and Wang,

2002). Lastly, FRAP analyses of the CPC component, Survivin, showed a highly dynamic cytosolic to centromere shuffling during prometaphase and metaphase (Delacour-Larose et al., 2004). These data suggest that Aurora B kinase alone or as part of the CPC at centromeres is not stable. Therefore, future experiments are needed to elucidate whether the dynamic association of Aurora B to centromeres affects the phosphorylation of the outer-localized kinetochore components.

In addition to a low diffusion rate from centromeres, the "spatial separation" model also assumes Aurora B primarily localizes to the inner centromere. However, in mammalian cells, an active pool Aurora B has been found to associate with outer kinetochores, with levels decreasing only slightly from early prometaphase to metaphase (DeLuca et al., 2011). In addition, in mouse spermatocytes, Aurora B is known to remain closely associated with kinetochores during metaphase I and metaphase II (Parra et al., 2006; Parra et al., 2003). Upon progression from prometaphase I to metaphase II, the inner-centromeric pool of Aurora B diminishes while the adjacent kinetochore pool is known to remain (Parra et al, 2006). Consistent with these findings, abrogating the inner centromere targeting of the homolog of Aurora B, lpl1 in budding yeast, did not disrupt proper chromosome segregation during mitosis or meiosis (Campbell and Desai, 2013). However, the function of this kinetochore pool remains poorly understood. Thus, future experiments by selectively disrupting the kinetochore pool should provide insights on the role of this population in stabilizing kinetochore-microtubule attachments.

The distance between sister kinetochores (inter-kinetochore stretch), was first proposed as a readout for tension (Waters et al., 1996). As a continuation of the tension-based concept, multiple groups proposed that tension exerted at the kinetochore upon microtubule attachment (intra-kinetochore stretch), regulates the stabilization of kinetochore-microtubule attachments (**Figure**

4.1A) (Mascara and Salmon, 2009; Uchida, et al., 2009). Indeed, disruption of the constitutive centromere-associated network (CCAN) components, CENP-C and CENP-T, which have been implicated in the generation of intra-kinetochore stretch, was shown to affect Aurora B-mediated phosphorylation of the outer kinetochore component, Ncd80 (Suzuki et al. 2014). However, only a 10 nm change in intra-kinetochore was observed and this small change alone cannot explain the sharp downregulation in phosphorylation that occurs at bi-oriented kinetochores. Importantly, it has been challenging to reach a definitive conclusion on whether tension (inter- or intra-kinetochore stretch) mediates the stabilization of microtubule attachments since the generation of tension depends on microtubule attachment and the stabilization of microtubule attachments depends on tension according to both tension models.

Recent studies, however, provide evidence for a new model based primarily on microtubule attachment. First, a study using a non-phosphorylatable version of the core microtubule-binding, Hec1 component found that changes in intra-kinetochore stretch are not required to regulate the stabilization of kinetochore-microtubule attachments (Tauchman et al., 2015; Etemad et al., 2015). Importantly, expressing this non-phosphorylatable mutant in cells can uncouple microtubule attachment from tension. In other words, cells expressing this non-phosphorylatable mutant can bind to microtubules tightly, but are unable to generate tension under conditions that prevent bi-orientation. Expressing this non-phosphorylatable mutant was sufficient to induce the stabilization of kinetochore-microtubule attachments and cells were able to progress through mitosis in the absence of tension. Second, time-lapse microscopy combined with electron microscopy analysis of taxol-treated cells, which disrupts intra-kinetochore stretch (**Figure 4.1B**), showed that targeting of the outer component and a well-characterized microtubule-attachment marker, Mad2 was sufficient to mediate mitotic progression (Waters et al., 1998; Magidson et al., 2016). In sum, these

results suggest that microtubule attachment is sufficient to promote the stabilization of kinetochore-microtubule attachments and not tension (inter- and/or intra-kinetochore stretch).

The unique structural features of CENP-E facilitate the stabilization of kinetochore-microtubule attachments before and after bi-orientation

The studies discussed thus far and the results presented in this thesis leads me to propose a new model: Aurora B-mediated phosphorylation of the outer kinetochore substrates is regulated by the microtubule capture activity of CENP-E. My model is supported by multiple observations: (1) Disruption of both inter- and intra- kinetochore stretch using taxol does not induce Aurora B-mediated phosphorylation of the Ndc80 complex, as predicted by the tension models, however inhibition of the motor motility of CENP-E induces an increase in Aurora B-mediated phosphorylation of the Ndc80 complex; (2) A decrease in inter-kinetochore stretch, which should according to the tension-based models, induce an increase in the Aurora B-mediated phosphorylation of Ndc80 complex, does not in cells depleted of CENP-E by RNAi; (3) Disruption of the motor motility of CENP-E either genetically or chemically, induces an increase in Aurora B-mediated phosphorylation of Ndc80 complex at bi-oriented attachments, which would otherwise be kept low under normal conditions; (4) At unaligned kinetochores that lack tension, perturbation of CENP-E function leads to an upregulation of Aurora B-mediated phosphorylation of the Ndc80 complex compared to control conditions; (5) Microtubule attachment alone, without inducing tension, is sufficient to decrease Aurora B-mediated phosphorylation of the Ndc80 complex, which is dependent on both the motor motility and the coiled-coil domain of CENP-E.

The discovery of CENP-E as a kinetochore-associated kinesin motor led to the proposal of CENP-E as being the major component responsible for powering chromosome movement along the microtubules of the mitotic spindle (Yen et al., 1991; Yen et al., 1992). Certainly, multiple

subsequent studies provide evidence for this role: (1) Antibodies addition against CENP-E blocks the microtubule depolymerization-dependent minus end–directed movement of purified chromosomes (Lombillo et al., 1995); (2) Immunodepletion of CENP-E from *Xenopus* egg extracts disrupts chromosome congression to the metaphase plate (Wood et al., 1997); (3) Microinjection of antibodies against CENP-E, RNAi-mediated depletion of CENP-E from mammalian cells, or genetic disruption of the *Cenp-e* gene in mice, prevents chromosome alignment and causes accumulation of misaligned chromosomes near the spindle poles (Schaar et al., 1997; Yao et al., 1997; Martin-Luesma et al., 2002; McEwen et al., 2001; Putkey et al., 2002); (4) Monooriented chromosomes near the poles are able to congress to the metaphase plate in a CENP-E-dependent manner (Kapoor et al., 2006). Thus, CENP-E is a prominent mitotic kinesin involved in chromosomal transport.

As other conventional kinesin motors, CENP-E has been proposed to be regulated by autoinhibition. In the absence of kinetochore association, CENP-E has been proposed to remain in an inhibited, folded-state (Espeut et al., 2008). *In vitro* studies showed that as a soluble molecule, the tail domain of CENP-E can bind to the motor domain, thus inhibiting the microtubule-stimulated ATPase activity. This inhibited state was proposed to be reversed by phosphorylation of the tail domain by the mitotic kinases cyclin B/Cdk1 or Mps1 (Espeut et al., 2008). A more recent study suggested that the coiled-coil domain of CENP-E mediates the autoinhibition of CENP-E (Vitre et al., 2014). Using a construct with a truncated shorter coiled-coil domain, similar to the Mini mutant described in this thesis, this truncated mutant failed to bind microtubules *in vitro* unless a cargo was bound via its C-terminal tail domain (Vitre et al., 2014). However, my data of the intra-molecular distance of CENP-E, suggest that expressing a similar truncated mutant did not produce a folded conformation. Rather, it showed a fully extended conformation, with only

a slight reduction at unaligned kinetochores. This suggests an experimental discrepancy, which could be attributed to *in vitro* systematic differences. Future experiments with higher temporal resolution in combination with biochemical and structural work should elucidate the role of the coiled-coil domain in regulating the autoinhibition of CENP-E molecules.

Nevertheless, it is important to mention that unlike conventional kinesin motors, purified CENP-E molecules were never found in a two-state conformation (Kim et al., 2008; Hirokawa et al.,1989). Instead, in *vitro* CENP-E assembles into various uncategorizable conformations, which are mediated by the 230 nm long and flexible coiled-coil domain (Kim et al., 2008). This feature to my knowledge has not been observed in other kinesin molecules. The intra-molecular distance analysis of kinetochore-associated CENP-E shown in this thesis supports this *in vitro* finding. In all cases analyzed including in the presence or absence of microtubule attachment, the intra-molecular distance of CENP-E at the kinetochore showed a high variability in length that did not relate linearly to the counter length of a fully-extended CENP-E molecule. Conversely, the intra-molecular distance of Ncd80 complex measured using similar experimental conditions was almost a constant 45 nm with a very low variance (Wan et al., 2009). Therefore, this suggests that the flexibility of CENP-E is likely maintained at the soluble state and upon association with kinetochores.

Taking the structural uniqueness of the coiled-coil domain into consideration, I hypothesize CENP-E has evolved from other kinesin members to mediate the stabilization of kinetochore-microtubule attachment in vertebrate cells, rather than to mediate canonical cargo transport. My hypothesis is supported by multiple observations: (1) While inhibition or removal of CENP-E from mammalian cells or disruption of the *Cenp-e* gene in mice leads to metaphase chromosome misalignment, the majority of chromosomes are still able to align at the metaphase plate (Yao et

al., 1997; Martin-Luesma et al., 2002; McEwen et al., 2001; Putkey et al., 2002); (2) Inhibition or depletion of CENP-E reduces the number of microtubules bound to kinetochores at both unaligned and aligned chromosomes (McEwen et al., 2001; Putkey et al., 2002; Weaver et al., 2003); (3) CENP-E can track both the polymerizing and the depolymerizing ends of dynamic microtubules *in vitro* (Gudimchuk et al., 2013), which suggest CENP-E can convert from a lateral transporter into a microtubule plus-end and minus-end tracker; (4) Disrupting the motor function genetically or chemically and genetic perturbations of the coiled-coil domain affects both the generation and the maintenance of chromosome alignment at the metaphase plate (Gudimchuk et al., 2013 and this thesis); (5) CENP-E regulates the Aurora B kinase activity, a major regulator involved in the stabilization of kinetochore-microtubule attachment (Guo at al., 2012 and this thesis); (6) In budding yeast, which have no functional CENP-E orthologue, chromosome movement is mediated by a kinesin-5 homologue, which has a coiled-coil domain similar to that of kinesin-1 family. Therefore, it is plausible to speculate that the unique coiled-coil domain of CENP-E is a specialized motor in vertebrate cells. These kinetochores are known to assemble larger complexes that bind 20-25 microtubules than those found in yeasts, which only bind one microtubule (Cheeseman and Desai, 2008).

According to the intra-molecular measurements of CENP-E, CENP-E undergoes a conformational change from 122.8 nm at unattached kinetochores to 81.5 nm at unaligned kinetochores and extends back to 123.5 nm at aligned kinetochores (**Figure 4.2**). Chemical inhibition of the plus-end-directed motor motility or perturbations of the flexible coiled-coil domain of CENP-E perturbs this change. Indirect immunofluorescence analysis of Mad1 (microtubule attachment marker) revealed a significant decrease in the fluorescence signal at unaligned kinetochores compared to unattached ones. Therefore, I propose the majority of these

unaligned kinetochores are laterally attached. However, since there is no bonafide marker for laterally-attached kinetochores identified to date, electron microscopy analysis should be use to confirm the microtubule composition of these unaligned kinetochores. Nevertheless, these data suggest that CENP-E undergoes a conformational change specifically at unaligned kinetochores where Aurora B-mediated phosphorylation of the outer-localized kinetochore substrates is high, which can provide important mechanistic insights into the stabilization of kinetochore-microtubule attachment prior to bi-orientation.

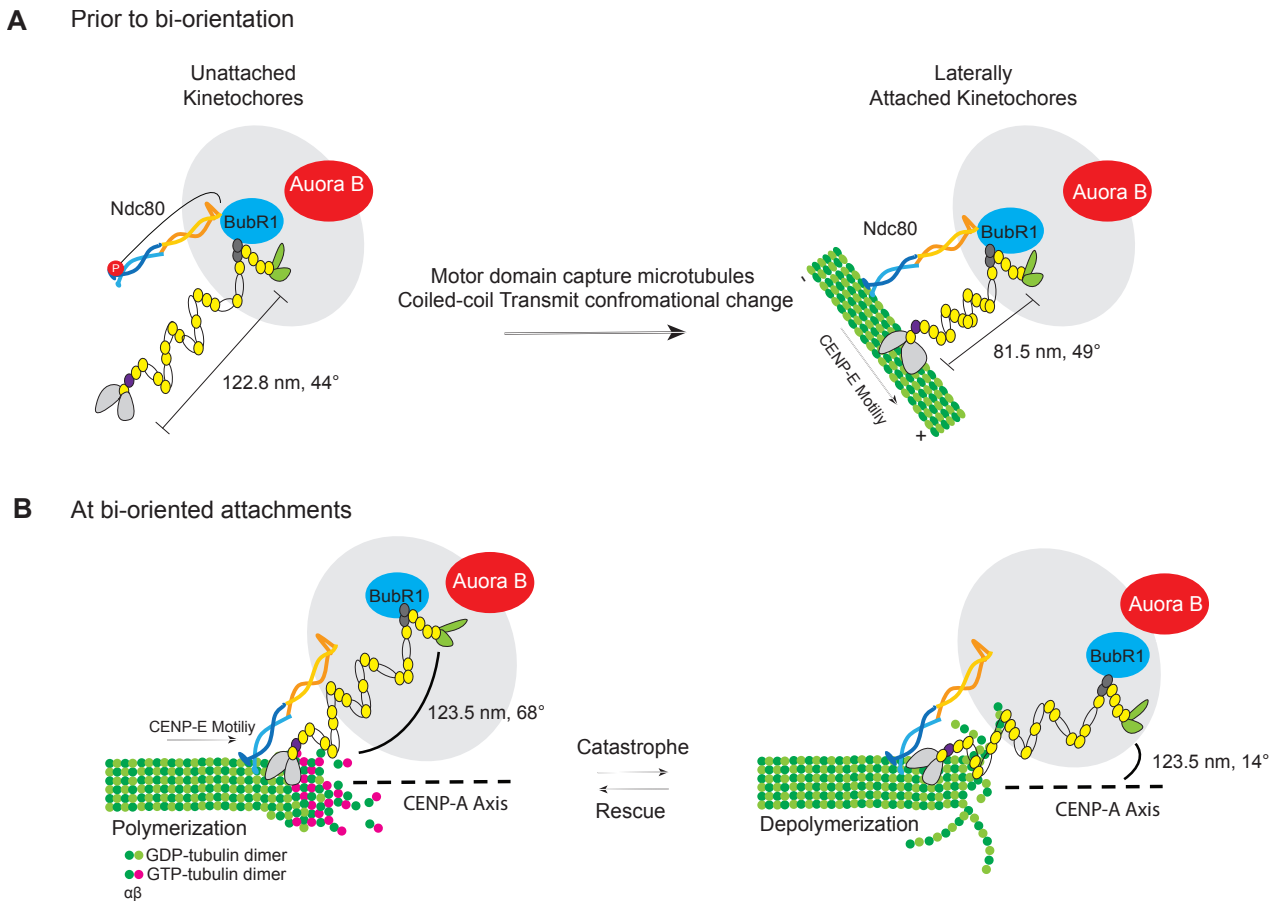

Figure 4.2 Proposed models for the role of CENP-E in the stabilization of kinetochore-microtubule attachments (**A**) Prior to bi-orientation, the motor domain captures microtubule by binding to the lateral walls of microtubules. Microtubule capture and the plus end-directed motility induces a conformational change that is transduced through the flexible coiled-coil domain of CENP-E. This conformation inactivates BubR1 kinase activity, which in turn downregulates Aurora B-mediated phosphorylation of the Ndc80 complex, leading to the stabilization of kinetochore-microtubule attachments (**B**) After bi-orientation is established, CENP-E facilitates the maintenance of the end-on configuration by tracking the growing and shrinking ends of microtubules by re-arranging into a two-state conformation.

Previous studies provide an important mechanistic possibility through the direct interaction of CENP-E with the kinetochore-associated mitotic kinase, BubR1. CENP-E has been shown to activate the kinase activity of BubR1 and microtubule capture by CENP-E inactivates BubR1 kinase activity *in vitro* (Mao et al., 2003; Mao et al., 2005). Further studies on the kinase function of BubR1, identified a BubR1 autophosphorylation site at Threonine 608 (Guo at al., 2012). Phosphorylation at this site was found to be dependent on both, the kinetochore localization of CENP-E, and the presence of kinetochore-microtubule attachments in mammalian cells (Guo at al., 2012). Bridging the BubR1-CENP-E interaction with the Aurora B pathway, this study also showed Aurora B-mediated phosphorylation of the Ndc80 complex was reduced in cells depleted of CENP-E and upon expression of a non-phosphorylatable mutant, but not the phosphomimetic, form of BubR1 (Guo at al., 2012). Importantly, previous studies showed that phosphorylation of BubR1 is reduced in laterally attached kinetochores (Guo, 2012).

To determine whether the microtubule capture activity of CENP-E affects BubR1 kinase activation/inactivation, I tested the levels of pT608-BubR1 in cells expressing a motorless construct (Tail) or mutants with a disrupted coiled-coil domain (Mini and Chimera) (**Figure 4.3**). Expressing the kinetochore Tail domain alone was sufficient to induce BubR1 phosphorylation at Threonine 608 in cells lacking microtubule attachments (**Figure 4.3, A and C**). Similarly, the Tail domain was also sufficient to stimulate Aurora B-mediated phosphorylation of pS55-Hec1 (**Figure 4.3, B and D)**. These results suggest CENP-E regulates Aurora B-mediated phosphorylation of outer kinetochore components through its interaction with BubR1. Therefore, I propose that upon lateral attachment, CENP-E undergoes a conformational change that can be transduced through BubR1 to regulate Aurora B-mediated phosphorylation of outer kinetochore components (**Figure 4.2A**). The plus-end directed motility of CENP-E induces a conformation change that can be

transmitted through the flexible coiled-coil domain of CENP-E. In turn, this inactivates BubR1 kinase activity, promoting the stabilization of kinetochore-microtubule attachment by downregulating Aurora B-mediated phosphorylation of outer kinetochore components.

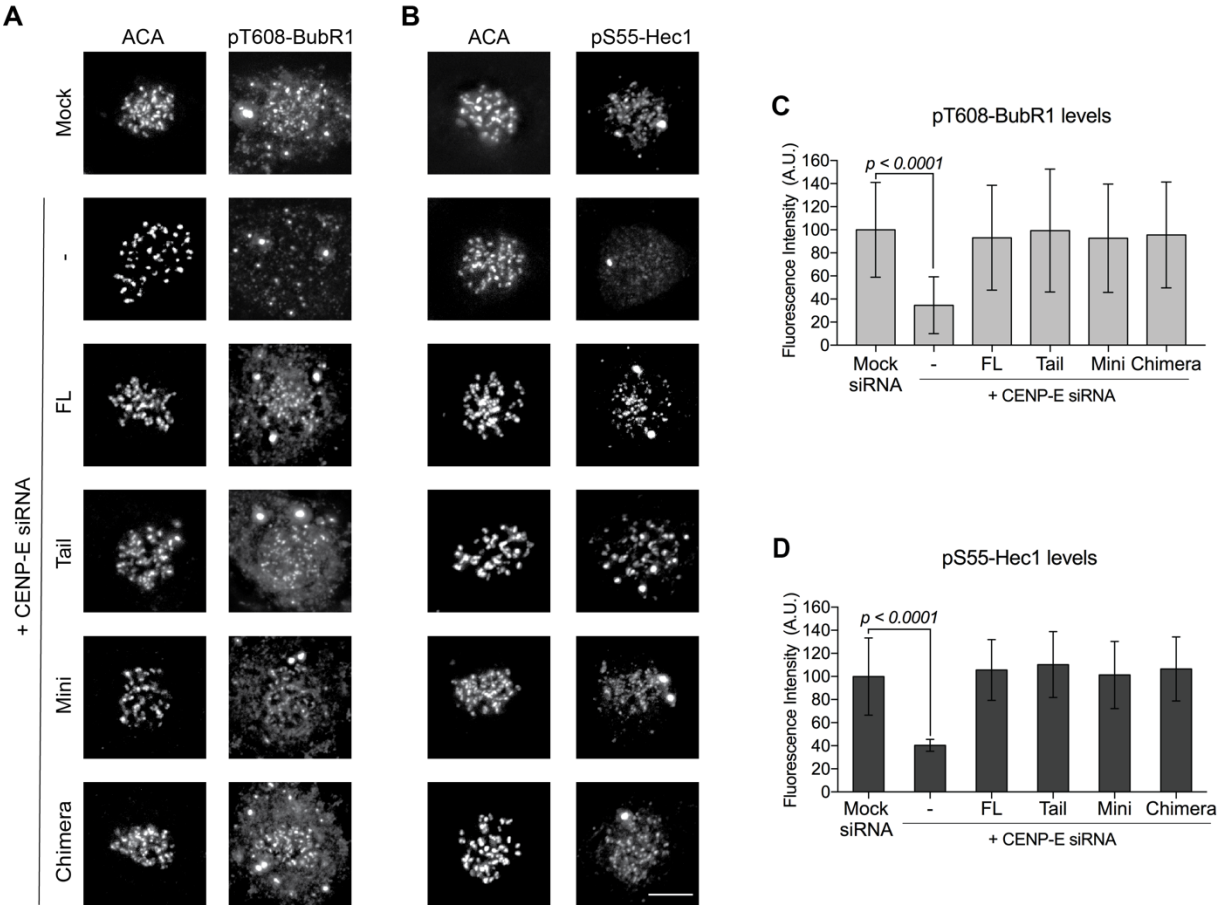

Figure 4.3 The tail domain of CENP-E is sufficient to induce BubR1 autophosphorylation and Aurora B-mediated Hec1 phosphorylation at unattached kinetochores. (**A**) Immunofluorescence analysis of nocodazole-treated T98G cells. Phosphorylation of BubR1 was assessed with a pT608-BubR1 antibody and kinetochores were stained with ACA. (**B**) Immunofluorescence analysis of nocodazole-treated T98G cells. Phosphorylation of Hec1 was assessed with a pS55-Hec1 antibody and kinetochores were stained with ACA. (**C**) Quantification of the relative fluorescence intensity of pS55-Hec1 at unattached kinetochores. Mean ± SD of three independent experiments are shown, ≥ 200 kinetochores per group quantified. (**D**) Quantification of the relative fluorescence intensity of pS55-Hec1 at unattached kinetochores. Mean ± SD of three independent experiments is shown, of ≥ 200 kinetochores per group quantified.

Future experiments should further confirm the lateral microtubule attachment sensing function of CENP-E. A FRET tension sensor should be used to confirm the structural behavior of CENP-E. Additionally, cells depleted of Hec1 can also be tested. Kinetochores depleted of Hec1 cannot establish end-on attachment are known to maintain lateral attachment through their interactions with Dynein and CENP-E (Kapoor et al., 2006; Cai et al., 2009). Assessment of these laterally-attached kinetochores will determine whether the phosphorylation of outer kinetochore substrates such as the mDia3 by Aurora B is affected in cells with perturbed CENP-E function.

In addition to the microtubule capture activity at lateral microtubules, CENP-E also actively maintains bi-oriented, end-on attachment at the metaphase plate (Gudimchuk et al., 2013). Consistent with this function, we found an upregulation in the Aurora B-mediated phosphorylation of the Ndc80 complex upon inhibition of the motor motility of CENP-E or perturbations of the coiled-coil domain. Strikingly, analysis of the angular conformation of full-length CENP-E along the kinetochore (CENP-A) axis yielded bi-modal distribution. On the other hand, this bi-modal distribution was not found at unattached or at unaligned kinetochores. This suggests CENP-E assumes two major conformations at end-on attached kinetochores.

Previous studies on the configuration of kinetochore components at end-on attached kinetochores identified a bent and rigid lateral linkage of the Ndc80 complex through an elongated interaction with the Mis12 complex and KNL1 (Wan et al., 2009). The study proposed the existence of a flexible linkage that could transmit the pulling forces generated by curling protofilaments of a microtubule to the inner kinetochore (Wan et al., 2009). However, no such linkage has been identified in vertebrate cells. I hypothesize, CENP-E undergoes a conformational change in response to microtubule dynamics by acting as a flexible linkage that helps track the depolymerizing and polymerizing ends of microtubule through the rigid binding of the Ndc80

complex (**Figure 4.2B**). Indeed, *in vitro* studies, have characterized CENP-E as a microtubule tip-tracker, tracking both the growing and shrinking end of microtubules (Gudimchuk et al., 2013).

The bi-modal distribution may be also attributed to CENP-E interactions with microtubule-associated proteins. Certainly, CENP-E has been shown to interact directly with the conserved kinetochore- and microtubule-associated proteins, CLASP1 and CLASP2, which are known to regulate kinetochore-microtubule dynamics (Maiato et al., 2003; Maffini et al., 2009). In human cells, RNAi-mediated depletion of CLASPs proteins or CENP-E caused a reduction in kinetochore-microtubule poleward flux and turnover rates (Maffini et al., 2009). Future experiments should elucidate whether this interaction is critical to sustaining the distinct distribution of CENP-E at end-on attached kinetochores.

Recruitment of phosphatases to the kinetochore balances the phosphorylation of outer kinetochore-associated components

The balance of phosphorylation of the outer-localized kinetochore components by Aurora B can be regulated by at least two different non-mutually exclusive mechanisms, either by regulating Aurora B kinase activation directly or by regulating the recruitment of phosphatases. I ruled out the possibility of a kinase targeting misregulation because I did not find any perturbation in the targeting of Aurora B to centromeres/kinetochores (data not shown). Additionally, the targeting of the outer kinetochore components including CENP-E, BubR1, and Mad1, a process that is dependent on Aurora B kinase activity was not disrupted under the different conditions analyzed. Therefore, a deregulation of the full-on kinase activation is unlikely. However, to further confirm this conclusion, I will determine whether the active pool of Aurora B association to centromeres/kinetochores is disrupted using a phospho-specific antibody that recognizes the active form of Aurora B kinase.

The serine/threonine phosphatases, PP1 and PP2A, are the most abundant phosphatases found in mammals that are known to counteract Aurora B-mediated phosphorylation of outer kinetochore substrates (De Wulf et al., 2009). However, the mechanism by which PP1 and PP2A contribute to the stabilization of kinetochore-microtubule attachments prior to bi-orientation is still unclear, especially since PP1 only localizes to kinetochores after bi-orientation and PP2A localizes to both centromeres and kinetochores from early prometaphase until metaphase (Liu et al., 2010; Posh et al., 2010; Foley et al., 2011). Therefore, the process that links these two phosphatase-mediated processes needs further investigation.

Nevertheless, there are several reported pathways known to mediate the recruitment of these phosphatases to kinetochores. PP2A and its regulatory domain have been shown to be recruited to kinetochores via an interaction with BubR1. Phosphorylation of the KARD domain of BubR1 by PLK1 kinase promotes direct interaction of BUBR1 with the PP2A-B56α phosphatase (**Figure 4.4A**) (Suijkerbuijk et al., 2012b). I tested whether PP2A-B56α recruitment to kinetochores is affected in cells expressing the mutant forms of CENP-E or upon inhibition of the motor motility of CENP-E (**Figure 4.4B, C, and D**). Indirect immunofluorescence analysis of PP2A-B56α did not show any significant difference in the kinetochore targeting of PP2A-B56α in cells expressing the mutant forms of CENP-E or upon inhibition of CENP-E's motor motility at both aligned or at unaligned kinetochores (**Figure 4.4B, C, and D**). This suggests that the BubR1-mediated recruitment of PP2A-B56α to kinetochores is unlikely to be involved in the regulation of the Aurora B-mediated phosphorylation of outer kinetochore components via the microtubule capture activity of CENP-E.

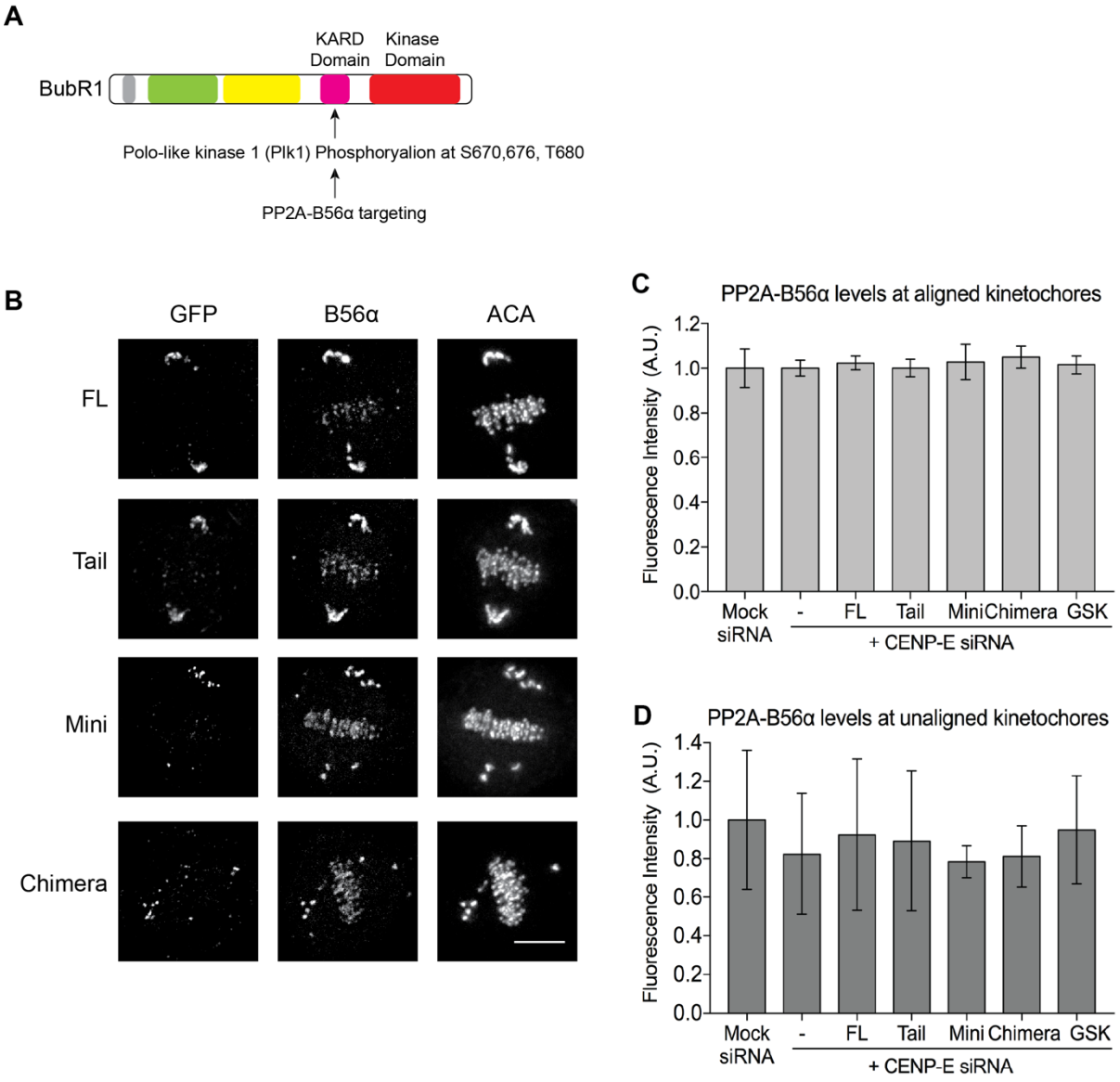

Figure 4.4 Perturbing CENP-E function does not affect PP2A-B56α recruitment to kinetochores. (**A**) Illustration depicting the site PP2A-B56α recruitment in BubR1. Phosphorylation of the KARD domain by Plk1 promotes PP2A-B56α recruitment. (**B**) Immunofluorescence analysis of pseudo-metaphase T98G cells with aligned and unaligned kinetochores expressing the full-length and mutant forms of CENP-E. GFP, B56α, and ACA were used to label CENP-E, PP2A-B56α, and kinetochores, respectively. (**C and D**) Quantification of the normalized relative fluorescence intensity PP2A-B56α at (**C**) aligned kinetochores and (**D**) unaligned kinetochores. (**C and D**) Mean ± SD of three independent experiments is shown, of ≥ 200 kinetochores per group quantified.

In vertebrate cells, two isoforms of PP1 are known to localized to the outer kinetochore (Trinkle-Mulcahy et al., 2006). PP1 is targeted to kinetochores by either an interaction with KNL1 or through an interaction with CENP-E (Liu et al., 2009 and Kim et al., 2010). Specifically, a docking site for PP1 can be found near the motor domain of CENP-E and phosphorylation of this domain by Aurora B disrupts the kinetochore targeting of PP1 (Kim et al., 2010) (**Figure 4.5A**). Hence, PP1 is a likely candidate to counteract Aurora B-mediated phosphorylation of outer kinetochore components following microtubule capture by CENP-E. Therefore, I assessed whether the isoform, PP1α recruitment to kinetochores is affected in pseudo-metaphase cells expressing the mutant forms of CENP-E or upon chemical inhibition of the motor motility of CENP-E (**Figure 4.5B, C, and D**). I found a significant decrease in PP1α immunofluorescence levels at both aligned and unaligned kinetochores in cells expressing the CENP-E mutant constructs and upon motor motility inhibition (**Figure 4.5B, C, and D**). These results suggest a decrease in PP1α are consisting with the upregulation in Aurora B-mediated phosphorylation observed in cells expressing the defective forms of CENP-E.

However, PP1α recruitment in CENP-E depleted cells was not affected as expected from previous studies (Kim et al., 2010). This suggests the recruitment of PP1α in the absence of CENP-E can be compensated by the KNL1 recruitment pathway. Alternatively, since there are two major isoforms of PP1 recruited to kinetochores, PP1α and PP1γ, future analysis of PP1 should determine whether there is a differential recruitment depending on the isoform as well as another possible pathway that mediates PP1 recruitment.

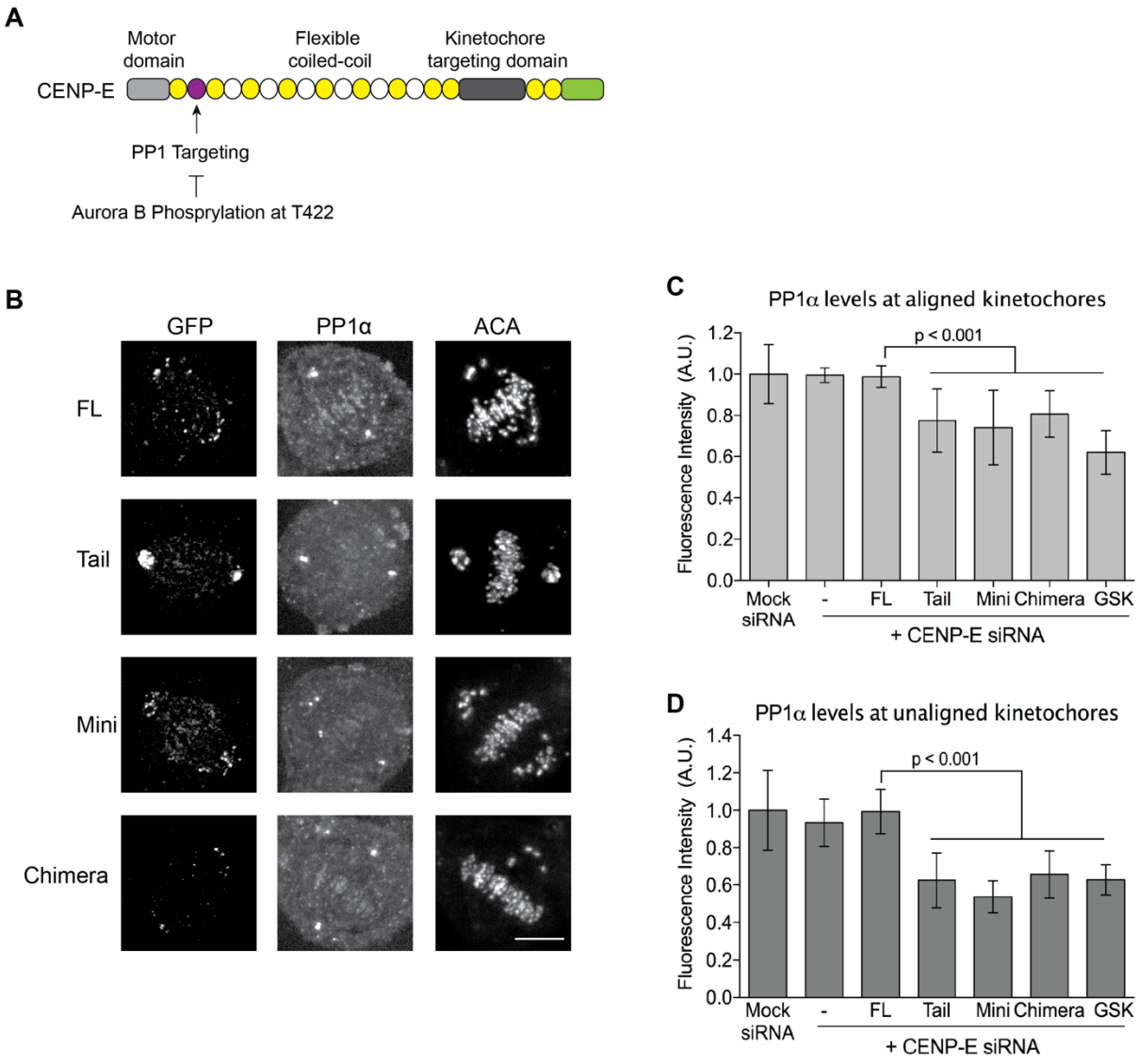

Figure 4.5 Perturbing CENP-E function affects PP1α recruitment to kinetochores. (**A**) Illustration depicting the site PP1α recruitment in CENP-E. Phosphorylation of the threonine 422 domain by Aurora B prevents PP1 recruitment (**B**) Immunofluorescence analysis of pseudo-metaphase T98G cells with aligned and unaligned kinetochores expressing the full-length and mutant forms of CENP-E. GFP, PP1α, and ACA were used to label CENP-E, PP1α, and kinetochores, respectively. (**C and D**) Quantification of the normalized relative fluorescence intensity PP1α at (**C**) aligned kinetochores and (**D**) unaligned kinetochores. (**C and D**) Mean ± SD of three independent experiments is shown, of ≥ 200 kinetochores per group quantified.

PART 2: Aurora B regulates the actin assembly function of mDia3

Aurora B-mediated phosphorylation activates the actin assembly function of the FH2 domain of mDia3

Previous studies of isolated FH2 fragments from various organisms, including the Bni1p from *S. cerevisiae,* the *S. pombe* Cdc12p, or the mammalian mDia1 showed a common property of affecting the barded ended actin assembly kinetics by a complete or partial capping mechanisms of filamentous actin (Pruyne et al. 2002; Sagot et al. 2002b; Pring et al. 2003; Kovar et al. 2003; Li and Higgs 2003). Structural work of isolated mouse mDia1 has shown the FH2 domain is composed of an elongated crescent-shape of almost exclusively α-helices (Shimada et al., 2004). The FH2 motif includes the residues (946–1010) originally identified as FH2 and is the best evolutionary conserved region of the formin family of proteins (Watanabe et al., 1999). Within this region, there is a highly conserved "GNXMN" motif (Shimada et al., 2004). Additionally, several lysine residues cluster found in this motif have been shown to play a role in the actin assembly function of the FH2 domain of mDia1 (Ishizaki et al., 2001).

I conducted a primary protein sequence alignment of mDia1 and mDia3 to determine where the Aurora B phosphorylation sites lie along this conserved motif and the consecutive lysine clusters (**Figure 4.6**). Strikingly, both the lysine residues and the GNXMN were found in the middle of the two Aurora B phosphorylatable sites of mDia3 (**Figure 4.6**). In particular, the region around the highly conserved GNXMN motif was previously shown to be really flexible (Shimada et al., 2004). Therefore, I hypothesize Aurora B-mediated phosphorylation of these two sites regulates the flexibility of this motif to stabilize the actin assembly function of the FH2 domain of mDia3. My results showed that replacement of the phosphorylatable residues to alanines residues completely arrogates the actin polymerization function of mDia3, whereas the phosphomimetic

form of mDia3 induced the actin polymerization function of mDia3. To test my hypothesis, I will replace mDia1 and mDia2 phosphomimetic residues to a serine or to alanines residues and test whether these replacements downregulates the actin polymerization function of the FH2 domain. Additionally, structural studies should elucidate whether the flexibility and stabilization around the highly conserved GNXMN motif and the lysine clusters is regulated by phosphorylation.

Besides the possibility of an intrinsic structural regulation, alternatively, phosphorylation of the FH2 domain of mDia3 by Aurora B might alter the actin polymerization function by interaction with other effectors molecules. Previous mass spectrometry studies using the FH2 domain of mDia3 as a bait identified several proteins that directly bind to the FH2 domain. Importantly these proteins uniquely interacted with the FH2 domain of mDia3 and not with the FH2 domain of mDia1 or mDia2 (Daou et al., 2014). Some of these unique interactions include cytoskeleton components, such as the prelamin-A/C (LMNA) and latent-transforming growth factor beta-binding protein 3 (LTBP3). Prelamin-A/C plays an important role in nuclear assembly, chromatin organization, nuclear membrane and telomere dynamics (Capell and Collins, 2006). LTBP3 has been described as a secreted protein that contributes to the extracellular matrix (Daou et al., 2014). Therefore, mDia3 might interact with a specific pool of LTBP3 that enters or remains in cells and with prelamin-A/C at the nucleus. Future experiments should confirm these interactions and their effects on the intracellular localization and the actin assembly function of mDia3.

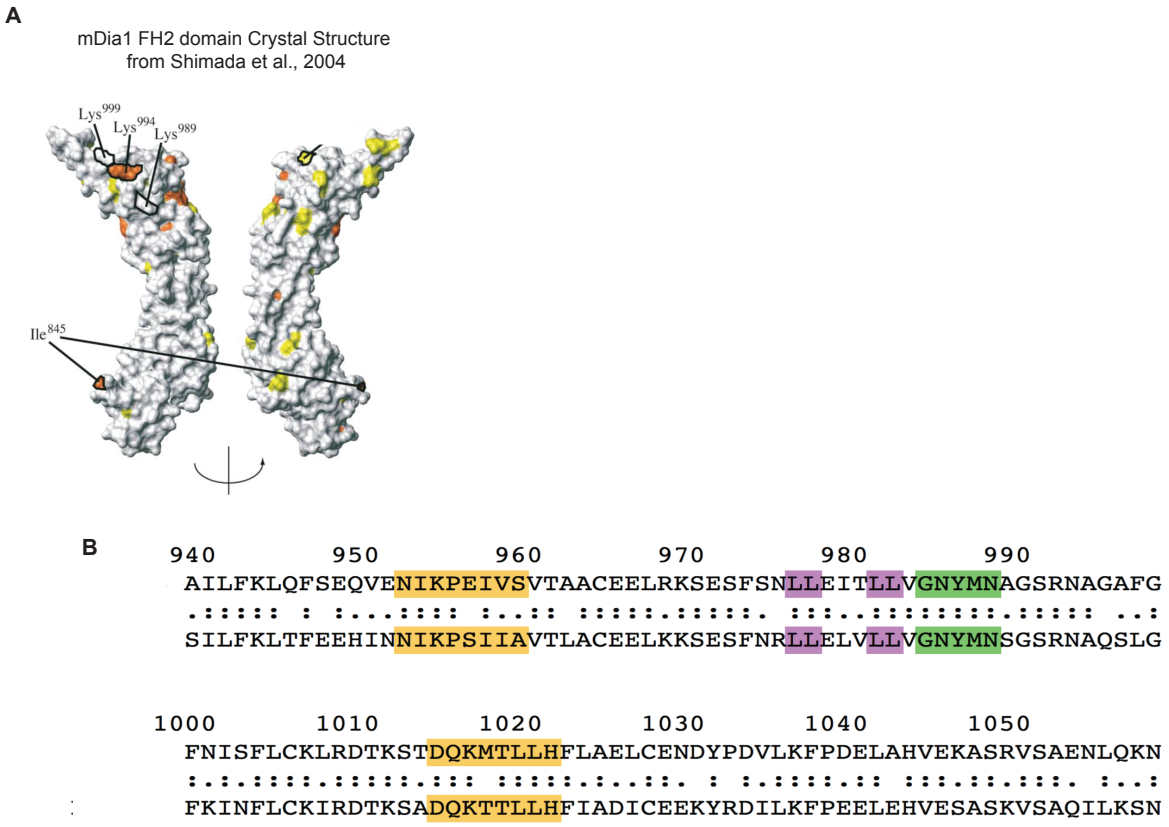

Figure 4.6. The highly conserved "GNXMN" motif and lysine residues are critical for the actin nucleation and elongation function of formins. (**A**) Monomeric structure of mouse FH2 domain adapted from *Shimada et al., 2004* showing the location lysine residues along the FH2 domain. (**B**) Primary sequence alignment of human mDia1 (top) and human mDia3 (bottom) were conducted using Pairwise Sequence Alignment (LALIGN) powered by the EMBL European Bioinformatics Institute. Note, all three isoforms of mDia3 showed conservation of these regions.

Aurora B-mediated phosphorylation of mDia3 regulates the 'crosstalk' between the actin and the microtubule function of mDia3

In addition to the role in actin assembly of mDia1, mDia2, and mDia3, they have also been shown to interact with the plus ends of microtubules to promote microtubule stabilization (Wen et al., 2004; Bartolini et al., 2008; Lewkowicz et al., 2008). This suggests formin-mediated processes can link both the actin and microtubule cytoskeletons. In mitotic cells, mDia3 stabilizes kinetochore-microtubule attachments independently from its actin assembly function (Cheng et al., 2011). Specifically, Aurora B-mediated phosphorylation of mDia3 failed to bind or stabilize microtubules *in vitro* and in cells expressing the phosphomimetic form of mDia3 (Cheng et al., 2011). On the other hand, the phosphomimetic form of mDia3 or in *vitro* phosphorylation of the FH2 domain of mDia3 induced the actin assembly function of mDia3 by localizing to cellular protrusions to regulate cell migration. Therefore, I hypothesize Aurora B regulates the spatiotemporal multi-functional role of mDia3. To test my hypothesis, I will determine the intracellular localization of the wild-type and phospho-mDia3 using fluorescence microscopy. This will allow me to distinguish among the sub-cellular organization of actin and microtubule cytoskeletal using co-staining with specific markers.

Although overlapping functions have been observed for the *Diaphanous* subfamily for mDia1, mDia2, and mDia3. For instance, knockout of both mDia1 and mDia3 locus is required to induce developmental defects in the brain of mice (Thumkeo et al., 2011; Shinohara et al., 2012). However, a growing number of studies suggest the diaphanous subfamily of formins regulate different cellular processes mainly through specific interactions with specific effector molecules at precise subcellular locations (Daou et al., 2013; Miki et al., 2008; Liu and Mao, 2016; Evangelista et al., 1997; Imamura et al., 1997; Ozaki-Kuroda et al., 2001; Pellegrin and Mellor

2005; Schirenbeck et al., 2005). The wild-type FH1FH2 purified fragment from mDia3 showed a substantially low actin polymerization activity compared to the previously studied FH1-FH2 purified fragment of mDia1 and mDia2 under similar conditions (Li and Higgs, 2003; Bartolini et al., 2008). Furthermore, the velocity of the wild-type mDia3 puncta measured in cells was ~0.244 μm/sec (unpublished data) compared to the wild-type mDia1 at ~2 μm/sec or mDia2 at ~ 0.5 μm/sec (Higashida et al., 2004; Bartolini et al., 2008). Given these differential actin assembly rates, I hypothesize the actin assembly functions of the diaphanous subfamily for mDia1-3 are differentially regulated by Aurora B at distinct actin structures during cell migration. To test my hypothesis, first, I will compare the actin polymerization of phosphomimetic and non-phosphorylatable mutants of mDia1-3 using *in vitro* kinetic assays and TIRF microscopy imaging to monitor the velocity of mDia1-3 puncta in cells. I will also compare the intracellular localization of the phosphomimetic and non-phosphorylatable mutants of mDia1-3.

Aurora B regulates the cytoskeleton in interphase cells

Previous studies identified the formin homology 2 (FH2) domain-containing protein 1 (FHOD1) as a major substrate of Aurora B (Floyd et al., 2013). RNAi-mediated depletion of FHOD1 affects the cell spreading after completion of cytokinesis. Importantly, phosphorylation of FHOD1 at five different sites, including one found in the FH2 domain, induced actin polymerization at the cell cortex. Furthermore, the retention of Aurora B at the cell cortex is dependent on the FHOD1 actin assembly function (Floyd et al., 2013). The non-phosphorylatable mutant of the FH2 domain of mDia3 severely disrupted the actin polymerization function of mDia3 *in vitro* and expression in cells disrupted the ability of cells to reorganize the actin cytoskeleton in Fibronectin-coated coverslips. Thus, the kinase activity of Aurora B regulates the remodeling of

the actin cytoskeleton to facilitate entrance to interphase. To further confirm the Aurora B-dependent process, I will use time-lapse microscopy to monitor cells upon mitotic exit and determine whether there are any overlapping functions for other diaphanous-related formins (DRFs) phosphorylation-dependent functions.

Previous studies have shown Aurora B predominantly accumulates in the nucleus at the end of the G2 phase of the cell cycle. Furthermore, the anaphase-promoting complex (APC/C) ubiquitin ligase was shown to target Aurora B for degradation after cell division completion (Lindon and Pines, 2004; Stewart and Fang, 2005). Thus, this suggests Aurora B kinase activity function has been proposed to be restricted by the cell cycle. However, once inside the nucleus Aurora B, was found to shuffle from the nucleus to the cytoplasm via the exportin1-mediated nuclear export-dependent pathway (Rannou et al., 2008). Therefore, I hypothesize the function of Aurora B persists throughout the cell cycle. To this end, I conducted immunofluorescence analysis of Aurora B to determine whether Aurora can be detected in interphase cells. A former colleague in the lab was able to detect Aurora localized at cellular protrusions using a commercially available mouse monoclonal antibody, which localized with the wild-type GFP-FH1FH2-mDia3 construct (**Figure 4.7A**). I confirmed these results using a different commercially available polyclonal antibody and found structures that were reminiscent of focal adhesions structures (**Figure 4.7B**). Together, this suggests Aurora B is not exclusively found inside the nucleus and it localizes to specific cellular structures. I will further investigate the role of the cytoplasmic pool of Aurora B using focal adhesion, lamellipodia and filopodia markers and total internal reflection (TIRF) microscopy analysis of fluorescently-labeled Aurora B.

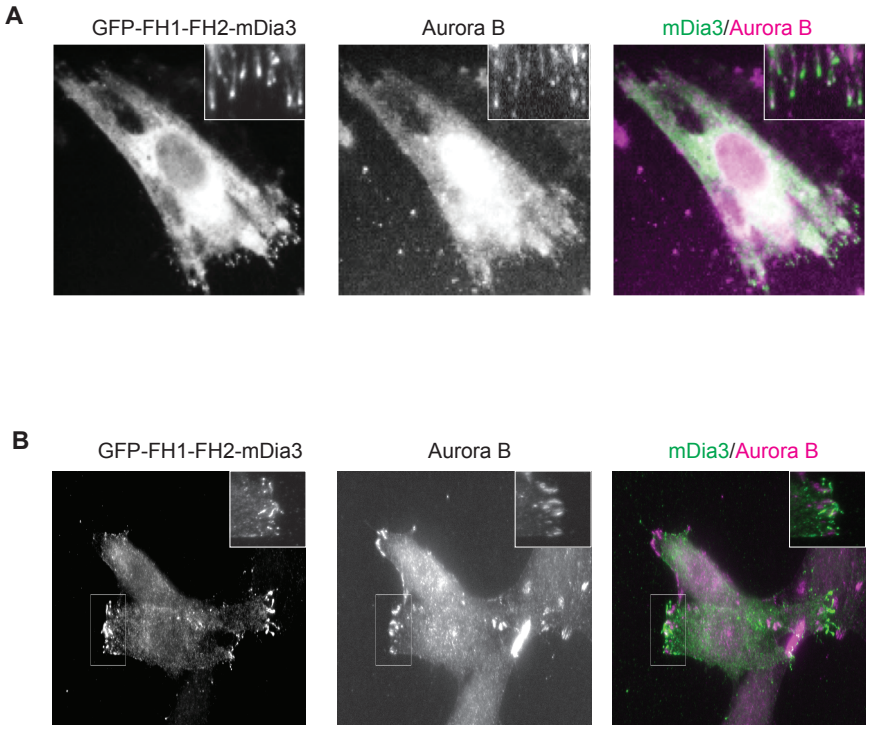

Figure 4.7. Aurora B localization during interphase. (**A**) Indirect immunofluorescence staining of NIH3T3 cells expressing the GFP-FH1FH2-mDia3. Cells were stained with a GFP antibody and a commercially available mouse monoclonal antibody (Abcam, Cat No, 3609)**.** Insets shows localization to 'filopodia-like' structures **(B)** Indirect immunofluorescence staining of NIH3T3 cells expressing the GFP-FH1FH2-mDia3. Cells were stained with a GFP antibody and a commercially available rabbit polyclonal antibody (Abcam, Cat No, 2254). Insets shows localization to 'focal adhesion-like' structures.

REFERENCES

Abrieu, A., Kahana, J.A., Wood, K.W. and Cleveland, D.W., 2000. CENP-E as an essential component of the mitotic checkpoint in vitro. *Cell*, 102(6), pp.817-826.

Alberts, A.S., 2001. Identification of a carboxyl-terminal diaphanous-related formin homology protein autoregulatory domain. *Journal of Biological Chemistry*, *276*(4), pp.2824-2830.

Andrews, P.D., Ovechkina, Y., Morrice, N., Wagenbach, M., Duncan, K., Wordeman, L. and Swedlow, J.R., 2004. Aurora B regulates MCAK at the mitotic centromere. *Developmental cell*, *6*(2), pp.253-268.

Ault, J.G. and Rieder, C.L., 1992. Chromosome mal-orientation and reorientation during mitosis. *Cell motility and the cytoskeleton*, *22*(3), pp.155-159.

Ashar, H.R., James, L., Gray, K., Carr, D., Black, S., Armstrong, L., Bishop, W.R. and Kirschmeier, P., 2000. Farnesyl transferase inhibitors block the farnesylation of CENP-E and CENP-F and alter the association of CENP-E with the microtubules. *Journal of Biological Chemistry*, *275*(39), pp.30451-30457.

Azimzadeh, J. and Bornens, M., 2007. Structure and duplication of the centrosome. *Journal of cell science*, *120*(13), pp.2139-2142.

Bakhoum, S.F., Thompson, S.L., Manning, A.L. and Compton, D.A., 2009. Genome stability is ensured by temporal control of kinetochore–microtubule dynamics. *Nature cell biology*, *11*(1), pp.27-35.

Barisic, M., Aguiar, P., Geley, S. and Maiato, H., 2014. Kinetochore motors drive congression of peripheral polar chromosomes by overcoming random arm-ejection forces. *Nature cell biology*, *16*(12), pp.1249-1256.

Bartolini, F., Moseley, J.B., Schmoranzer, J., Cassimeris, L., Goode, B.L. and Gundersen, G.G., 2008. The formin mDia2 stabilizes microtubules independently of its actin nucleation activity. *The Journal of cell biology*,*181*(3), pp.523-536.

Berg, J.S. and Cheney, R.E., 2002. Myosin-X is an unconventional myosin that undergoes intrafilopodial motility. *Nature cell biology*, *4*(3), pp.246-250.

Biggins, S., Severin, F.F., Bhalla, N., Sassoon, I., Hyman, A.A. and Murray, A.W., 1999. The conserved protein kinase Ipl1 regulates microtubule binding to kinetochores in budding yeast. *Genes & development*, *13*(5), pp.532-544.

Bione, S., Sala, C., Manzini, C., Arrigo, G., Zuffardi, O., Banfi, S., Borsani, G., Jonveaux, P., Philippe, C., Zuccotti, M. and Ballabio, A., 1998. A human homologue of the Drosophila melanogaster diaphanous gene is disrupted in a patient with premature ovarian failure: evidence

for conserved function in oogenesis and implications for human sterility. *The American Journal of Human Genetics*, *62*(3), pp.533-541.

Blower, M.D., Sullivan, B.A. and Karpen, G.H., 2002. Conserved organization of centromeric chromatin in flies and humans. *Developmental cell*, *2*(3), pp.319-330.

Bolton, M.A., Lan, W., Powers, S.E., McCleland, M.L., Kuang, J. and Stukenberg, P.T., 2002. Aurora B kinase exists in a complex with survivin and INCENP and its kinase activity is stimulated by survivin binding and phosphorylation. *Molecular biology of the cell*, *13*(9), pp.3064-3077.

Brown, K.D., Coulson, R.M., Yen, T.J. and Cleveland, D.W., 1994. Cyclin-like accumulation and loss of the putative kinetochore motor CENP-E results from coupling continuous synthesis with specific degradation at the end of mitosis. *The Journal of Cell Biology*, *125*(6), pp.1303-1312.

Brown, K.D., Wood, K.W. and Cleveland, D.W., 1996. The kinesin-like protein CENP-E is kinetochore-associated throughout poleward chromosome segregation during anaphase-A. *Journal of cell science*, *109*(5), pp.961-969.

Cahill, D.P., Lengauer, C., Yu, J., Riggins, G.J., Willson, J.K., Markowitz, S.D., Kinzler, K.W. and Vogelstein, B., 1998. Mutations of mitotic checkpoint genes in human cancers. *Nature*, *392*(6673), pp.300-303.

Cai, S., O'Connell, C.B., Khodjakov, A. and Walczak, C.E., 2009. Chromosome congression in the absence of kinetochore fibres. *Nature cell biology*, *11*(7), pp.832-838.

Campbell, C.S. and Desai, A., 2013. Tension sensing by Aurora B kinase is independent of survivin-based centromere localization. *Nature*, *497*(7447), pp.118-121.

Capell, B.C. and Collins, F.S., 2006. Human laminopathies: nuclei gone genetically awry. *Nature Reviews Genetics*, *7*(12), pp.940-952.

Carmena, M. and Earnshaw, W.C., 2003. The cellular geography of aurora kinases. *Nature reviews Molecular cell biology*, *4*(11), pp.842-854.

Castrillon, D.H. and Wasserman, S.A., 1994. Diaphanous is required for cytokinesis in Drosophila and shares domains of similarity with the products of the limb deformity gene. *Development*, *120*(12), pp.3367-3377.

Chan, G.K.T., Jablonski, S.A., Sudakin, V., Hittle, J.C. and Yen, T.J., 1999. Human BUBR1 is a mitotic checkpoint kinase that monitors CENP-E functions at kinetochores and binds the cyclosome/APC. *The Journal of cell biology*, *146*(5), pp.941-954.

Chan, Y.W., Jeyaprakash, A.A., Nigg, E.A. and Santamaria, A., 2012. Aurora B controls kinetochore–microtubule attachments by inhibiting Ska complex–KMN network interaction. *The Journal of cell biology*, *196*(5), pp.563-571.

Chang, F., Drubin, D. and Nurse, P., 1997. cdc12p, a protein required for cytokinesis in fission yeast, is a component of the cell division ring and interacts with profilin. *The Journal of cell biology*, *137*(1), pp.169-182.

Cheeseman, I.M. and Desai, A., 2008. Molecular architecture of the kinetochore–microtubule interface. *Nature reviews Molecular cell biology*,*9*(1), pp.33-46.

Cheeseman, I.M., Anderson, S., Jwa, M., Green, E.M., Kang, J.S., Yates, J.R., Chan, C.S., Drubin, D.G. and Barnes, G., 2002. Phospho-regulation of kinetochore-microtubule attachments by the Aurora kinase Ipl1p. *Cell*,*111*(2), pp.163-172.

Cheeseman, I.M., Niessen, S., Anderson, S., Hyndman, F., Yates, J.R., Oegema, K. and Desai, A., 2004. A conserved protein network controls assembly of the outer kinetochore and its ability to sustain tension. *Genes & development*, *18*(18), pp.2255-2268.

Cheeseman, I.M., Chappie, J.S., Wilson-Kubalek, E.M. and Desai, A., 2006. The conserved KMN network constitutes the core microtubule-binding site of the kinetochore. *Cell*, *127*(5), pp.983-997.

Cheng, L., Zhang, J., Ahmad, S., Rozier, L., Yu, H., Deng, H. and Mao, Y., 2011. Aurora B regulates formin mDia3 in achieving metaphase chromosome alignment. *Developmental cell*, *20*(3), pp.342-352.
Chesarone et al., 2010;

Churchman, L.S., Ökten, Z., Rock, R.S., Dawson, J.F. and Spudich, J.A., 2005. Single molecule high-resolution colocalization of Cy3 and Cy5 attached to macromolecules measures intramolecular distances through time. *Proceedings of the National Academy of Sciences of the United States of America*, *102*(5), pp.1419-1423.

Ciferri, C., Pasqualato, S., Screpanti, E., Varetti, G., Santaguida, S., Dos Reis, G., Maiolica, A., Polka, J., De Luca, J.G., De Wulf, P. and Salek, M., 2008. Implications for kinetochore-microtubule attachment from the structure of an engineered Ndc80 complex. *Cell*, *133*(3), pp.427-439.

Cimini, D., Moree, B., Canman, J.C. and Salmon, E.D., 2003. Merotelic kinetochore orientation occurs frequently during early mitosis in mammalian tissue cells and error correction is achieved by two different mechanisms. *Journal of cell science*, *116*(20), pp.4213-4225.

Cleveland, D.W., Mao, Y. and Sullivan, K.F., 2003. Centromeres and kinetochores: from epigenetics to mitotic checkpoint signaling. *Cell*, *112*(4), pp.407-421.

Collins, K.A., Castillo, A.R., Tatsutani, S.Y. and Biggins, S., 2005. De novo kinetochore assembly requires the centromeric histone H3 variant. *Molecular biology of the cell*, *16*(12), pp.5649-5660.

Daou, P., Hasan, S., Breitsprecher, D., Baudelet, E., Camoin, L., Audebert, S., Goode, B.L. and Badache, A., 2014. Essential and nonredundant roles for Diaphanous formins in cortical microtubule capture and directed cell migration. *Molecular biology of the cell*, *25*(5), pp.658-668.

Delacour-Larose, M., Molla, A., Skoufias, D.A., Margolis, R.L. and Dimitrov, S., 2004. Distinct dynamics of Aurora B and Survivin during mitosis. *Cell Cycle*, *3*(11), pp.1418-1426.

DeLuca, J.G., Moree, B., Hickey, J.M., Kilmartin, J.V. and Salmon, E.D., 2002. hNuf2 inhibition blocks stable kinetochore–microtubule attachment and induces mitotic cell death in HeLa cells. *The Journal of cell biology*, *159*(4), pp.549-555.

DeLuca, J.G., Gall, W.E., Ciferri, C., Cimini, D., Musacchio, A. and Salmon, E.D., 2006. Kinetochore microtubule dynamics and attachment stability are regulated by Hec1. *Cell*, *127*(5), pp.969-982.

DeLuca, K.F., Lens, S.M. and DeLuca, J.G., 2011. Temporal changes in Hec1 phosphorylation control kinetochore–microtubule attachment stability during mitosis. *J Cell Sci*, *124*(4), pp.622-634.

Desai, A. and Mitchison, T.J., 1997. Microtubule polymerization dynamics. *Annual review of cell and developmental biology*, *13*(1), pp.83-117.

Dewar, H., Tanaka, K., Nasmyth, K. and Tanaka, T.U., 2004. Tension between two kinetochores suffices for their bi-orientation on the mitotic spindle. *Nature*, *428*(6978), pp.93-97.

De Wulf, P., Montani, F. and Visintin, R., 2009. Protein phosphatases take the mitotic stage. *Current opinion in cell biology*, *21*(6), pp.806-815.

Ditchfield, C., Johnson, V.L., Tighe, A., Ellston, R., Haworth, C., Johnson, T., Mortlock, A., Keen, N. and Taylor, S.S., 2003. Aurora B couples chromosome alignment with anaphase by targeting BubR1, Mad2, and Cenp-E to kinetochores. *The Journal of cell biology*, *161*(2), pp.267-280.

Dominguez, R., 2010. Structural insights into de novo actin polymerization. Current opinion in structural biology, 20(2), pp.217-225.

Driscoll, D.A. and Gross, S., 2009. Prenatal screening for aneuploidy. *New England Journal of Medicine*, *360*(24), pp.2556-2562.

Drpic, D., Pereira, A.J., Barisic, M., Maresca, T.J. and Maiato, H., 2015. Polar ejection forces promote the conversion from lateral to end-on kinetochore-microtubule attachments on mono-oriented chromosomes. *Cell reports*, *13*(3), pp.460-468.

Elzinga, M., Collins, J.H., Kuehl, W.M. and Adelstein, R.S., 1973. Complete amino-acid sequence of actin of rabbit skeletal muscle. *Proceedings of the National Academy of Sciences*, *70*(9), pp.2687-2691.

Emanuele, M.J. and Stukenberg, P.T., 2007. Xenopus Cep57 is a novel kinetochore component involved in microtubule attachment. *Cell*, *130*(5), pp.893-905.

Emanuele, M.J., Lan, W., Jwa, M., Miller, S.A., Chan, C.S. and Stukenberg, P.T., 2008. Aurora B kinase and protein phosphatase 1 have opposing roles in modulating kinetochore assembly. *The Journal of cell biology*, *181*(2), pp.241-254.

Espeut, J., Gaussen, A., Bieling, P., Morin, V., Prieto, S., Fesquet, D., Surrey, T. and Abrieu, A., 2008. Phosphorylation relieves autoinhibition of the kinetochore motor Cenp-E. *Molecular cell*, *29*(5), pp.637-643.

Etemad, B., Kuijt, T.E. and Kops, G.J., 2015. Kinetochore-microtubule attachment is sufficient to satisfy the human spindle assembly checkpoint.*Nature communications*, *6*.

Evangelista, M., Blundell, K., Longtine, M.S., Chow, C.J., Adames, N., Pringle, J.R., Peter, M. and Boone, C., 1997. Bni1p, a yeast formin linking cdc42p and the actin cytoskeleton during polarized morphogenesis. *Science*,*276*(5309), pp.118-122.

Fang, G., Yu, H. and Kirschner, M.W., 1998. Direct binding of CDC20 protein family members activates the anaphase-promoting complex in mitosis and G1. *Molecular cell*, *2*(2), pp.163-171.

Feierbach, B. and Chang, F., 2001. Roles of the fission yeast formin for3p in cell polarity, actin cable formation and symmetric cell division. *Current Biology*, *11*(21), pp.1656-1665.

Floyd, S., Whiffin, N., Gavilan, M.P., Kutscheidt, S., De Luca, M., Marcozzi, C., Min, M., Watkins, J., Chung, K., Fackler, O.T. and Lindon, C., 2013. Spatiotemporal organization of Aurora-B by APC/CCdh1 after mitosis coordinates cell spreading through FHOD1. *J Cell Sci*, *126*(13), pp.2845-2856.

Foley, E.A. and Kapoor, T.M., 2013. Microtubule attachment and spindle assembly checkpoint signalling at the kinetochore. *Nature reviews Molecular cell biology*, *14*(1), pp.25-37.

Foley, E.A., Maldonado, M. and Kapoor, T.M., 2011. Formation of stable attachments between kinetochores and microtubules depends on the B56-PP2A phosphatase. *Nature cell biology*, *13*(10), pp.1265-1271.

Francisco, L., Wang, W. and Chan, C.S., 1994. Type 1 protein phosphatase acts in opposition to IpL1 protein kinase in regulating yeast chromosome segregation. *Molecular and cellular biology*, *14*(7), pp.4731-4740.

Friedl, P. and Gilmour, D., 2009. Collective cell migration in morphogenesis, regeneration and cancer. *Nature reviews Molecular cell biology*, *10*(7), pp.445-457.

Futamura, M., Arakawa, H., Matsuda, K., Katagiri, T., Saji, S., Miki, Y. and Nakamura, Y., 2000. Potential role of BRCA2 in a mitotic checkpoint after phosphorylation by hBUBR1. *Cancer research*, *60*(6), pp.1531-1535.

Gaillard, J., Ramabhadran, V., Neumanne, E., Gurel, P., Blanchoin, L., Vantard, M. and Higgs, H.N., 2011. Differential interactions of the formins INF2, mDia1, and mDia2 with microtubules. *Molecular biology of the cell*,*22*(23), pp.4575-4587.

Gardel, M.L., Schneider, I.C., Aratyn-Schaus, Y. and Waterman, C.M., 2010. Mechanical integration of actin and adhesion dynamics in cell migration.*Annual review of cell and developmental biology*, *26*, p.315.

Gasman, S., Kalaidzidis, Y. and Zerial, M., 2003. RhoD regulates endosome dynamics through Diaphanous-related Formin and Src tyrosine kinase.*Nature Cell Biology*, *5*(3), pp.195-204.

Gestaut, D.R., Graczyk, B., Cooper, J., Widlund, P.O., Zelter, A., Wordeman, L., Asbury, C.L. and Davis, T.N., 2008. Phosphoregulation and depolymerization-driven movement of the Dam1 complex do not require ring formation. *Nature cell biology*, *10*(4), pp.407-414.

Giet, R., Petretti, C. and Prigent, C., 2005. Aurora kinases, aneuploidy and cancer, a coincidence or a real link?. *Trends in cell biology*, *15*(5), pp.241-250.

Glotzer, M., Murray, A.W. and Kirschner, M.W., 1991. Cyclin is degraded by the ubiquitin pathway. *Nature*, *349*(6305), pp.132-138.

Goh, W.I., Lim, K.B., Sudhaharan, T., Sem, K.P., Bu, W., Chou, A.M. and Ahmed, S., 2012. mDia1 and WAVE2 proteins interact directly with IRSp53 in filopodia and are involved in filopodium formation. *Journal of Biological Chemistry*, *287*(7), pp.4702-4714.

Gomes, E.R., Jani, S. and Gundersen, G.G., 2005. Nuclear movement regulated by Cdc42, MRCK, myosin, and actin flow establishes MTOC polarization in migrating cells. *Cell*, *121*(3), pp.451-463.

Goode, B.L. and Eck, M.J., 2007. Mechanism and function of formins in the control of actin assembly. *Annu. Rev. Biochem.*, *76*, pp.593-627.

Goshima, G., Kiyomitsu, T., Yoda, K. and Yanagida, M., 2003. Human centromere chromatin protein hMis12, essential for equal segregation, is independent of CENP-A loading pathway. *The Journal of cell biology*, *160*(1), pp.25-39.

Gudimchuk, N., Vitre, B., Kim, Y., Kiyatkin, A., Cleveland, D.W., Ataullakhanov, F.I. and Grishchuk, E.L., 2013. Kinetochore kinesin CENP-E is a processive bi-directional tracker of dynamic microtubule tips. *Nature cell biology*, *15*(9), pp.1079-1088.

Gundersen, G.G. and Worman, H.J., 2013. Nuclear positioning. *Cell*, *152*(6), pp.1376-1389.

Guo, Y., Kim, C., Ahmad, S., Zhang, J. and Mao, Y., 2012. CENP-E–dependent BubR1 autophosphorylation enhances chromosome alignment and the mitotic checkpoint. *The Journal of cell biology*, *198*(2), pp.205-217.

Guo, Y., Kim, C. and Mao, Y., 2013. New insights into the mechanism for chromosome alignment in metaphase. *International review of cell and molecular biology*, *303*, p.237.

Hartigan, J.A. and Hartigan, P.M., 1985. The dip test of unimodality. The Annals of Statistics, pp.70-84.

Hartwell, L.H. and Kastan, M.B., 1994. Cell cycle control and cancer.*Science*, *266*(5192), p.1821.

Hauf, S., Cole, R.W., LaTerra, S., Zimmer, C., Schnapp, G., Walter, R., Heckel, A., Van Meel, J., Rieder, C.L. and Peters, J.M., 2003. The small molecule Hesperadin reveals a role for Aurora B in correcting kinetochore–microtubule attachment and in maintaining the spindle assembly checkpoint.*The Journal of cell biology*, *161*(2), pp.281-294.

Higashida, C., Miyoshi, T., Fujita, A., Oceguera-Yanez, F., Monypenny, J., Andou, Y., Narumiya, S. and Watanabe, N., 2004. Actin polymerization-driven molecular movement of mDia1 in living cells. *Science*, *303*(5666), pp.2007-2010.

Higgs, H.N. and Peterson, K.J., 2005. Phylogenetic analysis of the formin homology 2 domain. *Molecular biology of the cell*, *16*(1), pp.1-13.

Hirokawa, N., Pfister, K.K., Yorifuji, H., Wagner, M.C., Brady, S.T. and Bloom, G.S., 1989. Submolecular domains of bovine brain kinesin identified by electron microscopy and monoclonal antibody decoration. *Cell*, *56*(5), pp.867-878.

Hoffman, D.B., Pearson, C.G., Yen, T.J., Howell, B.J. and Salmon, E.D., 2001. Microtubule-dependent changes in assembly of microtubule motor proteins and mitotic spindle checkpoint proteins at PtK1 kinetochores. *Molecular biology of the cell*, *12*(7), pp.1995-2009.

Honda, R., Körner, R. and Nigg, E.A., 2003. Exploring the functional interactions between Aurora B, INCENP, and survivin in mitosis. *Molecular biology of the cell*, *14*(8), pp.3325-3341.

Howell, B.J., McEwen, B.F., Canman, J.C., Hoffman, D.B., Farrar, E.M., Rieder, C.L. and Salmon, E.D., 2001. Cytoplasmic dynein/dynactin drives kinetochore protein transport to the spindle poles and has a role in mitotic spindle checkpoint inactivation. *The Journal of cell biology*, *155*(7), pp.1159-1172.

Hoyt, M.A., Totis, L. and Roberts, B.T., 1991. S. cerevisiae genes required for cell cycle arrest in response to loss of microtubule function. *Cell*, *66*(3), pp.507-517.

Hsu, J.Y., Sun, Z.W., Li, X., Reuben, M., Tatchell, K., Bishop, D.K., Grushcow, J.M., Brame, C.J., Caldwell, J.A., Hunt, D.F. and Lin, R., 2000. Mitotic phosphorylation of histone H3 is governed by Ipl1/aurora kinase and Glc7/PP1 phosphatase in budding yeast and nematodes. *Cell*, *102*(3), pp.279-291.

Hwang, L.H., Lau, L.F., Smith, D.L., Mistrot, C.A., Hardwick, K.G., Hwang, E.S., Amon, A. and Murray, A.W., 1998. Budding yeast Cdc20: a target of the spindle checkpoint. *Science*, *279*(5353), pp.1041-1044.

Imamura, H., Tanaka, K., Hihara, T., Umikawa, M., Kamei, T., Takahashi, K., Sasaki, T. and Takai, Y., 1997. Bni1p and Bnr1p: downstream targets of the Rho family small G-proteins which interact with profilin and regulate actin cytoskeleton in Saccharomyces cerevisiae. *The EMBO journal*, *16*(10), pp.2745-2755.

Insall, R.H. and Machesky, L.M., 2009. Actin dynamics at the leading edge: from simple machinery to complex networks. *Developmental cell*, *17*(3), pp.310-322.

Ishizaki, T., Morishima, Y., Okamoto, M., Furuyashiki, T., Kato, T. and Narumiya, S., 2001. Coordination of microtubules and the actin cytoskeleton by the Rho effector mDia1. *Nature Cell Biology*, *3*(1), pp.8-14.

Iwanaga, Y., Chi, Y.H., Miyazato, A., Sheleg, S., Haller, K., Peloponese, J.M., Li, Y., Ward, J.M., Benezra, R. and Jeang, K.T., 2007. Heterozygous deletion of mitotic arrest–deficient protein 1 (MAD1) increases the incidence of tumors in mice. *Cancer research*, *67*(1), pp.160-166.

Jelluma, N., Brenkman, A.B., van den Broek, N.J., Cruijsen, C.W., van Osch, M.H., Lens, S.M., Medema, R.H. and Kops, G.J., 2008. Mps1 phosphorylates Borealin to control Aurora B activity and chromosome alignment. *Cell*,*132*(2), pp.233-246.

Kallio, M.J., McCleland, M.L., Stukenberg, P.T. and Gorbsky, G.J., 2002. Inhibition of aurora B kinase blocks chromosome segregation, overrides the spindle checkpoint, and perturbs microtubule dynamics in mitosis. *Current biology*, *12*(11), pp.900-905.

Kapoor, T.M., Mayer, T.U., Coughlin, M.L. and Mitchison, T.J., 2000. Probing spindle assembly mechanisms with monastrol, a small molecule inhibitor of the mitotic kinesin, Eg5. *The Journal of cell biology*, *150*(5), pp.975-988.

Kapoor, T.M., Lampson, M.A., Hergert, P., Cameron, L., Cimini, D., Salmon, E.D., McEwen, B.F. and Khodjakov, A., 2006. Chromosomes can congress to the metaphase plate before biorientation. *Science*, *311*(5759), pp.388-391.

Keating, P., Rachidi, N., Tanaka, T.U. and Stark, M.J., 2009. Ipl1-dependent phosphorylation of Dam1 is reduced by tension applied on kinetochores. *Journal of cell science*, *122*(23), pp.4375-4382.

Keen, N. and Taylor, S., 2004. Aurora-kinase inhibitors as anticancer agents. *Nature Reviews Cancer*, *4*(12), pp.927-936.

Keller, R., 2002. Shaping the vertebrate body plan by polarized embryonic cell movements. *Science*, 298(5600), pp.1950-1954.

Kelly, A.E. and Funabiki, H., 2009. Correcting aberrant kinetochore microtubule attachments: an Aurora B-centric view. *Current opinion in cell biology*, *21*(1), pp.51-58.

Kim, Y., Heuser, J.E., Waterman, C.M. and Cleveland, D.W., 2008. CENP-E combines a slow, processive motor and a flexible coiled coil to produce an essential motile kinetochore tether. *The Journal of cell biology*, *181*(3), pp.411-419.

Kim, Y., Holland, A.J., Lan, W. and Cleveland, D.W., 2010. Aurora kinases and protein phosphatase 1 mediate chromosome congression through regulation of CENP-E. *Cell*, *142*(3), pp.444-455.

Kimura, M., Kotani, S., Hattori, T., Sumi, N., Yoshioka, T., Todokoro, K. and Okano, Y., 1997. Cell cycle-dependent expression and spindle pole localization of a novel human protein kinase, Aik, related to Aurora of Drosophila and yeast Ipl1. *Journal of Biological Chemistry*, *272*(21), pp.13766-13771.

King, J.M. and Nicklas, R.B., 2000. Tension on chromosomes increases the number of kinetochore microtubules but only within limits. *Journal of Cell Science*, *113*(21), pp.3815-3823.

Kirschner, M. and Mitchison, T., 1986. Beyond self-assembly: from microtubules to morphogenesis. *Cell*, 45(3), pp.329-342.

Kitajima, T.S., Sakuno, T., Ishiguro, K.I., Iemura, S.I., Natsume, T., Kawashima, S.A. and Watanabe, Y., 2006. Shugoshin collaborates with protein phosphatase 2A to protect cohesin. *Nature*, *441*(7089), pp.46-52.

Kiyomitsu, T., Obuse, C. and Yanagida, M., 2007. Human Blinkin/AF15q14 is required for chromosome alignment and the mitotic checkpoint through direct interaction with Bub1 and BubR1. *Developmental cell*, *13*(5), pp.663-676.

Kline-Smith, S.L., Khodjakov, A., Hergert, P. and Walczak, C.E., 2004. Depletion of centromeric MCAK leads to chromosome congression and segregation defects due to improper kinetochore attachments. *Molecular biology of the cell*, *15*(3), pp.1146-1159.

Kline, S.L., Cheeseman, I.M., Hori, T., Fukagawa, T. and Desai, A., 2006. The human Mis12 complex is required for kinetochore assembly and proper chromosome segregation. *The Journal of cell biology*, *173*(1), pp.9-17.

Knowlton, A.L., Lan, W. and Stukenberg, P.T., 2006. Aurora B is enriched at merotelic attachment sites, where it regulates MCAK. *Current biology*,*16*(17), pp.1705-1710.

Koizumi, K., Takano, K., Kaneyasu, A., Watanabe-Takano, H., Tokuda, E., Abe, T., Watanabe, N., Takenawa, T. and Endo, T., 2012. RhoD activated by fibroblast growth factor induces cytoneme-like cellular protrusions through mDia3C. *Molecular biology of the cell*, *23*(23), pp.4647-4661.

Kole, T.P., Tseng, Y., Jiang, I., Katz, J.L. and Wirtz, D., 2005. Intracellular mechanics of migrating fibroblasts. *Molecular biology of the cell*, *16*(1), pp.328-338.

Kovar, D.R., Harris, E.S., Mahaffy, R., Higgs, H.N. and Pollard, T.D., 2006. Control of the assembly of ATP-and ADP-actin by formins and profilin. *Cell*,*124*(2), pp.423-435.

Kovar, D.R., Kuhn, J.R., Tichy, A.L. and Pollard, T.D., 2003. The fission yeast cytokinesis formin Cdc12p is a barbed end actin filament capping protein gated by profilin. *The Journal of cell biology*, *161*(5), pp.875-887.

Lammers, M., Rose, R., Scrima, A. and Wittinghofer, A., 2005. The regulation of mDia1 by autoinhibition and its release by Rho• GTP. *The EMBO journal*, *24*(23), pp.4176-4187.

Lampson, M.A. and Cheeseman, I.M., 2011. Sensing centromere tension: Aurora B and the regulation of kinetochore function. *Trends in cell biology*,*21*(3), pp.133-140.

Lan, W., Zhang, X., Kline-Smith, S.L., Rosasco, S.E., Barrett-Wilt, G.A., Shabanowitz, J., Hunt, D.F., Walczak, C.E. and Stukenberg, P.T., 2004. Aurora B phosphorylates centromeric MCAK and regulates its localization and microtubule depolymerization activity. *Current Biology*, *14*(4), pp.273-286.

Lauffenburger, D.A. and Horwitz, A.F., 1996. Cell migration: a physically integrated molecular process. *Cell*, *84*(3), pp.359-369.

Lens, Susanne MA, Rob MF Wolthuis, Rob Klompmaker, Jos Kauw, Reuven Agami, Thijn Brummelkamp, Geert Kops, and René H. Medema. "Survivin is required for a sustained spindle checkpoint arrest in response to lack of tension." *The EMBO journal* 22, no. 12 (2003): 2934-2947.

Lewkowicz, E., Herit, F., Le Clainche, C., Bourdoncle, P., Perez, F. and Niedergang, F., 2008. The microtubule-binding protein CLIP-170 coordinates mDia1 and actin reorganization during CR3-mediated phagocytosis. *The Journal of cell biology*, *183*(7), pp.1287-1298.

Li, F. and Higgs, H.N., 2003. The mouse Formin mDia1 is a potent actin nucleation factor regulated by autoinhibition. *Current biology*, *13*(15), pp.1335-1340.

Li, R. and Murray, A.W., 1991. Feedback control of mitosis in budding yeast. *Cell*, *66*(3), pp.519-531.

Liao, H., Li, G. and Yen, T.J., 1994. Mitotic regulation of microtubule cross-linking activity of CENP-E kinetochore protein. *Science*, *265*(5170), pp.394-398.

Lindon, C. and Pines, J., 2004. Ordered proteolysis in anaphase inactivates Plk1 to contribute to proper mitotic exit in human cells. *The Journal of cell biology*, *164*(2), pp.233-241.

Liu, C. and Mao, Y., 2016. Diaphanous formin mDia2 regulates CENP-A levels at centromeres. *The Journal of cell biology*, *213*(4), pp.415-424.

Liu, S.T., Chan, G.K., Hittle, J.C., Fujii, G., Lees, E. and Yen, T.J., 2003. Human MPS1 kinase is required for mitotic arrest induced by the loss of CENP-E from kinetochores. *Molecular biology of the cell*, *14*(4), pp.1638-1651.

Liu, D., Vleugel, M., Backer, C.B., Hori, T., Fukagawa, T., Cheeseman, I.M. and Lampson, M.A., 2010. Regulated targeting of protein phosphatase 1 to the outer kinetochore by KNL1 opposes Aurora B kinase. *The Journal of cell biology*, *188*(6), pp.809-820.

Liu, D., Vader, G., Vromans, M.J., Lampson, M.A. and Lens, S.M., 2009. Sensing chromosome bi-orientation by spatial separation of aurora B kinase from kinetochore substrates. *Science*, *323*(5919), pp.1350-1353.

Lombillo, V.A., Stewart, R.J. and McIntosh, J.R., 1994. Kinesin supports minus end-directed, depolymerization-driven motility of microspheres coupled shortening microtubules. *Nature*,*373*, pp.161-164.

Lombillo, V.A., Nislow, C., Yen, T.J., Gelfand, V.I. and McIntosh, J.R., 1995. Antibodies to the kinesin motor domain and CENP-E inhibit microtubule depolymerization-dependent motion of chromosomes in vitro. *The Journal of Cell Biology*, *128*(1), pp.107-115.

Lončarek, J., Kisurina-Evgenieva, O., Vinogradova, T., Hergert, P., La Terra, S., Kapoor, T.M. and Khodjakov, A., 2007. The centromere geometry essential for keeping mitosis error free is controlled by spindle forces. *Nature*,*450*(7170), pp.745-749.

Lu, J., Meng, W., Poy, F., Maiti, S., Goode, B.L. and Eck, M.J., 2007. Structure of the FH2 domain of Daam1: implications for formin regulation of actin assembly. *Journal of molecular biology*, *369*(5), pp.1258-1269.

Luster, A.D., Alon, R. and von Andrian, U.H., 2005. Immune cell migration in inflammation: present and future therapeutic targets. *Nature immunology*,*6*(12), pp.1182-1190.

Maffini, S., Maia, A.R., Manning, A.L., Maliga, Z., Pereira, A.L., Junqueira, M., Shevchenko, A., Hyman, A., Yates, J.R., Galjart, N. and Compton, D.A., 2009. Motor-independent targeting of CLASPs to kinetochores by CENP-E promotes microtubule turnover and poleward flux. *Current Biology*, *19*(18), pp.1566-1572.

Magidson, V., O'Connell, C.B., Lončarek, J., Paul, R., Mogilner, A. and Khodjakov, A., 2011. The spatial arrangement of chromosomes during prometaphase facilitates spindle assembly. *Cell*, *146*(4), pp.555-567.

Magidson, V., He, J., Ault, J.G., O'Connell, C.B., Yang, N., Tikhonenko, I., McEwen, B.F., Sui, H. and Khodjakov, A., 2016. Unattached kinetochores rather than intrakinetochore tension arrest mitosis in taxol-treated cells. *The Journal of cell biology*, *212*(3), pp.307-319.

Maiato, H., Fairley, E.A., Rieder, C.L., Swedlow, J.R., Sunkel, C.E. and Earnshaw, W.C., 2003. Human CLASP1 is an outer kinetochore component that regulates spindle microtubule dynamics. *Cell*, *113*(7), pp.891-904.

Maiato, H., Rieder, C.L. and Khodjakov, A., 2004. Kinetochore-driven formation of kinetochore fibers contributes to spindle assembly during animal mitosis. *The Journal of cell biology*, *167*(5), pp.831-840.

Mao, Y., Abrieu, A. and Cleveland, D.W., 2003. Activating and silencing the mitotic checkpoint through CENP-E-dependent activation/inactivation of BubR1. *Cell*, *114*(1), pp.87-98.

Mao, Y., Desai, A. and Cleveland, D.W., 2005. Microtubule capture by CENP-E silences BubR1-dependent mitotic checkpoint signaling. *The Journal of cell biology*, *170*(6), pp.873-880.

Maresca, T.J. and Salmon, E.D., 2009. Intrakinetochore stretch is associated with changes in kinetochore phosphorylation and spindle assembly checkpoint activity. *The Journal of cell biology*, *184*(3), pp.373-381.

Martin, P., 1997. Wound healing--aiming for perfect skin regeneration. *Science*, *276*(5309), pp.75-81.

Martin-Lluesma, S., Stucke, V.M. and Nigg, E.A., 2002. Role of Hec1 in spindle checkpoint signaling and kinetochore recruitment of Mad1/Mad2.*Science*, *297*(5590), pp.2267-2270.

Martin, P. and Leibovich, S.J., 2005. Inflammatory cells during wound repair: the good, the bad and the ugly. *Trends in cell biology*, *15*(11), pp.599-607.

Maas, R.L., Zeller, R., Woychik, R.P., Vogt, T.F. and Leder, P., 1990. Disruption of formin-encoding transcripts in two mutant limb deformity alleles. *Nature*, 853-855.

McCleland, M.L., Gardner, R.D., Kallio, M.J., Daum, J.R., Gorbsky, G.J., Burke, D.J. and Stukenberg, P.T., 2003. The highly conserved Ndc80 complex is required for kinetochore assembly, chromosome congression, and spindle checkpoint activity. *Genes & Development*, *17*(1), pp.101-114.

McEwen, B.F., Chan, G.K., Zubrowski, B., Savoian, M.S., Sauer, M.T. and Yen, T.J., 2001. CENP-E is essential for reliable bioriented spindle attachment, but chromosome alignment can be achieved via redundant mechanisms in mammalian cells. *Molecular Biology of the Cell*, *12*(9), pp.2776-2789.

Mejillano, M.R., Kojima, S.I., Applewhite, D.A., Gertler, F.B., Svitkina, T.M. and Borisy, G.G., 2004. Lamellipodial versus filopodial mode of the actin nanomachinery: pivotal role of the filament barbed end. *Cell*, *118*(3), pp.363-373.

Meraldi, P., Draviam, V.M. and Sorger, P.K., 2004. Timing and checkpoints in the regulation of mitotic progression. *Developmental cell*, *7*(1), pp.45-60.

Miki, T., Okawa, K., Sekimoto, T., Yoneda, Y., Watanabe, S., Ishizaki, T. and Narumiya, S., 2009. mDia2 shuttles between the nucleus and the cytoplasm through the importin-α/β-and CRM1-mediated nuclear transport mechanism. *Journal of Biological Chemistry*, *284*(9), pp.5753-5762.

Minoshima, Y., Kawashima, T., Hirose, K., Tonozuka, Y., Kawajiri, A., Bao, Y.C., Deng, X., Tatsuka, M., Narumiya, S., May, W.S. and Nosaka, T., 2003. Phosphorylation by aurora B converts MgcRacGAP to a RhoGAP during cytokinesis. *Developmental cell*, *4*(4), pp.549-560.

Mitchison, T. and Kirschner, M., 1984. Dynamic instability of microtubule growth. *nature*, *312*(5991), pp.237-242.

Murata-Hori, M. and Wang, Y.L., 2002. The kinase activity of aurora B is required for kinetochore-microtubule interactions during mitosis. *Current biology*, *12*(11), pp.894-899.

Musacchio, A. and Salmon, E.D., 2007. The spindle-assembly checkpoint in space and time. *Nature reviews Molecular cell biology*, *8*(5), pp.379-393.

Musinipally, V., Howes, S., Alushin, G.M. and Nogales, E., 2013. The microtubule binding properties of CENP-E's C-terminus and CENP-F. *Journal of molecular biology*, *425*(22), pp.4427-4441.

Nakano, K., Imai, J., Arai, R., Toh-e, A., Matsui, Y. and Mabuchi, I., 2002. The small GTPase Rho3 and the diaphanous/formin For3 function in polarized cell growth in fission yeast. *Journal of Cell Science*, *115*(23), pp.4629-4639.

Nicklas, R.B., 1997. How cells get the right chromosomes. *Science*,*275*(5300), pp.632-637.

Nicklas, R.B. and Koch, C.A., 1969. Chromosome micromanipulation III. Spindle fiber tension and the reorientation of mal-oriented chromosomes. *The Journal of cell biology*, *43*(1), pp.40-50.

Nicklas, R.B. and Ward, S.C., 1994. Elements of error correction in mitosis: microtubule capture, release, and tension. *The Journal of cell biology*,*126*(5), pp.1241-1253.

Nogales, E., Wolf, S.G. and Downing, K.H., 1998. Structure of the αβ tubulin dimer by electron crystallography. *Nature*, *391*(6663), pp.199-203.

Nogales, E., Whittaker, M., Milligan, R.A. and Downing, K.H., 1999. High-resolution model of the microtubule. *Cell*, *96*(1), pp.79-88.

Nousiainen, M., Silljé, H.H., Sauer, G., Nigg, E.A. and Körner, R., 2006. Phosphoproteome analysis of the human mitotic spindle. *Proceedings of the National Academy of Sciences*, *103*(14), pp.5391-5396.

Obuse, C., Iwasaki, O., Kiyomitsu, T., Goshima, G., Toyoda, Y. and Yanagida, M., 2004. A conserved Mis12 centromere complex is linked to heterochromatic HP1 and outer kinetochore protein Zwint-1. *Nature Cell Biology*, *6*(11), pp.1135-1141.

Ohi, R., Sapra, T., Howard, J. and Mitchison, T.J., 2004. Differentiation of cytoplasmic and meiotic spindle assembly MCAK functions by Aurora B-dependent phosphorylation. *Molecular biology of the cell*, *15*(6), pp.2895-2906.

Ozaki-Kuroda, K., Yamamoto, Y., Nohara, H., Kinoshita, M., Fujiwara, T., Irie, K. and Takai, Y., 2001. Dynamic localization and function of Bni1p at the sites of directed growth in Saccharomyces cerevisiae. *Molecular and Cellular Biology*, *21*(3), pp.827-839.

Parra, M.T., Gómez, R., Viera, A., Page, J., Calvente, A., Wordeman, L., Rufas, J.S. and Suja, J.A., 2006. A perikinetochoric ring defined by MCAK and Aurora-B as a novel centromere domain. *PLoS Genet*, *2*(6), p.e84.

Pellegrin, S. and Mellor, H., 2005. The Rho family GTPase Rif induces filopodia through mDia2. *Current Biology*, *15*(2), pp.129-133.

Peng, J., Wallar, B.J., Flanders, A., Swiatek, P.J. and Alberts, A.S., 2003. Disruption of the Diaphanous-related formin Drf1 gene encoding mDia1 reveals a role for Drf3 as an effector for Cdc42. *Current Biology*, *13*(7), pp.534-545.

Petersen, J., Nielsen, O., Egel, R. and Hagan, I.M., 1998. FH3, a domain found in formins, targets the fission yeast formin Fus1 to the projection tip during conjugation. *The Journal of cell biology*, *141*(5),
pp.1217-1228.

Pollard, T.D., 2007. Regulation of actin filament assembly by Arp2/3 complex and formins. *Annu. Rev. Biophys. Biomol. Struct.*, *36*, pp.451-477.

Posch, M., Khoudoli, G.A., Swift, S., King, E.M., DeLuca, J.G. and Swedlow, J.R., 2010. Sds22 regulates aurora B activity and microtubule–kinetochore interactions at mitosis. *The Journal of cell biology*, *191*(1), pp.61-74.

Pring, M., Evangelista, M., Boone, C., Yang, C. and Zigmond, S.H., 2003. Mechanism of formin-induced nucleation of actin filaments. *Biochemistry*,*42*(2), pp.486-496.

Pruyne, D., Evangelista, M., Yang, C., Bi, E., Zigmond, S., Bretscher, A. and Boone, C., 2002. Role of formins in actin assembly: nucleation and barbed-end association. *Science*, *297*(5581), pp.612-615.

Putkey, F.R., Cramer, T., Morphew, M.K., Silk, A.D., Johnson, R.S., McIntosh, J.R. and Cleveland, D.W., 2002. Unstable kinetochore-microtubule capture and chromosomal instability following deletion of CENP-E. *Developmental cell*, *3*(3), pp.351-365.

Rajagopalan, Harith, and Christoph Lengauer. "Aneuploidy and cancer."*Nature* 432, no. 7015 (2004): 338-341.

Rannou, Y., Troadec, M.B., Petretti, C., Hans, F., Dutertre, S., Dimitrov, S. and Prigent, C., 2008. Localization of aurora A and aurora B kinases during interphase: role of the N-terminal domain. *Cell Cycle*, *7*(19), pp.3012-3020.

Riedel, C.G., Katis, V.L., Katou, Y., Mori, S., Itoh, T., Helmhart, W., Gálová, M., Petronczki, M., Gregan, J., Cetin, B. and Mudrak, I., 2006. Protein phosphatase 2A protects centromeric sister chromatid cohesion during meiosis I. *Nature*, *441*(7089), pp.53-61.

Romero, S., Le Clainche, C., Didry, D., Egile, C., Pantaloni, D. and Carlier, M.F., 2004. Formin is a processive motor that requires profilin to accelerate actin assembly and associated ATP hydrolysis. *Cell*, *119*(3), pp.419-429.

Rose, R., Weyand, M., Lammers, M., Ishizaki, T., Ahmadian, M.R. and Wittinghofer, A., 2005. Structural and mechanistic insights into the interaction between Rho and mammalian Dia. *Nature*, *435*(7041), pp.513-518.

Ruchaud, S., Carmena, M. and Earnshaw, W.C., 2007. The chromosomal passenger complex: one for all and all for one. *Cell*, *131*(2), pp.230-231.

Sagot, I., Rodal, A.A., Moseley, J., Goode, B.L. and Pellman, D., 2002. An actin nucleation mechanism mediated by Bni1 and profilin. *Nature cell biology*, *4*(8), pp.626-631.

Santaguida, S. and Musacchio, A., 2009. The life and miracles of kinetochores. *The EMBO journal*, *28*(17), pp.2511-2531.

Santaguida, S., Vernieri, C., Villa, F., Ciliberto, A. and Musacchio, A., 2011. Evidence that Aurora B is implicated in spindle checkpoint signalling independently of error correction. *The EMBO journal*, *30*(8), pp.1508-1519.

Sardar, H.S., Luczak, V.G., Lopez, M.M., Lister, B.C. and Gilbert, S.P., 2010. Mitotic kinesin CENP-E promotes microtubule plus-end elongation. *Current Biology*, *20*(18), pp.1648-1653.

Sassoon, I., Severin, F.F., Andrews, P.D., Taba, M.R., Kaplan, K.B., Ashford, A.J., Stark, M.J., Sorger, P.K. and Hyman, A.A., 1999. Regulation of Saccharomyces cerevisiae kinetochores by the type 1 phosphatase Glc7p.*Genes & Development*, *13*(5), pp.545-555.

Sazer, S., 2005. Nuclear envelope: nuclear pore complexity. *Current biology*,*15*(1), pp.R23-R26.

Schaar, B.T., Chan, G.K.T., Maddox, P., Salmon, E.D. and Yen, T.J., 1997. CENP-E function at kinetochores is essential for chromosome alignment. *The Journal of cell biology*, *139*(6), pp.1373-1382.

Schafer-Hales, K., Iaconelli, J., Snyder, J.P., Prussia, A., Nettles, J.H., El-Naggar, A., Khuri, F.R., Giannakakou, P. and Marcus, A.I., 2007. Farnesyl transferase inhibitors impair chromosomal maintenance in cell lines and human tumors by compromising CENP-E and CENP-F function. *Molecular cancer therapeutics*, *6*(4), pp.1317-1328.

Schirenbeck, A., Bretschneider, T., Arasada, R., Schleicher, M. and Faix, J., 2005. The Diaphanous-related formin dDia2 is required for the formation and maintenance of filopodia. *Nature cell biology*, *7*(6), pp.619-625.

Schliekelman, M., Cowley, D.O., O'Quinn, R., Oliver, T.G., Lu, L., Salmon, E.D. and Van Dyke, T., 2009. Impaired Bub1 function in vivo compromises tension-dependent checkpoint function leading to aneuploidy and tumorigenesis. *Cancer research*, *69*(1), pp.45-54.

Severson, A.F., Baillie, D.L. and Bowerman, B., 2002. A Formin Homology protein and a profilin are required for cytokinesis and Arp2/3-independent assembly of cortical microfilaments in C. elegans. *Current biology*, *12*(24), pp.2066-2075.

Shan, R.F., Zhou, Y.F., Peng, A.F. and Jie, Z.G., 2014. Inhibition of Aurora-B suppresses HepG2 cell invasion and migration via the PI3K/Akt/NF-κB signaling pathway in vitro. *Experimental and therapeutic medicine*, *8*(3), pp.1005-1009.

Shimada, A., Nyitrai, M., Vetter, I.R., Kühlmann, D., Bugyi, B., Narumiya, S., Geeves, M.A. and Wittinghofer, A., 2004. The core FH2 domain of diaphanous-related formins is an elongated actin binding protein that inhibits polymerization. *Molecular cell*, *13*(4), pp.511-522.

Shinohara, R., Thumkeo, D., Kamijo, H., Kaneko, N., Sawamoto, K., Watanabe, K., Takebayashi, H., Kiyonari, H., Ishizaki, T., Furuyashiki, T. and Narumiya, S., 2012. A role for mDia, a Rho-regulated actin nucleator, in tangential migration of interneuron precursors. *Nature neuroscience*, *15*(3), pp.373-380.

Shrestha, R.L. and Draviam, V.M., 2013. Lateral to end-on conversion of chromosome-microtubule attachment requires kinesins CENP-E and MCAK. *Current biology*, *23*(16), pp.1514-1526.

Silkworth, W.T. and Cimini, D., 2012. Transient defects of mitotic spindle geometry and chromosome segregation errors. *Cell division*, *7*(1), p.1.

Stewart, S. and Fang, G., 2005. Destruction Box–Dependent Degradation of Aurora B Is Mediated by the Anaphase-Promoting Complex/Cyclosome and Cdh1. *Cancer research*, *65*(19), pp.8730-8735.

Suetsugu, S., Miki, H. and Takenawa, T., 1999. Identification of two human WAVE/SCAR homologues as general actin regulatory molecules which associate with the Arp2/3 complex. *Biochemical and biophysical research communications*, *260*(1), pp.296-302.

Suijkerbuijk, S.J., Vleugel, M., Teixeira, A. and Kops, G.J., 2012. Integration of kinase and phosphatase activities by BUBR1 ensures formation of stable kinetochore-microtubule attachments. *Developmental cell*, *23*(4), pp.745-755.

Sundin, L.J., Guimaraes, G.J. and DeLuca, J.G., 2011. The NDC80 complex proteins Nuf2 and Hec1 make distinct contributions to kinetochore–microtubule attachment in mitosis. *Molecular biology of the cell*, *22*(6), pp.759-768.

Suzuki, A., Hori, T., Nishino, T., Usukura, J., Miyagi, A., Morikawa, K. and Fukagawa, T., 2011. Spindle microtubules generate tension-dependent changes in the distribution of inner kinetochore proteins. *The Journal of cell biology*, *193*(1), pp.125-140.

Suzuki, A., Badger, B.L., Wan, X., DeLuca, J.G. and Salmon, E.D., 2014. The architecture of CCAN proteins creates a structural integrity to resist spindle forces and achieve proper intrakinetochore stretch. *Developmental cell*, *30*(6), pp.717-730.

Swan, K.A., Severson, A.F., Carter, J.C., Martin, P.R., Schnabel, H., Schnabel, R. and Bowerman, B., 1998. cyk-1: a C. elegans FH gene required for a late step in embryonic cytokinesis. *Journal of cell science*, *111*(14), pp.2017-2027.

Tanaka, K., 2013. Regulatory mechanisms of kinetochore–microtubule interaction in mitosis. *Cellular and Molecular Life Sciences*, *70*(4), pp.559-579.

Tang, Z., Shu, H., Qi, W., Mahmood, N.A., Mumby, M.C. and Yu, H., 2006. PP2A is required for centromeric localization of Sgo1 and proper chromosome segregation. *Developmental cell*, *10*(5), pp.575-585.

Tauchman, E.C., Boehm, F.J. and DeLuca, J.G., 2015. Stable kinetochore-microtubule attachment is sufficient to silence the spindle assembly checkpoint in human cells. *Nature communications*, *6*.

Thrower, D.A., Jordan, M.A. and Wilson, L., 1996. Modulation of CENP-E organization at kinetochores by spindle microtubule attachment. *Cell motility and the cytoskeleton*, *35*(2), pp.121-133.

Thumkeo, D., Shinohara, R., Watanabe, K., Takebayashi, H., Toyoda, Y., Tohyama, K., Ishizaki, T., Furuyashiki, T. and Narumiya, S., 2011. Deficiency of mDia, an actin nucleator, disrupts integrity of neuroepithelium and causes periventricular dysplasia. *PLoS One*, *6*(9), p.e25465.

Tominaga, T., Sahai, E., Chardin, P., McCormick, F., Courtneidge, S.A. and Alberts, A.S., 2000. Diaphanous-related formins bridge Rho GTPase and Src tyrosine kinase signaling. *Molecular cell*, *5*(1), pp.13-25.

Trinkle-Mulcahy, L., Andrews, P.D., Wickramasinghe, S., Sleeman, J., Prescott, A., Lam, Y.W., Lyon, C., Swedlow, J.R. and Lamond, A.I., 2003. Time-lapse imaging reveals dynamic relocalization of PP1γ throughout the mammalian cell cycle. *Molecular biology of the cell*, *14*(1), pp.107-117.

Trinkle-Mulcahy, L., Andersen, J., Lam, Y.W., Moorhead, G., Mann, M. and Lamond, A.I., 2006. Repo-Man recruits PP1γ to chromatin and is essential for cell viability. *The Journal of cell biology*, *172*(5), pp.679-692.

Tung, H.Y., Wang, W. and Chan, C.S., 1995. Regulation of chromosome segregation by Glc8p, a structural homolog of mammalian inhibitor 2 that functions as both an activator and an inhibitor of yeast protein phosphatase 1. *Molecular and cellular biology*, *15*(11), pp.6064-6074.

Uchida, K.S., Takagaki, K., Kumada, K., Hirayama, Y., Noda, T. and Hirota, T., 2009. Kinetochore stretching inactivates the spindle assembly checkpoint. *The Journal of cell biology*, *184*(3), pp.383-390.

Van Hooser, A.A., Ouspenski, I.I., Gregson, H.C., Starr, D.A., Yen, T.J., Goldberg, M.L., Yokomori, K., Earnshaw, W.C., Sullivan, K.F. and Brinkley, B.R., 2001. Specification of kinetochore-forming chromatin by the histone H3 variant CENP-A. *Journal of Cell Science*, *114*(19), pp.3529-3542.

Verhey, K.J., Kaul, N. and Soppina, V., 2011. Kinesin assembly and movement in cells. *Annual review of biophysics*, *40*, pp.267-288.

Vigneron, S., Prieto, S., Bernis, C., Labbé, J.C., Castro, A. and Lorca, T., 2004. Kinetochore localization of spindle checkpoint proteins: who controls whom?. *Molecular biology of the cell*, *15*(10), pp.4584-4596.

Vitre, B., Gudimchuk, N., Borda, R., Kim, Y., Heuser, J.E., Cleveland, D.W. and Grishchuk, E.L., 2014. Kinetochore–microtubule attachment throughout mitosis potentiated by the elongated stalk of the kinetochore kinesin CENP-E. *Molecular biology of the cell*, *25*(15), pp.2272-2281.

Walczak, C.E. and Heald, R., 2008. Chapter Three-Mechanisms of Mitotic Spindle Assembly and Function. *International review of cytology*, *265*, pp.111-158.

Wallar, B.J., DeWard, A.D., Resau, J.H. and Alberts, A.S., 2007. RhoB and the mammalian Diaphanous-related formin mDia2 in endosome trafficking. *Experimental cell research*, *313*(3), pp.560-571.

Wan, X., O'Quinn, R.P., Pierce, H.L., Joglekar, A.P., Gall, W.E., DeLuca, J.G., Carroll, C.W., Liu, S.T., Yen, T.J., McEwen, B.F. and Stukenberg, P.T., 2009. Protein architecture of the human kinetochore microtubule attachment site. *Cell*, *137*(4), pp.672-684.

Wang, H.W., Long, S., Ciferri, C., Westermann, S., Drubin, D., Barnes, G. and Nogales, E., 2008. Architecture and flexibility of the yeast Ndc80 kinetochore complex. *Journal of molecular biology*, *383*(4), pp.894-903.

Watanabe, S., Okawa, K., Miki, T., Sakamoto, S., Morinaga, T., Segawa, K., Arakawa, T., Kinoshita, M., Ishizaki, T. and Narumiya, S., 2010. Rho and anillin-dependent control of mDia2 localization and function in cytokinesis. *Molecular biology of the cell*, *21*(18), pp.3193-3204.

Watanabe, N., Madaule, P., Reid, T., Ishizaki, T., Watanabe, G., Kakizuka, A., Saito, Y., Nakao, K., Jockusch, B.M. and Narumiya, S., 1997. p140mDia, a mammalian homolog of Drosophila diaphanous, is a target protein for Rho small GTPase and is a ligand for profilin. *The EMBO journal*, *16*(11), pp.3044-3056.

Watanabe, N., Kato, T., Fujita, A., Ishizaki, T. and Narumiya, S., 1999. Cooperation between mDia1 and ROCK in Rho-induced actin reorganization. *Nature cell biology*, *1*(3), pp.136-143.

Waters, J.C., Skibbens, R.V. and Salmon, E.D., 1996. Oscillating mitotic newt lung cell kinetochores are, on average, under tension and rarely push. *Journal of cell science*, *109*(12), pp.2823-2831.

Waters, J.C., Chen, R.H., Murray, A.W. and Salmon, E.D., 1998. Localization of Mad2 to kinetochores depends on microtubule attachment, not tension. *The Journal of cell biology*, *141*(5), pp.1181-1191.

Weaver, B.A., Bonday, Z.Q., Putkey, F.R., Kops, G.J., Silk, A.D. and Cleveland, D.W., 2003. Centromere-associated protein-E is essential for the mammalian mitotic checkpoint to prevent aneuploidy due to single chromosome loss. *The Journal of cell biology*, *162*(4), pp.551-563.

Weaver, B.A., Silk, A.D., Montagna, C., Verdier-Pinard, P. and Cleveland, D.W., 2007. Aneuploidy acts both oncogenically and as a tumor suppressor. *Cancer cell*, *11*(1), pp.25-36.

Webb, D.J., Donais, K., Whitmore, L.A., Thomas, S.M., Turner, C.E., Parsons, J.T. and Horwitz, A.F., 2004. FAK–Src signalling through paxillin, ERK and MLCK regulates adhesion disassembly. *Nature cell biology*, *6*(2), pp.154-161.

Wei, R.R., Al-Bassam, J. and Harrison, S.C., 2007. The Ndc80/HEC1 complex is a contact point for kinetochore-microtubule attachment. *Nature structural & molecular biology*, *14*(1), pp.54-59.

Weiss, E. and Winey, M., 1996. The Saccharomyces cerevisiae spindle pole body duplication gene MPS1 is part of a mitotic checkpoint. *The Journal of cell biology*, *132*(1), pp.111-123.

Welburn, J.P., Vleugel, M., Liu, D., Yates, J.R., Lampson, M.A., Fukagawa, T. and Cheeseman, I.M., 2010. Aurora B phosphorylates spatially distinct targets to differentially regulate the kinetochore-microtubule interface.*Molecular cell*, *38*(3), pp.383-392.

Wen, Y., Eng, C.H., Schmoranzer, J., Cabrera-Poch, N., Morris, E.J., Chen, M., Wallar, B.J., Alberts, A.S. and Gundersen, G.G., 2004. EB1 and APC bind to mDia to stabilize microtubules downstream of Rho and promote cell migration. *Nature cell biology*, *6*(9), pp.820-830.

Wigge, P.A. and Kilmartin, J.V., 2001. The Ndc80p complex from Saccharomyces cerevisiae contains conserved centromere components and has a function in chromosome segregation. *The Journal of cell biology*,*152*(2), pp.349-360.

Wojcik, E., Basto, R., Serr, M., Scaërou, F., Karess, R. and Hays, T., 2001. Kinetochore dynein: its dynamics and role in the transport of the Rough deal checkpoint protein. *Nature cell biology*, *3*(11), pp.1001-1007.

Wood, K.W., Sakowicz, R., Goldstein, L.S. and Cleveland, D.W., 1997. CENP-E is a plus end–directed kinetochore motor required for metaphase chromosome alignment. *Cell*, *91*(3), pp.357-366.

Wood, K.W., Lad, L., Luo, L., Qian, X., Knight, S.D., Nevins, N., Brejc, K., Sutton, D., Gilmartin, A.G., Chua, P.R. and Desai, R., 2010. Antitumor activity of an allosteric inhibitor of centromere-associated protein-E. *Proceedings of the National Academy of Sciences*, *107*(13), pp.5839-5844.

Wood, K.W., Chua, P., Sutton, D. and Jackson, J.R., 2008. Centromere-associated protein E: a motor that puts the brakes on the mitotic checkpoint. *Clinical Cancer Research*, *14*(23), pp.7588-7592.

Wordeman, L., Wagenbach, M. and von Dassow, G., 2007. MCAK facilitates chromosome movement by promoting kinetochore microtubule turnover. *The Journal of cell biology*, *179*(5), pp.869-879.

Woychik, R.P., Maas, R.L., Zeller, R., Vogt, T.F. and Leder, P., 1990. 'Formins': proteins deduced from the alternative transcripts of the limb deformity gene.

Wu, J.C., Chen, T.Y., Chang-Tze, R.Y., Tsai, S.J., Hsu, J.M., Tang, M.J., Chou, C.K., Lin, W.J., Yuan, C.J. and Huang, C.Y.F., 2005. Identification of V23RalA-Ser194 as a critical mediator for Aurora-A-induced cellular motility and transformation by small pool expression screening. *Journal of Biological Chemistry*, *280*(10), pp.9013-9022.

Xu, Y., Moseley, J.B., Sagot, I., Poy, F., Pellman, D., Goode, B.L. and Eck, M.J., 2004. Crystal structures of a Formin Homology-2 domain reveal a tethered dimer architecture. *Cell*, *116*(5), pp.711-723.

Yamamoto, A., Guacci, V. and Koshland, D., 1996. Pds1p, an inhibitor of anaphase in budding yeast, plays a critical role in the APC and checkpoint pathway (s). *The Journal of cell biology*, *133*(1), pp.99-110.

Yang, C., Czech, L., Gerboth, S., Kojima, S.I., Scita, G. and Svitkina, T., 2007. Novel roles of formin mDia2 in lamellipodia and filopodia formation in motile cells. *PLoS biol*, *5*(11), p.e317.

Yao, X., Anderson, K.L. and Cleveland, D.W., 1997. The microtubule-dependent motor centromere–associated protein E (CENP-E) is an integral component of kinetochore corona fibers that link centromeres to spindle microtubules. *The Journal of cell biology*, *139*(2), pp.435-447.

Yao, X., Abrieu, A., Zheng, Y., Sullivan, K.F. and Cleveland, D.W., 2000. CENP-E forms a link between attachment of spindle microtubules to kinetochores and the mitotic checkpoint. *Nature Cell Biology*, *2*(8), pp.484-491.

Yardimci, H., Van Duffelen, M., Mao, Y., Rosenfeld, S.S. and Selvin, P.R., 2008. The mitotic kinesin CENP-E is a processive transport motor. *Proceedings of the National Academy of Sciences*, *105*(16), pp.6016-6021.

Yasuda, S., Oceguera-Yanez, F., Kato, T., Okamoto, M., Yonemura, S., Terada, Y., Ishizaki, T. and Narumiya, S., 2004. Cdc42 and mDia3 regulate microtubule attachment to kinetochores. *Nature*, *428*(6984), pp.767-771.

Yasui, Y., Urano, T., Kawajiri, A., Nagata, K.I., Tatsuka, M., Saya, H., Furukawa, K., Takahashi, T., Izawa, I. and Inagaki, M., 2004. Autophosphorylation of a newly identified site of Aurora-B is indispensable for cytokinesis. *Journal of Biological Chemistry*, *279*(13), pp.12997-13003.

Yen, T.J., Compton, D.A., Wise, D., Zinkowski, R.P., Brinkley, B.R., Earnshaw, W.C. and Cleveland, D.W., 1991. CENP-E, a novel human centromere-associated protein required for progression from metaphase to anaphase. *The EMBO journal*, *10*(5), p.1245.

Yen, T.J., Li, G., Schaar, B.T., Szjlak, I., and Cleveland, D.W 1992. CENP-E is a putative kinetochore motor that accumulates just before mitosis. *Nature*, *359*.

Yucel, J.K., Marszalek, J.D., McIntosh, J.R., Goldstein, L.S., Cleveland, D.W. and Philp, A.V., 2000. CENP-meta, an essential kinetochore kinesin required for the maintenance of metaphase chromosome alignment in Drosophila. *The Journal of cell biology*, *150*(1), pp.1-12.

Zachos, G., Black, E.J., Walker, M., Scott, M.T., Vagnarelli, P., Earnshaw, W.C. and Gillespie, D.A., 2007. Chk1 is required for spindle checkpoint function. *Developmental cell*, *12*(2), pp.247-260.

Zhang, X.D., Goeres, J., Zhang, H., Yen, T.J., Porter, A.C. and Matunis, M.J., 2008. SUMO-2/3 modification and binding regulate the association of CENP-E with kinetochores and progression through mitosis. *Molecular cell*,*29*(6), pp.729-741.

Zhou, L.D., Xiong, X., Long, X.H., Liu, Z.L., Huang, S.H. and Zhang, W., 2014. RNA interference-mediated knockdown of Aurora-B alters the metastatic behavior of A549 cells via modulation of the phosphoinositide 3-kinase/Akt signaling pathway. *Oncology letters*, *8*(5), pp.2063-2068.

Zhu, X.P., Liu, Z.L., Peng, A.F., Zhou, Y.F., Long, X.H., Luo, Q.F., Huang, S.H. and Shu, Y., 2014. Inhibition of Aurora-B suppresses osteosarcoma cell migration and invasion. *Experimental and therapeutic medicine*, *7*(3), pp.560-564.

Zigmond, S.H., Evangelista, M., Boone, C., Yang, C., Dar, A.C., Sicheri, F., Forkey, J. and Pring, M., 2003. Formin leaky cap allows elongation in the presence of tight capping proteins. *Current Biology*, *13*(20), pp.1820-1823.